

Institute of Crop Science

University of Hohenheim

Field: Nutritional Crop Physiology (340h)

Prof. Dr. Uwe Ludewig

**Comprehensive analyses of DNA methylation profile, regulation
on flowering, and seed mineral accumulation in *Arabidopsis*
thaliana in response to zinc deficiency**

Dissertation

submitted in fulfillment of the regulations to acquire the degree

“Doktor der Agrarwissenschaften”

(Dr. sc. agr. in Agricultural Sciences)

to the

Faculty of Agricultural Sciences

Presented by

Xiaochao Chen

Anhui, China

2016

The thesis was accepted as a doctoral thesis (Dissertation) in fulfillment of the regulations to acquire the doctoral degree “Doktor der Agrarwissenschaften – Doctor scientiarum agriculturæ (Dr. sc. agr.)” by the Faculty of Agricultural Sciences at the University of Hohenheim on 26.01.2017.

Date of the oral examination: 10.02.2016

Examination Committee

Head of Committee: Prof. Dr. Jörn Bennewitz

1st examiner: Prof. Dr. Uwe Ludewig

2nd examiner: Prof. Dr. Claudia Oecking

3rd examiner: Prof. Dr. Karl Schmid

Table of Contents

1 Summary-Zusammenfassung	1
1.1 Summary	1
1.2 Zusammenfassung	4
2 General introduction.....	7
2.1 Zinc: a multifunctional but bioavailability-limited micronutrient	7
2.2 Transcriptional responses to adapt to Zn deficiency in <i>Arabidopsis thaliana</i>	7
2.3 Epigenome and epigenetic adaptation to stress in plants	8
2.4 Flowering pathways in <i>Arabidopsis thaliana</i>	10
2.5 Mineral concentrations in <i>Arabidopsis</i> seeds	11
2.6 Natural variation and genome-wide association studies in <i>Arabidopsis thaliana</i> ..	13
2.7 Research objectives	14
3 Publications	16
4 Chapter I	17
Limited contribution of zinc deficiency-induced DNA demethylation to transcription in <i>Arabidopsis thaliana</i>	17
5 Chapter II	55
Zinc controls leaf size by promotion of <i>FLOWERING LOCUS T</i> in early-flowering <i>Arabidopsis thaliana</i>	55
6 Chapter III	93
Natural genetic variation of seed micronutrients of <i>Arabidopsis thaliana</i> grown in zinc-deficient and zinc-amended soil	93
7 General discussion.....	94
7.1 How to limit Zn bioavailability in <i>Arabidopsis</i> ?	94
7.2 How to perform a powerful GWAS?	95
7.3 How does <i>Arabidopsis thaliana</i> respond to Zn deficiency?	96
7.3.1 Transcriptional and epigenetic responses to Zn deficiency in roots	97
7.3.2 Zn-dependence of flowering and leaf size	99
7.3.3 Seed Zn accumulation under adverse Zn deficiency condition	100
7.4 Future perspectives	102
8 References	104
9 Acknowledgement	116

10 Curriculum vitae.....	117
--------------------------	-----

1 Summary-Zusammenfassung

1.1 Summary

Zinc (Zn) is an essential micronutrient for plant growth and development, which plays important roles in DNA binding, metabolic, catalytic and transcriptional regulator activities. However, Zn deficiency is a worldwide problem due to its limited bioavailability in soils in many agricultural areas, often as a result of high CaCO_3 content and high pH. In addition, phytic acid is able to strongly chelate cations, such as Zn^{2+} , Fe^{2+} , Ca^{2+} and Mg^{2+} to form the phytate salts. Phytate cannot be digested by human beings or other monogastric animals due to lack of phytase, an enzyme that can hydrolyze phytate. Therefore, Zn bioavailability in seeds (or grains) is restricted by phytate. Moreover, seed Zn concentration is also reduced by elevated CO_2 , especially in C3 plants, such as wheat, rice and soybean. Regarding to the crucial roles but limited bioavailability of Zn, here I present a comprehensive analysis on roots, leaves (and flowering) and seeds in response to Zn deficiency in the model plant *Arabidopsis thaliana* via three experiments.

First, I investigated the transcriptional response and whole-genome DNA methylation profile upon Zn deficiency in roots using next-generation sequencing. Ionome analysis on shoots showed that Zn concentration was strongly reduced in Zn deficiency, whereas other nutrients were not affected. Microarray Analysis identified several known Zn-deficiency responsive genes, confirming the effectiveness of Zn deficiency in this work. However, bisulfite sequencing results revealed that DNA methylation was eliminated by Zn deficiency in transposable elements and slightly in gene bodies as well. The DNA demethylation response to nutrient stress was a novel finding, as reversed to previous reports about phosphate stress which accumulated methylation. Surprisingly, further analysis suggested that DNA methylation occurred independent of gene transcription. Nevertheless, non-CpG methylation has a potential impact on flower development in response to Zn deficiency.

Summary-Zusammenfassung

The second experiment investigated the relationship between rosette size and flowering, and how rosette size and flowering time were regulated by Zn deficiency. Using natural variation population (168 *Arabidopsis* accessions), I found that flowering time was positively correlated with rosette size in early-flowering accessions but not in late-flowering accessions. Intriguingly, the flowering time was delayed by Zn deficiency in these early-flowering plants and resulting in promotion of vegetative biomass. However, Zn-regulated flowering time was independent of previously reported flowering pathways. Then genome-wide association study identified the underlying candidate gene was *FLOWERING LOCUS T (FT)* which was strongly inhibited by Zn deficiency in all accessions. Detailed genetic analysis confirmed this result as well. Furthermore, the promotion of leaf size in Zn deficiency was found being contributed by cell proliferation (cell number) but not cell size.

Lastly, in the third experiment I was interested in the natural genetic variation in seed Zn concentration, together with iron (Fe) and manganese (Mn), in response to Zn deficiency. Across around 100 accessions, average seed Zn concentration decreased from $47.4 \mu\text{g g}^{-1}$ to $31.3 \mu\text{g g}^{-1}$ due to Zn deficiency. To identify candidate genes affecting seed Zn, Fe and Mn concentrations, genome-wide association mapping was performed. A candidate gene, inositol 1,3,4-trisphosphate 5/6-kinase 3 gene (*ITPK3*), was associated which is involved in phytate synthesis pathways. However, loss of this gene in *itpk3-1* did neither affect phytate seed levels nor seed Zn, Fe and Mn. Nevertheless, large natural variance of micronutrient seed levels was identified in the population and several accessions maintained high seed Zn despite growth in Zn-deficient conditions.

Altogether, this study presents comprehensive analyses in how *Arabidopsis* adapts to Zn deficiency in regard of root transcription and DNA methylation, flowering and leaf regulation, and seed mineral accumulation. I provided new possibilities of correlation between DNA methylation and gene transcription, which is much more complex than previously reported. I also opened a novel insight into flowering regulation on leaf size, resulting in promotion of vegetative

Summary-Zusammenfassung

biomass in nutrient deficiency. Substantial natural variation of seed experiment indicated that the evolution process was involved in seed mineral accumulation in *Arabidopsis*, especially those accessions maintaining Zn concentration in Zn-deficient soils are valuable for further investigations. I believe these findings in *Arabidopsis* also provide precious knowledge for plant breeders and agronomists who work on crops.

1.2 Zusammenfassung

Zink (Zn) ist ein essentieller Mikronährstoff für das Wachstum und die Entwicklung einer Pflanze. Seine wesentlichen Funktionen liegen in der Bindung von DNA sowie in metabolischen, katalytischen und transkriptionell regulatorischen Aktivitäten. Aufgrund der begrenzten Bioverfügbarkeit von Zink im Boden, stellt Zinkmangel ein weltweites Problem dar. Vor allem landwirtschaftlich genutzte Böden mit hohen pH-Werten und Kalkgehalten limitieren die Zinkaufnahme. Zusätzlich werden Kationen (wie Zn^{2+} , Fe^{2+} , Ca^{2+} and Mg^{2+}) von im Boden enthaltenen Phytinsäuren chelatiert und bilden zusammen das schwerlösliche Salz Phytat. Phytat kann nicht von monogastrischen Lebewesen wie dem Menschen aufgespalten werden, da das dazu benötigte Enzym Phytase nicht im Verdauungstrakt vorkommt. Die Bioverfügbarkeit von Zn ist deshalb in pflanzlichen Samen durch den Phytatgehalt limitiert. Zudem führt der ansteigende CO_2 -Gehalt zu einer reduzierten Zn Konzentration im Samen, vor allem in C3-Pflanzen wie Weizen, Reis und Soja.

Aufgrund der wichtigen biologischen Funktionen von Zink, aber seiner begrenzten Bioverfügbarkeit, wurden in diesem Forschungsprojekt verschiedene Effekte des Zinkmangels in der Modellpflanze *Arabidopsis thaliana* genauer analysiert.

Zunächst wurden unter Zinkmangel transkriptionelle Veränderungen per Microarray und das genomweite DNA Methylierungsmuster durch genomweite Bisulfit-Sequenzierung in Wurzeln bestimmt. Dabei zeigte die Ionom-Analyse im Spross eine deutlich reduzierte Zn Konzentration in Zinkmangel-ernährten Pflanzen ohne Veränderungen anderer Nährstoffkonzentrationen. Auch die Microarray-Daten belegten einen spezifischen Zinkmangeleffekt durch Expressionsänderungen von mehreren Zinkmangelgenen. Die Ergebnisse der Bisulfit-Sequenzierung wiesen eine Reduzierung der DNA Methylierung durch Zinkmangel auf, welche, wenn vorhanden, hauptsächlich in Transposonelementen und teilweise in kodierenden Genregionen lokalisiert war.

Summary-Zusammenfassung

Die hier durch Stress verursachte Demethylierung unterschied sich zu bereits beschriebenen Veränderungen der Methylierung durch Phosphormangel – dies könnte zu neuen Erkenntnissen im Bereich der epigenetischen Anpassung führen. Interessanterweise zeigten weitere Untersuchungen, dass das DNA Methylierungsmuster keinen direkten Einfluss auf die Genexpression hatte. Nicht-CpG-Methylierungen könnten unter Zinkmangel möglicherweise aber die Blütenentwicklung beeinflussen.

Im zweiten Experiment wurde der Zusammenhang zwischen Rosettengröße und Blütezeit unter Zinkmangel bei natürlichen Population von *Arabidopsis* (168 Akzessionen) genauer untersucht: Bei Frühblüher-Akzessionen korrelierte der Blütezeitpunkt positiv mit der Rosettengröße; Dies traf allerdings nicht bei Spätblütler-Akzessionen zu. Zusätzlich wurde bei diesen Frühblütlern ein bis dato unbekannter, verspäteter Blütezeitpunkt unter Zinkmangel beobachtet, welcher zu einem verstärkten vegetativen Wachstum und dadurch zu einer erhöhten Biomasse führte. Das dafür verantwortliche Gen *FLOWERING LOCUS T (FT)*, das unter Zinkmangel in allen *Arabidopsis* Akzessionen stark inhibiert war, wurde mittels einer genomweiten Assoziationsstudie identifiziert. Des Weiteren konnte das verstärkte vegetative Blattwachstum unter Zinkmangel auf eine erhöhte Zellproliferation (Zellzahl) und nicht auf eine erhöhte Zellgröße zurückgeführt werden.

Im letzten Versuch wurde unter Zinkmangel die natürliche genetische Variation der Zn (sowie Fe und Mn) Konzentration in Samen analysiert. In etwa 100 Akzessionen verringerte sich unter Zinkmangel die durchschnittliche Zn Konzentration im Samen von $47.4 \mu\text{g g}^{-1}$ auf $31.3 \mu\text{g g}^{-1}$. Eine erneute genomweite Assoziationsstudie identifizierte das Inositol 1,3,4-triphosphate 5/6-kinase 3 (*ITPK3*) Gen, welches in der Phytatsynthese beteiligt ist, als möglichen Kandidaten für die Beeinflussung der Zn, Fe und Mn Konzentration im Samen. Jedoch führte der Verlust dieses Gens in der *iptk-1* Mutante weder zu einem verringerten Phytatgehalt noch zu veränderten Zn, Fe oder Mn Konzentrationen im Samen. Trotz Wachstum auf Zinkmangelboden wurde in der untersuchten

Summary-Zusammenfassung

Arabidopsis Population ein hoher Mikronährstoffgehalt im Samen quantifiziert und mehrere Akzessionen zeigten sogar trotz Zinkmangel einen hohen Zinkgehalt im Samen, was auf eine evolutionäre Anpassung hindeuten könnte.

Zusammengefasst kann gesagt werden, dass diese Studie einen umfassenden Einblick in die Zinkmangelanpassung von *Arabidopsis thaliana* liefert. Dabei konnten neue Erkenntnisse über die komplexe Beziehung zwischen DNA Methylierung und Genexpression gewonnen werden, über das Blühzeit-beeinflusste vegetative Wachstum und über die natürliche Variation des Mikronährstoffhaushalts im Samen. Diese aus *Arabidopsis* stammenden Ergebnisse könnten auf Kulturpflanzen übertragbar sein und damit hilfreich für die Züchtung von Kulturpflanzen.

2 General introduction

2.1 Zinc: a multifunctional but bioavailability-limited micronutrient

Zinc (Zn) is an essential micronutrient required for plant growth and development, and in the meantime an important dietary source of mineral for humans (Marschner, 2012). Average total Zn concentration in soils is 64 mg kg^{-1} , across India, China, England & Wales, Baltic Region, New Zealand, USA, Germany and France (Alloway, 2009). Zn is taken up predominantly as divalent cation (Zn^{2+}); whereas at high pH, also taken up as a monovalent (ZnOH^+) (Marschner, 2012). In plant system, Zn plays a crucial role in binding, catalytic and transcriptional regulator activities (Broadley et al., 2007). In *Arabidopsis thaliana*, over 2000 genes were found to be associated to Zn functionally, including Zn-finger transcription factors (Broadley et al., 2007). Thus Zn deficiency induces severe growth and development problems in leaves and seeds (Talukdar and Aarts, 2007).

Regardless of the crucial function of Zn, plant Zn deficiency is a widespread issue due to the limited soil bioavailability of Zn, often as a result of high CaCO_3 content and high pH, in many agricultural areas (Cakmak, 2007; Alloway, 2008). In addition, evidence accumulated that elevated CO_2 decreased Zn concentration in plants, including grains that are consumed as food by animals and humans (Mcgrath and Lobell, 2013; Loladze, 2014; Myers et al., 2014). Furthermore, Zn bioavailability in seeds is strongly reduced by phytate, a hexa-phosphorylated inositol that serves as the major storage form of phosphorus in seeds (Raboy, 2009). As a result, the inadequate dietary Zn intake has become a pretty prevalent public health problem, particularly in Sub-Saharan Africa and South Asia (Wessells and Brown, 2012). Therefore, Zn has attracted growing interests because of its multifunction and limited bioavailability.

2.2 Transcriptional responses to adapt to Zn deficiency in *Arabidopsis thaliana*

Unlike adaptation to nitrogen or phosphorus deficiency, root system architecture has limited response to Zn deficiency except for slight increment of lateral root

density (Gruber et al., 2013; Jain et al., 2013; Ristova and Busch, 2014). However, the molecular responses still widely occur in the whole plants. In the past two decades, impressive progress has been achieved in identification and characterization of Zn transporter genes responding to Zn deficiency.

The *ZIP* (*ZRT, IRT-LIKE PROTEIN*) gene family is the important metal transporter family in transporting several cations, including Zn, iron (Fe) and Manganese (Mn); and *Arabidopsis* contains 15 *ZIP* genes (Guerinot, 2000). Among them, *ZIP1* to *ZIP5*, *ZIP9* to *ZIP12* and *IRT3* are highly expressed under Zn deficiency (Grotz et al., 1998; Mortel et al., 2006; Krämer et al., 2007; Lin et al., 2009). *ZIP1* and *ZIP3* are expressed in roots, suggesting that they transport Zn from the soils into the plants (Grotz et al., 1998). *BZIP19* (*BASIC-REGION LEUCINE ZIPPER 19*) and *BZIP23* were the transcription factors that respond to Zn deficiency, binding to a specific motif (RTGTCGACAY) conserved in the plant kingdom (Assunção et al., 2010). In the *bzip19bzip23* double mutant, several Zn transporter genes are down-regulated, indicating the crucial function of *BZIP19* and *BZIP23* in controlling the expression of Zn responsive genes. In addition, *HMA* (*HEAVY METAL ATPASE*) family genes were also induced in response to Zn deficiency, like *HMA2* and *HMA4* (Hussain et al., 2004; Verret et al., 2004; Mortel et al., 2006). *HMA2* and *HMA4* are known to be involved in the Zn loading from root symplast to xylem (Olsen and Palmgren, 2014). Zn does not travel as free ion, but forming the Zn-nicotianamine complex. Thus *NAS* (*NICOTIANAMINE SYNTHASE*) family genes act in Zn stress as well, including *NAS2* and *NAS4* (Mortel et al., 2006; Deinlein et al., 2012; Clemens et al., 2013). Lastly, defensin-like family proteins were recently found to be up-regulated in Zn-deficiency assay as well (Zargar et al., 2014).

2.3 Epigenome and epigenetic adaptation to stress in plants

In plants, chromatin structure and DNA transcription are regulated by several epigenetic mechanisms, including DNA methylation, histone modifications and small-interfering RNA (siRNA) pathways (Henderson and Jacobsen, 2007; Zhang, 2008; Chen, 2009; Liu et al., 2010; He et al., 2011). DNA methylation is the

addition of methyl groups from S-adenosyl methionine to cytosines to form 5'-methylcytosines (Chan et al., 2005; Law and Jacobsen, 2010). In plants, DNA methylation occurs in the symmetric contexts CpG and CHG (where H=A, T or C), and the asymmetric context CHH, each of which is established and maintained in independent pathways (Chan et al., 2005; Law and Jacobsen, 2010; Stroud et al., 2013). In brief, CpG methylation is maintained by *METHYLTRANSFERASE 1* (*MET1*) and CHG methylation is maintained by *CHROMOMETHYLASE 3* (*CMT3*) by requiring the H3K9 methylation. CHH methylation is established and maintained by *DOMAINS REARRANGED METHYLTRANSFERASES 1* (*DRM1*) and *DRM2*, via the RNA-directed DNA methylation (RdDM) pathway. 24 nucleotide (24 nt) siRNAs are involved in RdDM pathway in establishing *de novo* methylation. Histone modifications are another important epigenetic marker in chromatin structuring and gene regulating. The fundamental unit of chromatin is named nucleosome that consists of around 140 nucleotides of DNA wrapped on histone octamer. Histone octamer contains two copies of histone proteins, termed H2A, H2B, H3 and H4. The amino tails of the histones are subject to be modified chemically, such as methylation, acetylation and phosphorylation (Liu et al., 2010). *Arabidopsis* vernalization is one classical case that the cold treatment changes the histone modifications of *FLOWERING LOCUS C* (*FLC*) leading to the acceleration of flowering (Sung and Amasino, 2004; Kim et al., 2009; Sheldon et al., 2009).

DNA methylation plays essential roles in stabilization of genome against transposable elements (TEs), regulation of DNA transcription and as well as alternative splicing (Chan et al., 2005; Zilberman et al., 2007; Law and Jacobsen, 2010; Lev Maor et al., 2015). In *Arabidopsis thaliana*, CpG methylation is enriched at TEs as well as gene bodies, whereas CHG and CHH methylation predominantly occurs at TEs (Cokus et al., 2008; Lister et al., 2008; Stroud et al., 2013). Recent years, abundant studies revealed the potential involvement of DNA methylation in response to environmental stress, using low-resolution approaches (Chinnusamy and Zhu, 2009; Zhong et al., 2009; Tan, 2010; Wang et al., 2010; Karan et al., 2012). However, the high resolution analyses of whole-

genome DNA methylation to respond stress are still limited. Using bisulfite sequencing, Downen *et al.* (2012) presented that salicylic acid stress can induce alteration of widespread *Arabidopsis* DNA methylation and regulate the expression of neighboring genes (Downen et al., 2012). Dubin *et al.*, (2015) found that CHH methylation increased with temperature at TEs (Dubin et al., 2015). In regard to nutrient stress, it was reported that phosphate deficiency changes the DNA methylation pattern predominantly at TEs close to highly induced genes (Secco et al., 2015).

2.4 Flowering pathways in *Arabidopsis thaliana*

The appropriate decision for flowering in annual plants is crucial for their lifespan and under very complex genetic control by over 360 genes (Fornara et al., 2010; Bouché et al., 2016). The transition to flowering depends on several endogenous and environmental signals in *Arabidopsis thaliana*. Several flowering pathways were identified, such as photoperiod, temperature, vernalization, gibberellin and sugar pathways (Searle and Coupland, 2004; Fornara et al., 2010; Capovilla et al., 2014; Bouché et al., 2016).

Flowering is promoted by exposure to long days compared to short days, via regulating the transcription factor *CONSTANS* (*CO*); *CO* is able to induce the expression of flowering integrator *FLOWERING LOCUS T* (*FT*) (Putterill et al., 1995; Searle and Coupland, 2004). The MADS-box transcription factor genes *FLOWERING LOCUS M* (*FLM*) and *SHORT VEGETATIVE PHASE* (*SVP*) have key roles in controlling flowering time in response to ambient temperature by antagonistic splicing variants *FLM-β* and *FLM-δ* (Posé et al., 2013). The *SVP-FLM-β* complex is predominately formed at low temperatures to repress flowering, whereas the competing *SVP-FLM-δ* complex acts as an activator of flowering at higher temperatures. Another important environmental stimulus that contributes to flowering transition is vernalization, by requiring a few weeks cold treatment in prior to normal growth condition. Vernalization accelerates flowering in *Arabidopsis* via repression of the floral repressor *FLC* locus. *FLC* was inhibited due to the trimethylation of Lys27 of Histone H3 (H3K27me3) in exposure to cold,

and the repression can be maintained in subsequent mitosis at normal growth temperature (Sung and Amasino, 2004; Kim et al., 2009; Sheldon et al., 2009). Gibberellins also function as an activator of flowering transition, through the promotion of floral integrators *FLOWERING LOCUS T (FT)* and *SUPPRESSOR OF OVEREXPRESSION OF CONSTANS 1 (SOC1)* (Hisamatsu and King, 2008; Mutasa-Göttgens and Hedden, 2009). In addition to the four major flowering pathways mentioned above, recent findings also shed light on the sugar pathway. Briefly, the trehalose-6-phosphate was found to control flowering time and the loss of *TREHALOSE-6-PHOSPHATASE SYNTHASES 1 (TPS1)* plants extremely delayed the flowering in *Arabidopsis* (Wahl et al., 2013; Yu et al., 2013). Other flowering pathways involve micro RNAs. For example, miR-156 regulates the expression of transcription factor *SQUAMOSA PROMOTER BINDING LIKE (SPL)* in the aging pathway (Wang et al., 2009; Fornara et al., 2010).

In the past decade, accumulated evidence indicated that nutrients also play important roles in controlling flowering time. General poor-nutrition accelerates flowering, which was usually assumed that plants are eager to finish their life cycles in response to stress (Kolář and Seňková, 2008; Wada et al., 2010). Similarly, low nitrate also induces flowering while acting independently of photoperiod, gibberellin and autonomous pathways, by showing null-mutants effects (Marín et al., 2010). Furthermore, nitrate and phosphate were presented to play antagonistic roles in regulating flowering, where low nitrate induced flowering, but low phosphate delayed flowering (Kant et al., 2011). In addition, Cadmium stress (50 μ M in *Arabidopsis*) promotes flowering via up-regulating the expression of *CO* and *FT*, whereas down-regulating the expression of *FLC* (Wang et al., 2012).

2.5 Mineral concentrations in *Arabidopsis* seeds

High yield and superior nutrition of seeds and grains are the ultimate pursuit for crop breeders and agronomists. However, seed mineral concentrations are threatened by several factors. One of them is phytate. The major phosphorus (P)

source in seeds is phytic acid, which is a myo-inositol hexakisphosphoric acid; phytic acid is able to strongly chelate cations, such as Zn^{2+} , Fe^{2+} , Ca^{2+} and Mg^{2+} to form the phytate salts (Maathuis, 2009; Raboy, 2009; Kumar et al., 2010; Lei et al., 2013). Phytate cannot be digested by human beings or other monogastric animals due to lack of phytase, the enzyme that can hydrolyze phytate (Holm et al., 2002; Raboy, 2009; Lei et al., 2013). However, detailed analysis of barley grains revealed that Zn and Fe clearly have different speciation and Fe was co-fractionated with phytate, while most Zn was co-eluted with a sulfur containing fraction, meaning that Zn binds to peptides, rather than phytate (Persson et al., 2009). Nevertheless, the chelated minerals are deficient biologically in human intestine. Another important factor is elevated CO_2 which severely threatens human nutrition, especially reduced Zn and Fe concentration in C3 plants (Loladze, 2014; Myers et al., 2014). CO_2 concentration is increasing, leading to the stronger photosynthesis for C3 plants but also a reduction of nutrients. Several potential reasons were supposed: carbohydrate dilution with increased photosynthesis; reduced transpiration also reduces mass flow of mineral nutrients; physiological changes alter requirements for minerals as protein cofactors (Mcgrath and Lobell, 2013; Loladze, 2014; Myers et al., 2014). Meanwhile, Zn deficiency in soils worldwide is also a problem we are facing, because of the reduced Zn loading in plant seeds, which also potentially affects human health (Alloway, 2009; Wessells and Brown, 2012). Altogether, hidden hunger is a new challenge for us.

The accumulation of edible seeds depends on a series of complex processes: the ion bioavailability in soils, uptake efficiency by roots, translocation to shoot and loading into seeds (Grusak and DellaPenna, 1999; Olsen and Palmgren, 2014). It is very hard to identify the underlying genetics responsible for the seed mineral concentrations, as the multitude processes involved and mineral-specific uptake mechanisms. The relationship of different mineral nutrients is also pretty complicated. In *Arabidopsis*, several studies using natural variation and/or recombinant inbred lines (RILs) concluded that the correlation between ion concentrations in different tissues was highly dependent on the growth conditions

and target organs (Buescher et al., 2010; Baxter et al., 2012; Ghandilyan et al., 2012).

2.6 Natural variation and genome-wide association studies in *Arabidopsis thaliana*

Tremendous natural variation exists in plant growth and development within *Arabidopsis* species that originally growth in distant geographically regions, also termed natural accessions (Nordborg and Weigel, 2008; Weigel, 2012; Ogura and Busch, 2015). Different accessions are able to present extremely diversity in numerous phenotypes, such as root architecture, leaf shape, flowering time and nutrients accumulation (Pérez-Pérez et al., 2002; Lempe et al., 2005; Richard et al., 2011; Baxter et al., 2012; Stetter et al., 2015). Meanwhile, natural variation also presents a very big fundamental challenge of biology and genetics, to answer how the genotypic variation contributes to phenotypic variation (Nordborg and Weigel, 2008). Beneficial from the high-throughput next-generation sequencing approaches, the 1001 Genomes project enables a convenient evaluation of the genome, transcriptome and DNA methylome information with over 1000 *Arabidopsis* accessions (Alonso-Blanco et al., 2016; Kawakatsu et al., 2016).

Forward genetics is a powerful tool to connect phenotype and genotype. In principle, any quantitative phenotypic differences identified can be connected to the underlying causative loci via mapping, including quantitative trait locus (QTL) mapping (Korte and Farlow, 2013). QTL mapping has been powerfully used to identify genome regions responsible for interested quantitative traits (e.g. flowering time), using RIL populations (Alonso-Blanco et al., 1998). However, due to the low resolution and intensive labor, there is a great interest to select or combine it with another efficient technique termed genome-wide association study (GWAS) (Nordborg and Weigel, 2008; Korte and Farlow, 2013). GWAS is conducted in a relatively large natural population that is at least partially sequenced, as its molecular markers are single nucleotide polymorphisms (SNPs). Small population potentially reduces the statistical significance and

convenience of the outcome (Ogura and Busch, 2015). However, 96 accessions have already been proven to be enough to produce promising candidates (Atwell et al., 2010). Additionally, population structure is a strong confounding factor to produce false discovery results, which can just be partially overcome by specific robust models, such as the multi-locus mixed model (Cardon and Palmer, 2003; Platt et al., 2010; Segura et al., 2012). Therefore, the best approach is to combine GWAS and QTL to increase the resolution and at the meantime to reduce the false discovery rate (FDR) (Nordborg and Weigel, 2008; Chao et al., 2012; Chao et al., 2014a). Nevertheless, GWAS has been widely performed in enormous traits in *Arabidopsis*. As a landmark, Atwell et al. (2010) opened a novel insight for plant workers by presenting comprehensive GWAS in 107 phenotypes in *Arabidopsis* though without biological confirmation (Atwell et al., 2010). Since then, great advances have been achieved in identification of different *Arabidopsis* phenotypes using GWAS, including nutrients accumulation, flowering time, light sensitivity and root architecture (Brachi et al., 2010; Chao et al., 2012; Chao et al., 2014a; Meijón et al., 2014; Chao et al., 2014b). In addition, Seren et al., (2012) presented GWAPP, a web application to carry out GWAS user-friendly (Seren et al., 2012). GWAPP contains 1386 accessions and 206,000 SNPs for analysis, and mixed model is available to eliminate noise of population structure as well.

2.7 Research objectives

Based on the previous knowledge in *Arabidopsis* of root Zn transporters, flowering regulation pathways and the mechanisms of seed mineral accumulation, this study was conceived to obtain more comprehensive knowledge in the adaptation strategies upon Zn deficiency. In this work, DNA methylome and transcriptome were analyzed, and association mapping was also conducted based on the natural variation. Overall, our objectives were:

- (1) To investigate the DNA methylation profile and the potential relationship with transcriptome in response to Zn deficiency in *Arabidopsis* roots;

General introduction

- (2) To evaluate the correlation between flowering time and leaf size, and how they are regulated by Zn genetically;
- (3) To identify the candidate genes underlying the accumulation of seed Zn, Fe and Mn concentrations by comparing Zn-deficient and Zn-amended growth conditions.

To achieve these objectives, three articles were produced, respectively.

3 Publications

The present thesis consists of three scientific articles as reflected by chapter I-III. Three articles have been submitted (chapter I-II) or published (chapter III).

Chapter I

Chen X, Schönberger B, Menz J and Ludewig U. Limited contribution of zinc deficiency-induced DNA demethylation to transcription in *Arabidopsis thaliana*

Chapter II

Chen X and Ludewig U. Zinc controls leaf size by promotion of *FLOWERING LOCUS T* in early-flowering *Arabidopsis thaliana*.

Chapter III

Chen X, Yuan L and Ludewig U (2016) Natural genetic variation of seed micronutrients of *Arabidopsis thaliana* grown in zinc-deficient and zinc-amended soil. *Front. Plant Sci.* 7:1070

4 Chapter I

Limited contribution of zinc deficiency-induced DNA demethylation to transcription in *Arabidopsis thaliana*.

Xiaochao Chen, Brigitte Schönberger, Jochen Menz and Uwe Ludewig

Institute of Crop Science, Nutritional Crop Physiology, University of Hohenheim, Fruwirthstr. 20, 70593 Stuttgart, Germany

Abbreviations: DEG: differentially expressed gene; DMR: differentially methylated region; FDR: false discovery rate; ^mC: methylated cytosine; TE: transposable element; TSS: transcription start site; Zn: zinc

Summary

DNA methylation is a genome modification that regulates transposon silencing and gene expression, and maintains genome stability in response to environmental conditions. Nutritional deficiencies are a common environmental stress, but little is known about whether and how these alter DNA methylation and whether this impacts on gene expression. The essential micronutrient zinc (Zn) is widely involved in many molecular and metabolic functions, and its deficiency activates a small set of well-known genes. Here, we found that plants lacking non-CpG methylation were strongly impaired by Zn deficiency. To get more insight into the potential role of DNA-methylation in the Zn deficiency response, the whole-genome methylation profile of roots was analyzed. Widespread differentially methylated regions, preferentially localized in transposable elements (TEs) were identified, irrespective of the methylation contexts. Genic CpG methylation was also eliminated to adapt to the adverse Zn situation. While highly expressed genes were more methylated in the CpG context, low expressed genes were predominantly methylated in non-CpG

contexts, but genic regions were preferentially hypomethylated by Zn deficiency, irrespective of the methylation contexts. Unexpectedly, Zn deficiency-induced DNA de-methylation had very limited contribution to transcriptomic changes in response to Zn deficiency. Overall, Zn deficiency leads to DNA methylation loss in roots that is not mirrored by differential gene transcription, while the relationship of Zn and non-CpG methylation needs further investigation.

Keywords: bisulfate sequencing, DNA methylation, transcriptome, microarray, microRNA, S-adenosyl methionine, transposable element, zinc

Introduction

Zinc (Zn) is an essential micronutrient for many living organisms due to its multifunction in molecular binding, metabolism regulation and signal transduction (Marschner, 2012). In *Arabidopsis thaliana*, over 2000 Zn-related genes have been assigned based on the Gene Ontology molecular functions, primarily with binding, catalytic and transcriptional regulator activity, including Zn fingers (Broadley et al., 2007). Zn finger is a DNA-binding domain, where the Zn ion (Zn^{2+}) is often ligated into two cysteines and two histidines by an inner hydrophobic core (Klug, 2010). Zn fingers are able to recognize specific DNA sites and regulate transcription, therefore they are integrated in the genome engineering tool ZFNs (Zinc-finger nucleases) (Klug, 2010; Gaj et al., 2013).

Despite of the importance of Zn, Zn deficiency is a widespread problem in plants due to the limited Zn bioavailability in soils, often as a result of high CaCO_3 content and high pH, in many agricultural areas (Cakmak, 2007; Alloway, 2008). Thus, plants have developed strategies to cope with low Zn availability. Unlike the adaptation to nitrogen or phosphorus deficiency, root system architecture has limited response to Zn deficiency except for slight increment of lateral roots (Gruber et al., 2013; Ristova and Busch, 2014; Zargar et al., 2014). However, the molecular responses still widely occur in the whole plant, and the Zn deficiency responsive genes have been largely identified in the past two decades. *ZIP* (*ZRT*, *IRT-LIKE PROTEIN*) family genes are the major group to transport Zn,

including *ZIP1* to *ZIP5*, *ZIP9* to *ZIP12* and *IRT3* (Grotz et al., 1998; Mortel et al., 2006; Krämer et al., 2007; Lin et al., 2009). In addition to *ZIP* family genes, *HMA* (*HEAVY METAL ATPASE*) and *NAS* (*NICOTIANAMINE SYNTHASE*) family genes were also reported to be involved in the Zn deficiency response (Hussain et al., 2004; Verret et al., 2004; Mortel et al., 2006; Deinlein et al., 2012; Clemens et al., 2013). Further, recent findings exhibited the up-regulation of defensin-like family proteins in Zn-deficiency assay as well (Zargar et al., 2014). Interestingly, the specific Zn-deficiency motif (RTGTCGACAY) was characterized, which was bound by the transcription factors *BZIP19* (*BASIC-REGION LEUCINE ZIPPER 19*) and *BZIP23* (Assunção et al., 2010).

DNA methylation is a heritable epigenetic modification in living organisms, which plays essential roles in stabilization of the genome against transposable elements, regulation of transcription and alternative splicing (Chan et al., 2005; Zilberman et al., 2007; Law and Jacobsen, 2010; Lev Maor et al., 2015). In *Arabidopsis*, DNA methylation occurs in the symmetric contexts CpG and CHG (where H represents A, T or C), and the asymmetric context CHH, each of which is established and maintained in independent pathways (Chan et al., 2005; Law and Jacobsen, 2010). Briefly, CpG methylation is maintained by *METHYLTRANSFERASE 1* (*MET1*) and CHG methylation is maintained via *CHROMOMETHYLASE 3* (*CMT3*) by requiring the H3K9 methylation. CHH methylation is established and maintained by *DOMAINS REARRANGED METHYLTRANSFERASES 1* (*DRM1*) and *DRM2* via the RNA-directed DNA methylation (RdDM) pathway. CpG methylation is enriched at transposable elements (TEs) as well as gene bodies, whereas CHG and CHH methylation predominantly occurs at TEs (Cokus et al., 2008; Lister et al., 2008; Stroud et al., 2013). Non-CpG methylation is more flexible to be hypermethylated in response to external stress, such as suboptimal temperature or phosphate deficiency (Dubin et al., 2015; Secco et al., 2015). Though extensive studies were performed on the transcriptional level in response to Zn stress, only a limited number of studies have assessed the potential involvement of DNA methylation or histone modifications. In rats, S-adenosyl methionine (methyl donors) level

was reported to be decreased under Zn deficiency, therefore DNA and histone were both hypomethylated under Zn stress (Sharif et al., 2012). MicroRNAs are endogenous small RNA regulatory molecules of 20 - 24 nucleotides, which are also involved in response to biotic and abiotic stress in plants (Khraiwesh et al., 2012; Bej and Basak, 2014). MiR399, miR395 and miR398 were described to regulate phosphate, sulfate and copper homeostasis, respectively in plants (Chiou et al., 2006; Buhtz et al., 2008; Khraiwesh et al., 2012). In addition to the canonical RNA-directed DNA methylation (RdDM) pathway by small interfering RNAs, microRNAs also mediate DNA methylation in plants.

Here, we investigated the changes in transcription and DNA methylation in response to Zn deficiency (-Zn) in roots. Initially, we found that -Zn severely impaired plant development in *ddc* mutants (lacking non-CpG methylation). Hence, we further performed a comprehensive analysis of Zn-dependent DNA methylation in the root. The ionome and transcriptome analyses confirmed the presence of Zn-deficiency and the whole-genome DNA methylome revealed that DNA was predominantly demethylated, especially in TEs and intergenic regions, in response to Zn deficiency. Unexpectedly, the Zn deficiency-induced hypomethylation was unrelated to gene transcription changes. MicroRNAs and SAM level were also stable in response to Zn deficiency. Our findings provide novel insights into the dynamics of cytosine methylation under Zn stress. Though non-CpG methylation is important to maintain normal growth under Zn-deficiency, while DNA is preferentially hypomethylated, the genome wide demethylation induced by Zn stress was independent of transcriptional changes.

Results

Mutant plants lacking non-CpG methylation were strongly impaired by Zn deficiency

Non-CpG methylation, maintained by *DRM1*, *DRM2* and *CMT3*, was described to change in response to stress more flexibly than CpG methylation (Law and Jacobsen, 2010; Stroud et al., 2013). On the other hand, *ROS1* (*REPRESSOR*

OF SILENCING1) plays an important role in DNA demethylation (Le et al., 2014). Therefore, we investigated the impact of Zn-deficiency (-Zn) on the non-CpG hypomethylated triple mutant *ddc* (lacking *DRM1*, *DRM2* and *CMT3*, (Stroud et al., 2013)) and the hypermethylated *ros1* mutants. Both mutants had only mild growth phenotypes under control hydroponic growth conditions, as reported earlier. However, a bushy growth, together with shorter stems and reduced flower development was apparent in the *ddc* mutant under Zn deficiency in long days, while the flowering time was not affected by -Zn (Fig. 1 A and B). -Zn reduced the shoot biomass of the wild type, the *ddc* and the *ros1* mutants (Fig. 1C), a consequence of the low concentrations of the essential Zn in the shoot under deficiency (Fig. 1D). Moreover, the reduced shoot biomass of *ddc* was accompanied by reduced root growth under control conditions, but interestingly, -Zn stimulated root growth in the *ddc* mutant to a level similar to wild type (Fig. 1E). Furthermore, the Zn concentration in *ddc* roots was larger than in the wild type, potentially indicating that root growth, Zn uptake and/or translocation was targeted by non-CpG methylation (Fig. 1F).

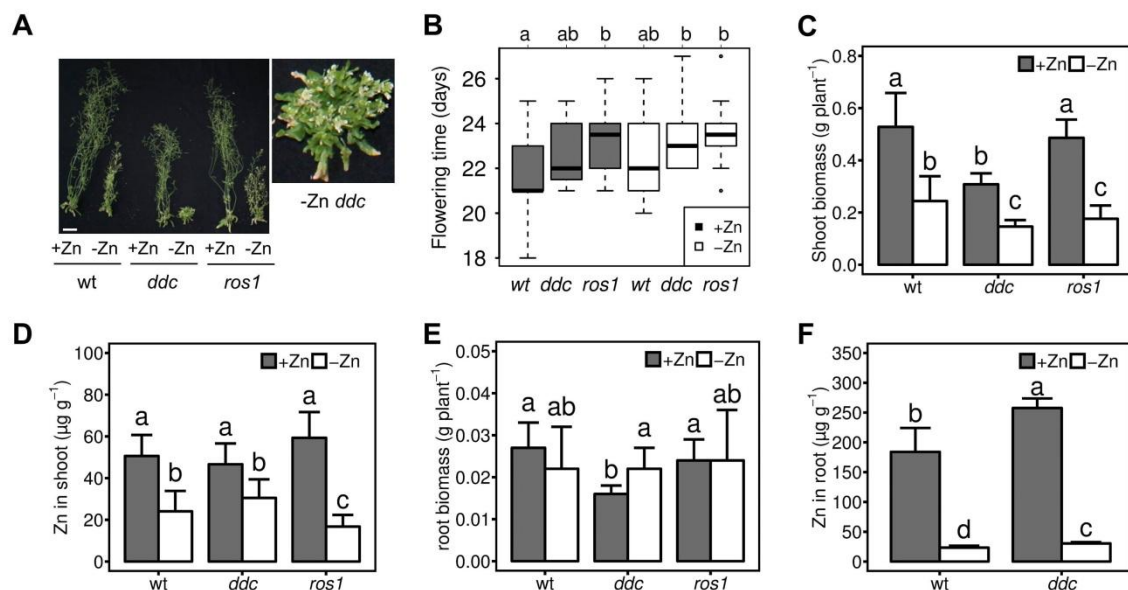


Figure 1: Zn deficiency strongly impaired flower development in *Arabidopsis* plants lacking non-CpG methylation. A, Phenotypic difference of wild type (Col-0), *ddc* mutant and *ros1* mutant under +Zn (2 μ M ZnSO₄) and -Zn conditions. Scale bar: 5

cm. -Zn *ddc* mutant plant was enlarged in the right panel. **B**, Flowering time was slightly affected by mutants. **C** and **D**, Shoot biomass and shoot Zn concentration in wild type and mutants. **E** and **F**, Root biomass and root Zn concentration in wild type and mutants. Data plotted are mean + SD. Different letters indicate significant difference at the $p < 0.05$ level.

Transcriptional responses of *Arabidopsis* root to Zn deficiency

As the *ddc* mutant presented an interesting phenotype under the -Zn condition, we hypothesized that there is some interconnection between the DNA methylome and Zn. In order to capture also long-term processes induced by mild Zn-deficiency occurring over weeks and involving many cell divisions, we selected another *Arabidopsis* accession, Sf-2 instead of Col-0, which has a different Zn demand, flowers later and produces larger biomass than Col-0. Plants with full nutrition (+Zn) and Zn deficiency (-Zn) received with or without 2 μM ZnSO_4 , respectively. Plants were harvested at 40-days, when Zn-deficiency symptoms in leaves were visible (Fig. 2A), but shoot biomass had not changed by -Zn at this stage (Fig. 2B). Ionome analysis of the shoot by inductively coupled plasma mass spectrometry (ICP-MS) confirmed the specific Zn-deficiency. Indeed, Zn concentration in the shoot ranged between +Zn ($72.8 \mu\text{g g}^{-1}$) and -Zn ($11.1 \mu\text{g g}^{-1}$) (Fig. 2C). All other nutrients were in the sufficient range, although copper (Cu) and calcium (Ca) concentrations were also slightly changed (Fig. 2C and D).

Microarray analysis was conducted on root samples in triplicate, to identify the differentially expressed genes (DEGs) induced by -Zn. Surprisingly, using strict significance thresholds, only 15 transcripts were identified at the $p < 0.05$ level (Table 1, Supporting table S1). As expected, typical Zn transporter family genes, such as *ZIP1*, *ZIP3*, *ZIP4*, *ZIP5* and *IRT3*, were up-regulated under -Zn, as well as *NAS2*, *NAS4*, *HMA2* and the purple acid phosphatase gene *PAP27*. Interestingly, four defensin-like family proteins were also highly up-regulated by -

Zn. The only transcript, which was down-regulated by Zn deficiency, was *TERMINAL FLOWERING 1 (TFL1)*, a gene involved in the flowering process. qRT-PCR confirmed the microarray results (Fig. S1).

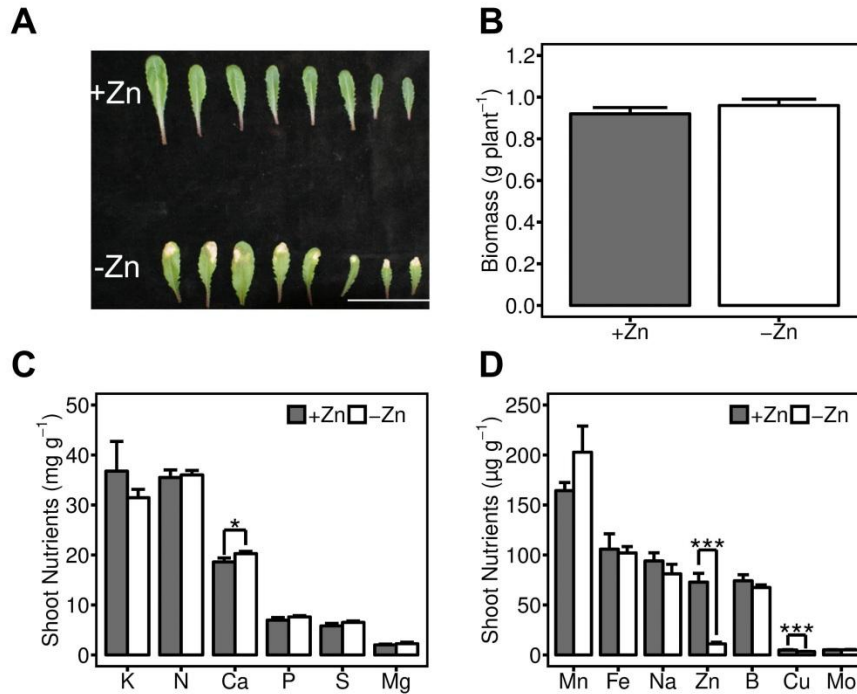


Figure 2: Effectiveness of Zn deficiency. A, Visible Zn-deficiency symptoms in *Arabidopsis* leaves at 40 days. Necrosis appeared in young leaves. Scale bar: 5 cm. B, Dry shoot biomass in full nutrition (+Zn, 2 μM ZnSO₄) and Zn deficiency (-Zn) at 40 days. C and D, Mineral concentrations of +Zn and -Zn shoots. Data plotted are mean + SD. * and *** indicate significant differences at the p<0.05 and p<0.001 level, respectively.

Genome-wide DNA methylation profiling of *Arabidopsis* roots upon Zn deficiency

To explore whether -Zn affects the genomic DNA methylation profile at single-base resolution in *Arabidopsis*, whole-genome bisulfite sequencing was performed on root samples under +Zn and -Zn, each in triplicate. Bisulfite

sequencing yielded approximately 40 million clean paired-end reads for each sample (Supplemental table S2). Altogether, average coverage was 22.3x (7.8x to 29.9x) and average unique mapping rate amounted 32.3 % (15.5 % to 41.3 %). The relatively low mapping rate resulted from strict alignment settings to limit aligning mismatches (see materials and methods for details). Nevertheless, bisulfite non-conversion rates were very low (Supplemental table S2).

Among the aligned mCs (methylated cytosines), the proportion of CpG, CHG and CHH amounted 53.3 %, 18.0 % and 28.6 % for +Zn and 54.0 %, 16.7 % and 29.3 % for -Zn (Fig. 3A). The methylation levels of CpG, CHG and CHH were 22.7 %, 7.6 % and 3.0 % in +Zn, and were slightly lower in -Zn (Fig. 3B). The microRNA level was also decreased under -Zn conditions, which was consistent with the demethylation trend (Fig. 3C). Methylation was mainly distributed either at a very low level (0-10%) or a very high level (90-100%), irrespective of the different contexts (Supporting Fig. S2A-C). In addition, methylation was highly correlated between +Zn and -Zn in all contexts (Supporting Fig. S2D-F).

Further, we examined the methylation profile in different genomic features, including the coding sequence (CDS), intron, 5_UTR, 3_UTR, TE and intergenic space. As expected, TEs showed a higher methylation level than gene body regions. Introns were slightly more methylated than exons (Fig. 3 D-F). In comparison to CpG methylation, non-CpG methylation was decreased in CDS.

Subsequently, the methylation profile across genes and TEs were characterized. Cytosines were rarely methylated in gene transcription start sites (TSS), but then increased gradually in gene body sequences (Supporting Fig. S3A-C). In contrast to TSS of coding regions, the TSS of TEs showed a higher methylation level in all cytosine contexts (Supporting Fig. S3D-F). In general, higher methylation was found in +Zn in genes and TEs. This was consistent with the whole-genome pattern in Fig. 3B. However, -Zn occasionally also established novel CHG and CHH methylation in all replicates, indicating a complex interaction between Zn nutrition and DNA methylation.

Table 1. Differentially expressed transcripts identified in microarray and methylation level

Number	Name	AGI code	Annotation	Log ₂ FC	Adjusted p value	Intensity	CG		CHG		CHH	
							+Zn	-Zn	+Zn	+Zn	-Zn	+Zn
1	<i>ZIP1</i>	<i>AT3G12750.1</i>	Zinc transporter 1 precursor	2.18	0.018	5257	3.0	3.1	0.3	0.4	0.3	0.5
2	<i>ZIP3</i>	<i>AT2G32270.1</i>	Zinc transporter 3 precursor	2.41	0.005	6747	0.4	0.5	0.6	0.5	0.3	0.4
3	<i>ZIP4</i>	<i>AT1G10970.1</i>	Zinc transporter 4 precursor	2.67	0.015	3616	17.9	15.5	0.8	1.0	0.4	0.4
4	<i>ZIP5</i>	<i>AT1G05300.1</i>	Zinc transporter 5 precursor	2.80	0.021	1965	0.2	0.3	0.2	0.2	0.3	0.3
5	<i>ZIP5</i>	<i>AT1G05300.2</i>	Zinc transporter 5 precursor	2.25	0.015	36	0.2	0.3	0.2	0.2	0.3	0.3
6	<i>IRT3</i>	<i>AT1G60960.1</i>	Iron regulated transporter 3	2.15	0.007	6562	6.2	5.6	0.4	0.2	0.3	0.3
7	<i>NAS2</i>	<i>AT5G56080.1</i>	Nicotianamine synthase 2	4.49	0.012	186	1.1	0.6	0.7	0.2	0.3	0.3
8	<i>NAS4</i>	<i>AT1G56430.1</i>	Nicotianamine synthase 4	5.62	0.023	71	6.2	2.4	2.3	0.2	1.0	0.4
9	<i>HMA2</i>	<i>AT4G30110.1</i>	Heavy metal atpase 2	4.43	0.026	495	6.4	6.5	0.3	0.4	0.3	0.3

Table 1. Continued

Number	Name	AGI code	Annotation	Log ₂ FC	Adjusted p value	Intensity	CG		CHG		CHH	
							+Zn	-Zn	+Zn	+Zn	-Zn	+Zn
10	<i>PAP27</i>	<i>AT5G50400.1</i>	Purple acid phosphatase 27	2.01	0.025	1911	12.7	10.3	0.4	0.3	0.4	0.3
11	<i>DEFL</i>	<i>AT1G34047.2</i>	Defensin-like family protein	10.49	0.008	530	0.6	0.6	0.3	0.4	0.3	0.6
12	<i>DEFL</i>	<i>AT2G36255.1</i>	Defensin-like family protein	10.60	0.012	313	0.2	0.3	0.0	0.0	0.5	0.5
13	<i>DEFL</i>	<i>AT3G59930.1</i>	Defensin-like family protein	8.71	0.036	512	2.5	0.3	2.0	0.2	1.1	0.5
14	<i>DEFL</i>	<i>AT4G11393.1</i>	Defensin-like family protein	8.50	0.012	372	0.0	0.1	0.0	0.2	0.0	0.2
15	<i>TFL1</i>	<i>AT5G03840.1</i>	Terminal flower 1	-1.48	0.025	91	0.1	0.6	0.5	0.3	0.4	0.4

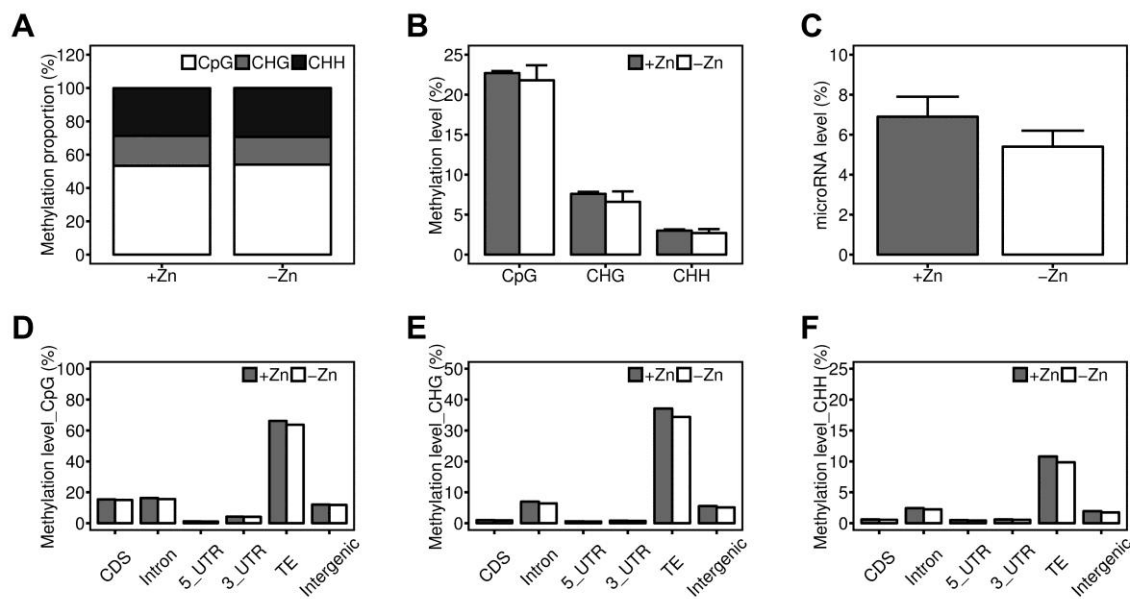


Figure 3: Description of methylation profile. **A**, Relative proportion of CpG, CHG and CHH methylation. **B**, Methylation level of CpG, CHG and CHH under +Zn and -Zn conditions. Data plotted are mean + SD. **C**, microRNA level in the harvested root samples. **D-F**, Methylation level in CDS, intron, 5-UTR, 3-UTR, TE and intergenic region.

Differentially methylated regions induced by Zn deficiency

Next we set out to identify Zn-induced differentially methylated regions (DMRs), by Bioconductor's bsseq package (Hansen et al., 2012). Default settings were carried out to find DMRs. In brief, methylation calls with coverage of at least 2x in at least 2 replicates were included in further analysis. Subsequently, DMRs were eliminated, that did not have at least 3 ^mCs and a mean difference between +Zn and -Zn less than 0.1, at the FDR < 0.025 level. Thereby, 4809 DMRs in CpG, 1701 DMRs in CHG and 547 DMRs in CHH were determined (Fig. 4 B-D). DMRs in the CpG context were mainly located in CDS, TEs and intergenic regions, whereas DMRs in non-CpG contexts occurred predominantly in TEs (Fig.4). Interestingly, most DMRs belonged to the hypomethylated group (lower methylation in -Zn relative to +Zn), indicating the demethylation under -Zn. However, -Zn also recruited new methylation, but those non-CpG

hypermethylation preferentially occurred in TEs rather than in gene body (Fig. 4 C-D). The DMR density across the genes provided a clear landscape that most CpG-DMRs appeared in the gene body, whereas non-CpG DMRs predominantly occurred in flanking regions (Supplementary Fig. S4A-C). Nevertheless, most DMRs were found in TEs, while very few were detected in flanking regions (Supplementary Fig. S4D-F).

Effects of DNA methylation on gene expression

To determine whether genomic DNA methylation affects global gene expression, we divided all transcripts into three classes based on their average expression intensity in the microarray analysis, namely high-expression (top 1/3, N=10709), medium-expression (middle 1/3, N=10709) and low-expression (bottom 1/3, N=10710). As shown in Supporting Fig. S5, average expression density was approximately 10.5 in high-expression genes, 6.8 in medium-expression genes and only 3.0 in low-expression genes. Non-methylated regions were excluded before calculating the average methylation level in different groups, as these regions diluted the methylation level across genes. In general, the methylation level in CpG was much higher than in non-CpG across all genes (Fig. 5 A-C). A slightly higher CpG methylation pattern was detected in high-expression genes, whereas non-CpG methylation was preferentially found in low-expression genes. As expected, +Zn significantly increased the methylation level, irrespective of the expression intensity and the methylation contexts (Fig.5 A-C). This was compatible with the whole-genome methylation profile.

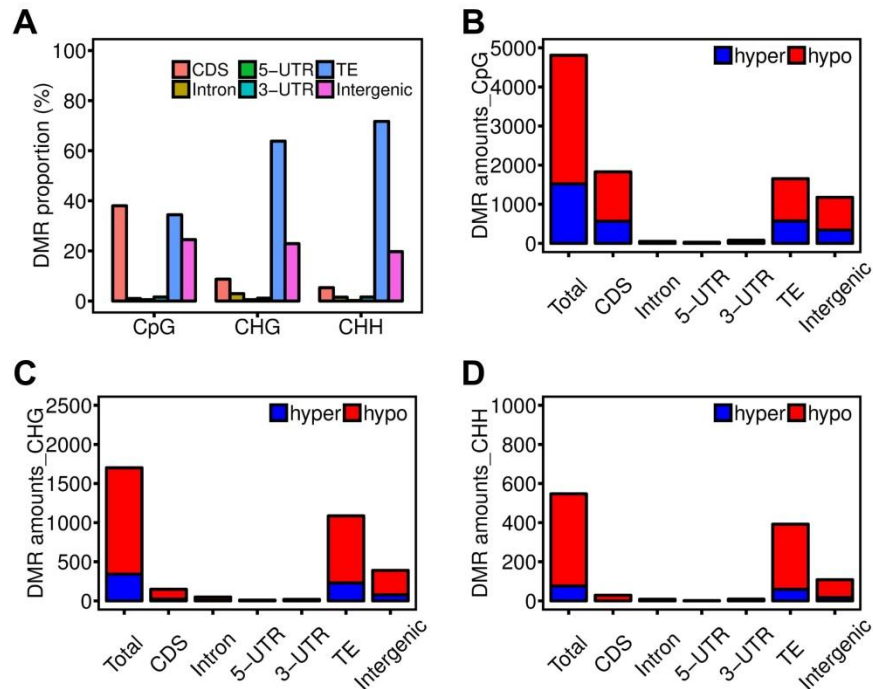


Figure 4: Distribution of differentially methylated regions (DMRs) in different genomic features. **A**, DMR proportion in different genomic features. **B-D**, DMR amounts in different genomic features. Hyper and hypo indicate hypermethylation and hypomethylation in the -Zn relative to the +Zn treatment.

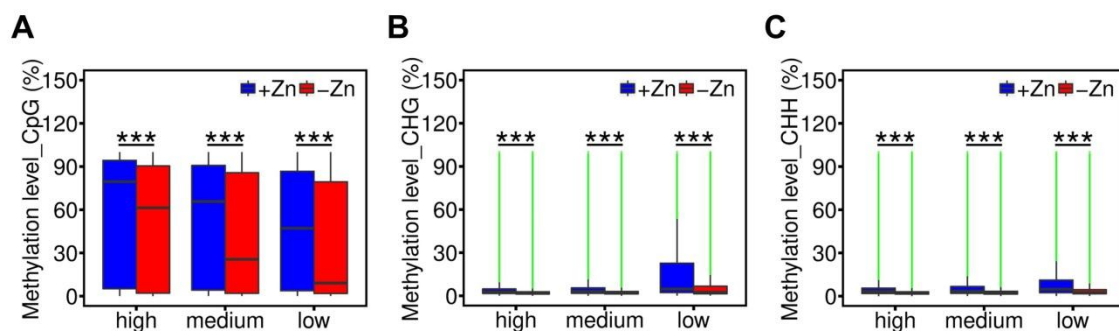


Figure 5: Gene body methylation level in different expressed gene groups in the whole genome. *** indicate significant difference at $p < 0.001$ level. Green lines in **B** and **C** present the deviated values.

A slightly higher CpG methylation pattern was detected in high-expression genes, whereas non-CpG methylation was preferentially found in low-expression genes. As expected, +Zn significantly increased the methylation level, irrespective of the expression intensity and the methylation contexts (Fig.5 A-C). This was compatible with the whole-genome methylation profile.

Next we asked whether methylation and/or differential methylation occurred in Zn-deficiency responsive genes that encode those fifteen transcripts that were identified in the microarray analysis (Table 1). The gene bodies of these DEGs were rarely methylated in all contexts (Table 1). The closest DMRs indicated hypomethylation in nearby regions, but not all of these transcripts overlapped with DMRs (Table 2). Especially the CHH methylation was far distant to these genes. Considering a distance of maximally 3 kb between DMRs and genes that might still be relevant to transcription, upstream hypomethylation in *ZIP1* and *ZIP3*, but downstream hypomethylation was found in *IRT3* and *NAS2*. *PAP27* was the only transcript hypomethylated in upstream and gene body regions. *AT1G34047.2*, located very close to DMRs, was hypermethylated in the CpG context, but hypomethylated in the CHG context. Additionally, the defensin-encoding *DEFL AT4G11393.3*, was hypermethylated in downstream sequences. However, there was no consistent pattern, questioning a causal relationship between DEGs and DMRs. Nevertheless, Zn deficiency tended to erase methylations in or nearby to DEGs.

Then we selected genes that were covered by DMRs, in gene body and 2-kb upstream sequences. Furthermore, we also selected genes that are in 2-kb distance associated to TEs, which were covered by DMRs. For these genes, -Zn induced methylation alterations and transcriptional changes were compared. Surprisingly, there was clearly a lack of correlation between differential methylation and mRNA abundance, irrespective of the ^mC contexts (Fig. 6), indicating that both processes are independent. Moreover, this pattern was also found in the entire genome (Supporting Fig. S6).

Table 2. Closest DMRs to the differentially expressed transcripts.

Transcripts			Closest DMR_CpGs			Closest DMR_CHGs			Closest DMR_CHHs		
Number	Name	AGI code	Type	Location	Distance (bp)	Type	Location	Distance (bp)	Type	Location	Distance (bp)
1	<i>ZIP1</i>	<i>AT3G12750.1</i>	hypo	upstream	1413	hyper	downstream	112111	hypo	downstream	65491
2	<i>ZIP3</i>	<i>AT2G32270.1</i>	hypo	upstream	1612	hypo	upstream	1367	hypo	downstream	69565
3	<i>ZIP4</i>	<i>AT1G10970.1</i>	hypo	downstream	8035	hypo	downstream	117338	hyper	downstream	159313
4	<i>ZIP5</i>	<i>AT1G05300.1</i>	hypo	downstream	22332	hypo	downstream	99594	hypo	upstream	22212
5	<i>ZIP5</i>	<i>AT1G05300.2</i>	hypo	downstream	22442	hypo	downstream	99704	hypo	upstream	22322
6	<i>IRT3</i>	<i>AT1G60960.1</i>	hypo	downstream	1950	hyper	downstream	27221	hypo	downstream	145289
7	<i>NAS2</i>	<i>AT5G56080.1</i>	hypo	downstream	2452	hypo	downstream	35942	hypo	downstream	198989
8	<i>NAS4</i>	<i>AT1G56430.1</i>	hypo	downstream	6882	hyper	upstream	8086	hypo	upstream	52813
9	<i>HMA2</i>	<i>AT4G30110.1</i>	hypo	upstream	46524	hypo	upstream	88708	hypo	upstream	459915

Table 2. Continued.

Transcripts			Closest DMR_CpGs			Closest DMR_CHGs			Closest DMR_CHHs		
Number	Name	AGI code	Type	Location	Distance (bp)	Type	Location	Distance (bp)	Type	Location	Distance (bp)
10	<i>PAP27 AT5G50400.1</i>		hypo	gene body	1217	hypo	upstream	1187	hypo	downstream	113440
11	<i>DEFL AT1G34047.2</i>		hyper	upstream	190	hypo	upstream	557	hypo	upstream	53258
12	<i>DEFL AT2G36255.1</i>		hypo	downstream	10721	hypo	downstream	66379	hyper	upstream	67029
13	<i>DEFL AT3G59930.1</i>		hypo	downstream	18844	hypo	downstream	18792	hypo	upstream	19932
14	<i>DEFL AT4G11393.1</i>		hyper	downstream	20906	hyper downstream	2246		hypo	downstream	86277
15	<i>TFL1 AT5G03840.1</i>		hyper	downstream	52498	hypo	downstream	148868	hypo	upstream	317983

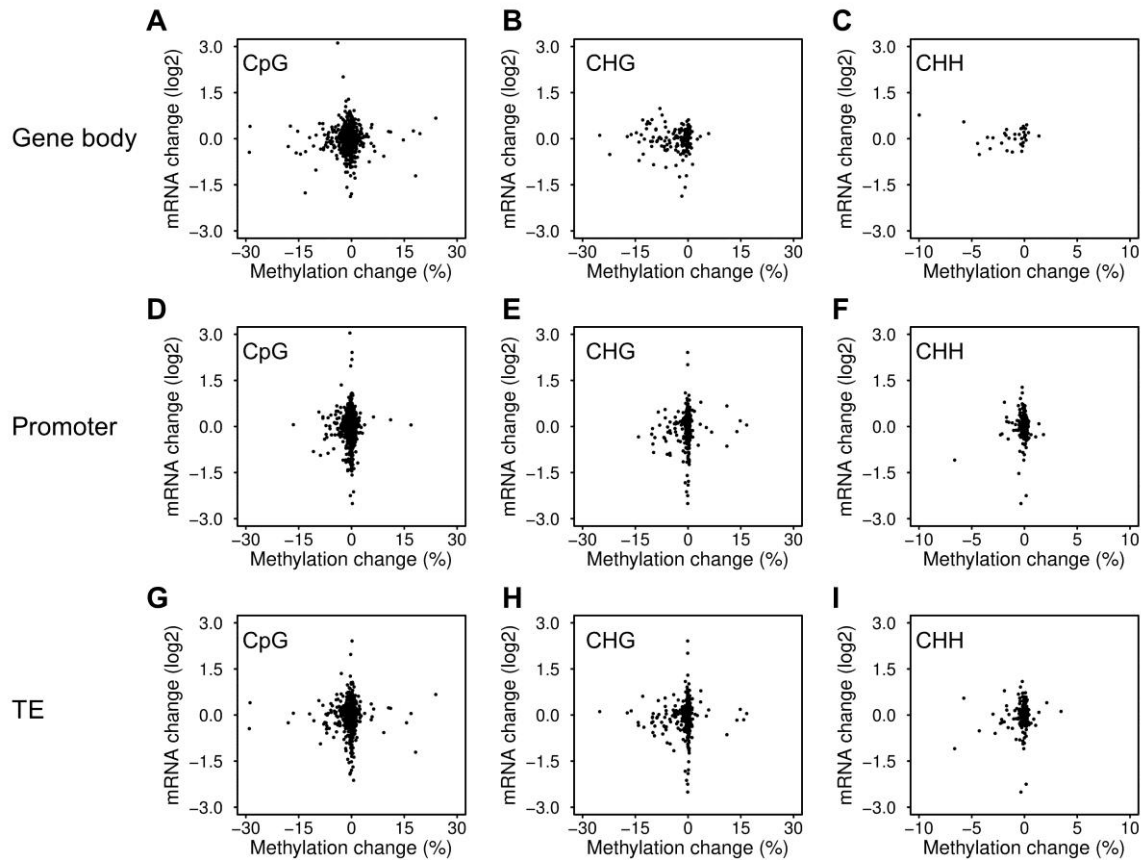


Figure 6: Independence of gene transcription from DNA methylation at DMRs. A-C, Gene body methylation. **D-F,** Promoter methylation. Promoter was defined as 2-kb upstream distance to transcription start site (TSS). **G-I,** Transposable element (TE) methylation. TEs either overlapped with gene bodies, or located at 2-kb upstream distance to gene transcription start sites.

Single-cytosine Methylation in Zn deficiency responsive motif

On account of limited DNA methylation alteration in DEGs, we further analyzed the single-cytosine methylation in Zn deficiency responsive motif (RTGTCGACAY) in promoters, which was previously identified to be bound by transcription factors *BZIP19* and *BZIP23* in response to Zn deficiency (Assunção et al., 2010). This 10 bp motif contains two cytosines, which are CpG and CHH methylation, respectively. By alignment to TAIR10, we found 84 genes contain this motif in their promoters without mismatch, including *ZIP4*, *ZIP5*, *IRT3* and two defensin-like genes (*AT1G34047* and *AT4G11393*), which were identified in microarray analysis (Supporting Table S3). Then 57 of 84 genes

were overlapped with the methylome data due to the sequencing coverage. Methylation level of first cytosine (CpG) was 3.01 in +Zn and 3.06 in -Zn across all these genes, while it was 0.19 and 0.36 for second cytosine (CHH) (Supporting Table S4).

S-adenosyl methionine level in response to Zn deficiency

Due to the unexpected preferential demethylation induced by Zn deficiency, the amounts of S-adenosyl methionine (SAM), the donor of methyl groups, were quantified. However, the SAM level was maintained under Zn deficiency, excluding the possibility that this substrate was limiting in -Zn (Supporting Fig. S7).

Discussions

Plants have developed a number of strategies to adapt to environmental stress. Nutritional deficiency is considered to be a crucial stress for plants. As an essential micronutrient, Zn is involved in vital molecular and metabolic functions (Broadley et al., 2007). However, little is known about DNA methylation or chromatin profile in response to Zn deficiency and its potential impact on transcription. Therefore, we performed a growth experiment with DNA methylation mutants to test whether the Zn status interacts with DNA methylation. Interestingly, we found that Zn deficiency altered plant development in plants lacking non-CpG methylation (*ddc* mutant), but increased the root biomass compared to control conditions (Fig. 1). However, *ros1* mutants showed a similar phenotype as wild type plants (Col-0). This suggested an interaction between Zn and non-CpG methylation, which might target also flower development. Previous studies reported that the *SUPERMAN* gene is silenced by hypermethylation in *SUPERMAN* epigenetic alleles, resulting in an abnormal flower structure compared to wild type (Jacobsen and Meyerowitz, 1997; Ito et al., 2003). Furthermore, *FWA* (*FLOWERING WAGENINGEN*) is a floral repressor; and hypermethylation in promoters of *FWA* inhibits the gene expression in wild type, whereas *fwa-1* mutants showed late flowering due to lack of methylation (Soppe et al., 2000). In addition to flowering regulation, *ddc* mutants presented higher Zn

accumulation in roots compared to the wild type, indicating an interaction between Zn supply and DNA methylation in roots as well. Hence, we further conducted a comprehensive analysis in gene transcription and DNA methylation of the root.

We then established Zn-deficient growth conditions with minimal phenotypic consequences, to reduce secondary developmental effects and focus on the Zn-deficiency response. The *Arabidopsis thaliana* accession Sf-2, which is late flowering and able to produce a higher biomass than Col-0, was therefore selected. After 6 weeks, Zn deficiency-induced necrosis appeared in leaves without changing the whole shoot biomass. $11.1 \mu\text{g g}^{-1}$ of Zn was still accumulated under -Zn conditions, although no additional Zn was supplied, indicating a Zn contamination from the used chemicals. The pots, deionized distilled water or the around $40 \mu\text{g g}^{-1}$ of Zn per seed (Chen et al., 2016) were excluded as contaminants. Nevertheless, Zn-supplied plants accumulated significantly higher Zn. In addition, -Zn stress did not affect other nutrients homeostasis, although Ca and Cu uptake was slightly changed, but both were still sufficient for optimal growth (Fig. 2). Therefore, the abnormal symptoms in -Zn plants were definitely caused by Zn deficiency. Moreover, the transcriptional responses confirmed Zn-deficiency specificity. Surprisingly, only fifteen transcripts were differentially expressed upon Zn deficiency, including the important Zn-deficiency responsive genes *ZIP1*, *ZIP3*, *ZIP4*, *ZIP5*, *IRT3*, *NAS2*, *NAS4*, *HMA2* and *PAP27* (Grotz et al., 1998; Mortel et al., 2006; Wong et al., 2009). Further, several genes encoding defensin-like proteins, previously not transcriptionally up-regulated by Zn-deficiency were among the most differentially regulated genes. Interestingly, defensin-like proteins had been identified in the Zn-deficiency response proteome (Zargar et al., 2014). All these transcripts were up-regulated, to mobilize Zn or increase uptake of Zn. By contrast, *TFL1* was down-regulated under -Zn, potentially indicating an involvement of Zn in the flowering regulation of *Arabidopsis*. Taken together, the ionome and transcriptome data confirmed a Zn-specific effect in the current study.

Previous microarray analysis identified over 300 differentially expressed transcripts in response to Zn deficiency (Mortel et al., 2006). The smaller number of identified genes in this study might be a consequence of the different accession, different growth conditions and the heterogeneity among the three biological replicates. Indeed, using less stringent quality parameters, another 50 transcripts, including additional Zn transporters and carbonic anhydrases, appeared also 4-fold differentially expressed between +Zn and -Zn (Supplemental table S1). On the other hand, the relatively late harvest developmental stage (long days in this study, compared to short days in the previous microarray analysis (Mortel et al., 2006), potentially induced nutrient reallocation to the following reproductive growth. Secco et al. (2015) also found that large amount phosphate-deficiency responsive genes were recovered at 52 days compared to 21 days due to floral transition in rice (Secco et al., 2015).

To date, limited studies have investigated the whole-genome DNA methylation profile upon adverse nutritional stress and potential regulation on transcription (Downen et al., 2012; Dubin et al., 2015; Secco et al., 2015). Secco et al., (2015) recently presented that phosphate deficiency-induced gene expression drove DNA hypermethylation at adjacent TEs to stabilize the genome in rice, but almost not in *Arabidopsis*, implying species-specific mechanisms. However, our study showed that Zn-deficiency impacts on DNA methylation (and vice versa) in *Arabidopsis*. Further, Zn deficiency-induced DMRs were not only enriched in TEs in non-CpG contexts, but also occurred in exons and TEs in CpG contexts (Fig. 4). All these observations implicated a nutrient-specific effect on the DNA methylation response.

DNA methylation plays crucial roles in regulating transcription and alternative splicing (Chan et al., 2005; Zilberman et al., 2007; Law and Jacobsen, 2010; Lev Maor et al., 2015). However, little interaction was established between Zn-induced DMRs and transcriptional responses in the present work. Only seven DEGs were differentially methylated in 3-kb distances to the genomic regions and only in CpG and CHG contexts, whereas most of the *de novo* CHH methylation was not changed by Zn deficiency in or close to DEGs (Table 2). This was

inconsistent with previous findings, where the CHH methylation is described to be the most flexible context to adapt to environmental stress (Downen et al., 2012; Dubin et al., 2015; Secco et al., 2015). The lack of correlation between methylation differences and mRNA changes implied stress-specific effects in plants. On the other hand, it was argued that gene body methylation is a consequence of transcription rather than a cause (Teixeira and Colot, 2009; Inagaki and Kakutani, 2012). Kawakatsu *et al.*, (2016) recently showed that the *Arabidopsis* accession Cvi-0 presented much less methylation, but a similar whole-genome transcription level, in comparison to other accessions (Kawakatsu et al., 2016). Additionally, Secco *et al.*, (2015) suggested that transcriptional changes occur prior to methylation changes in rice as well (Secco et al., 2015). All these assertions demonstrated that transcription does not rely on DNA methylation, and the latter is also strongly determined by specific stresses. Single-cytosine methylation was further analyzed in the 57 genes that contains Zn deficiency motif (RTGTCGACAY) in promoters. Not all 15 DEGs were included in these genes that contains the motif might because of few base-pair mismatches as previously reported (Assunção et al., 2010). Methylation level of these cytosines was also not distinguishable between two Zn treatments (Supporting Table S4). It was recently reported that only 76% (248 of 327) transcription factors shape the *Arabidopsis* epigenome (O'Malley et al., 2016).

Furthermore, due to the general demethylation pattern in Zn deficiency, we also investigated whether the methyl donors were affected by -Zn. In rats, the S-adenosyl methionine level has been reported to be decreased under Zn deficiency, therefore DNA and histones were both hypomethylated under Zn stress (Sharif et al., 2012). However, *Arabidopsis* S-adenosyl methionine level was maintained in Zn deficiency, excluding the possibility of scarce methyl donor effect in the downstream regulation (Supporting Fig. S7).

Altogether, we assumed that Zn deficiency erased DNA methylation in TEs irrespective of the cytosine contexts (Fig. 7). Genic CpG methylation was also removed to adapt to the adverse Zn situation. However, a causal correlation between Zn deficiency responsive genes and DNA methylation appears unlikely.

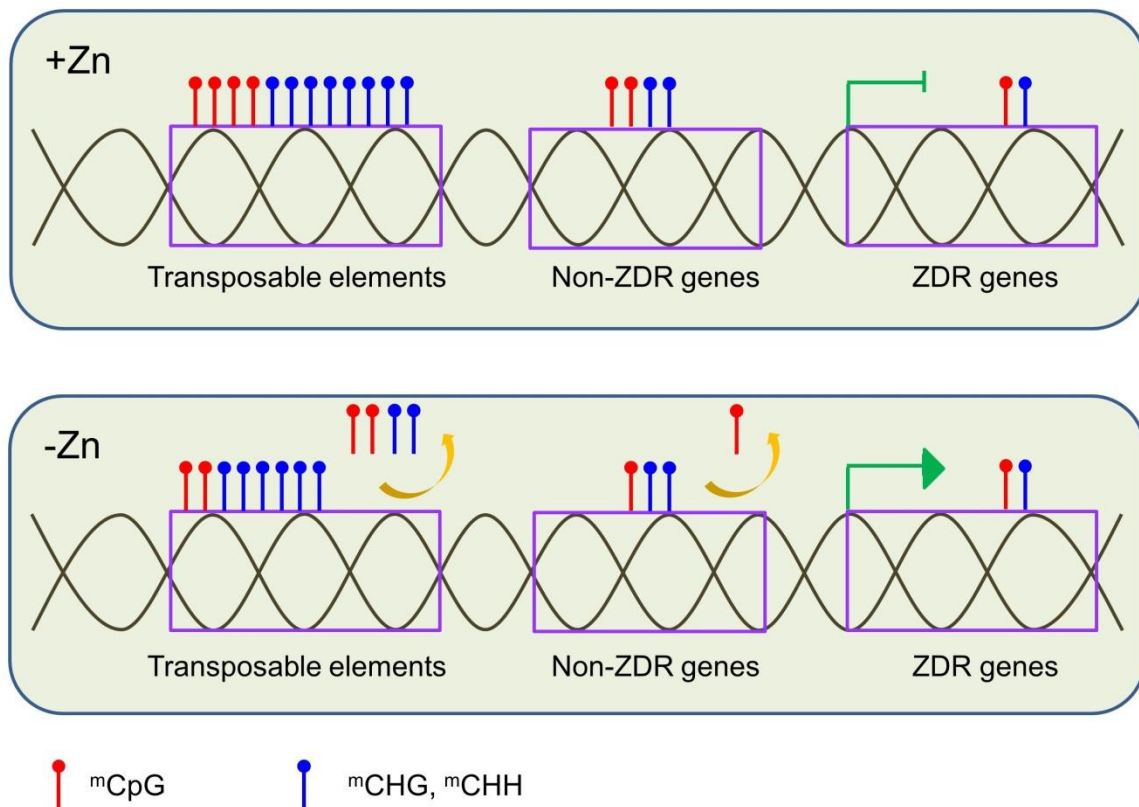


Figure 7: Schematic model of DNA methylation in response to Zn deficiency. Zn deficiency erased DNA methylation in TEs in CpG and non-CpG contexts. Genic CpG methylation of non-ZDR genes was also removed to adapt to the adverse Zn situation. ZDR genes were rarely methylated, and those methylations were not affected by Zn deficiency. ZDR genes represent Zn deficiency responsive genes.

Conclusion

This study presented that Zn deficiency impaired development in *ddc* mutants. Therefore, we further analyzed Zn deficiency-induced DNA methylation and transcriptional changes in roots. Ionome and transcriptome data confirmed the Zn-deficiency effectiveness. Whole-genome bisulfite sequencing was performed to provide insights in the Zn stress-induced methylation profile. However, unlike the phosphate or suboptimal temperature stress, Zn deficiency predominantly erased methylation in TEs in non-CpGs, and also removed CpG methylation in both genic regions and TEs. Unexpectedly, the Zn deficiency-induced demethylation made limited contribution to the transcriptional response. This study suggests that the relationship between stress-induced transcription and methylation was much more complex than previously described.

Experimental Procedures

Plant materials, growth conditions and sample collection

Arabidopsis thaliana accession Col-0 was used in the mutant experiments. *ddc* and *ros1* mutants were in Col-0 background. Another accession Sf-2 was used for all other studies, due to a higher biomass production, beneficial to limit Zn bioavailability in plants. Plants were grown in hydroponic system in a growth chamber in triplicate. A modified Hoagland's solution was supplied, containing 1 mM NH_4NO_3 , 1 mM KH_2PO_4 , 0.5 mM MgSO_4 , 1 mM CaCl_2 , 0.1 mM $\text{Na}_2\text{EDTA-Fe}$, 2 μM ZnSO_4 , 9 μM MnSO_4 , 0.32 μM CuSO_4 , 46 μM H_3BO_3 , 0.016 μM Na_2MoO_4 and with or without 2 μM ZnSO_4 , resulting in +Zn or -Zn conditions. The growth conditions were generally set as: long days (16h light / 8h dark), 22°C light / 20°C dark, 120-140 $\mu\text{mol m}^{-2} \text{s}^{-1}$ and 60% humidity. At 40-days, shoot and root samples were separately harvested with liquid nitrogen, before storing in -80°C for further analysis.

Ionome analysis

Harvested samples were dried at 60 °C before grinding. Around 0.5 g ground material was digested with 5 ml 69 % HNO₃ and 4 ml 30 % HCl for 1 hour. Afterwards, samples were microwaved at 170 °C for 25 min and followed by 40 min at 200 °C. The extract was measured by ICP (Inductively Coupled Plasma), to determine concentrations of P, K, Ca, Mg, B, Zn, Cu, Fe, Mn, Mo and Na. Additionally, approximately 5 mg ground material was used to quantify N and S concentrations by Elemental Analyser (HEKAteck GmbH, Germany).

Total RNA isolation and transcriptome analysis

Total RNA of 40-days-old root samples was extracted using the innuPREP Plant RNA Kit (Analytik Jena, Germany). Each treatment contained three independent biological replicates. All RNA samples were sent to OakLabs (Germany) for transcriptome analysis on single-channel microarrays. Raw data analysis was performed using Bioconductor's limma package (Ritchie et al., 2015). Differentially expressed genes were calculated after background correction, data normalization and linear modelling. The resulting p values were adjusted by the Benjamini-Hochberg approach to control the false discovery rate (Benjamini and Hochberg, 1995). Genes were considered to be significantly different expressed, if the adjusted p value < 0.05.

Genomic DNA extraction and bisulfite sequencing

Genomic DNA of 40-days-old root samples was extracted using the DNeasy Plant Mini Kit (Qiagen, Germany) in triplicate for each treatment. DNA samples were sent to Beijing Genomics Institute (BGI, China) for whole-genome bisulfite sequencing. Briefly, the MethylC-Seq library was constructed and sequenced with 100 bp paired-end, using Illumina Hiseq2000.

DNA methylation data processing

Raw data was filtered to remove the low-quality reads, including three types: adapter sequences, N base number over 10%, number of low-quality base (less than 20) over 10%. Clean data was mapped to TAIR 10 reference genome (The

Arabidopsis Information Resource, <http://www.arabidopsis.org/>), using Bismark (Krueger and Andrews, 2011). Default settings were carried out except that the *score_min* was set as *L,0,-0.6*, before removing PCR duplicates with SAMtools (Li et al., 2009). *Bismark_methylation_extractor* was conducted to call the cytosine methylation in CpG, CHG and CHH contexts. Then 5 bp and 3 bp bias bases were removed from 5'-end and 3'-end respectively, according to the M-bias plots produced by the Bismark methylation extractor.

DMR calling was performed using BSmooth in Bioconductor's bsseq package with default settings (Hansen et al., 2012). Briefly, bedGraph output files were smoothed, before computing t-statistics. Only keeping CpGs/CHGs/CHHs where at least 2 replicates in each treatment have at least coverage of 2x. Then dmrFinder was used to find DMRs. DMRs were filtered out, which did not cover at least 3 CpGs/CHGs/CHHs or showed a mean difference less than 0.1. The *qcutoff* and *maxGap* was set as 0.025 and 300 bp.

DMRs were mapped to genomic elements using TAIR10 annotations. Positions and regions were hierarchically assigned to annotated features in the order CDS > intron > 5-UTR > 3-UTR > transposable element > intergenic region. Intergenic regions were defined as those that were neither annotated with gene bodies nor transposable elements. The mapping was performed using bedtools (Quinlan and Hall, 2010). 2-kb upstream sequences of gene bodies were also overlapped with DMRs to indicate promoter regions.

Quantitative RT-PCR analysis

Around 1 µg of total RNA was used to synthesis the cDNA library using the QuantiTect Reverse Transcription Kit (Qiagen, Germany). Gene-specific primes for qRT-PCR were designed according to the *Arabidopsis* genome sequence information of TAIR 10 (<https://www.arabidopsis.org/>) and Primer-BLAST (<http://www.ncbi.nlm.nih.gov/tools/primer-blast/>). Additionally, primer quality was controlled using PCR Primer Stats (http://www.bioinformatics.org/sms2/pcr_primer_stats.html). Primers were ordered from Invitrogen (United States) and listed in the Supplemental Table S3.

Chapter I

For the PCR procedure, 15 µl reactions were carried out, containing 6 µl 20x diluted cDNA, 7.5 µl SYBR Green Supermix (KAPA Biosystems, United States), 0.3 µl forward primers, 0.3 µl reverse primers and 0.9 µl RNase-free H₂O. The reactions were conducted in 384-well plates in RT-PCR systems (Bio-Rad, United States). The standard protocol was set as: 3 min at 95 °C, followed by 44 cycles of 3 sec at 95 °C, 25 sec at 60 °C, and then 5 sec at 65 °C for providing the melt curve. Two reference genes, *SAND* (*At2g28390*) and *PDF2* (*At1g13320*), were used. Reactions were performed in 3 technical replicates and 3 biological replicates. Relative transcript levels were calculated with the 2- $\Delta\Delta$ CT method by the Bio-Rad software (Livak and Schmittgen, 2001).

MicroRNA extraction and quantification

MicroRNA was extracted using innuPREP Micro RNA Kit (Analytik Jena, Germany), followed by a quantification using the Small RNA Analysis Kit in Agilent 2100 Bioanalyzer (Agilent, United States), according to the manual instructions.

S-adenosyl methionine determination

The S-adenosyl methionine level was determined with Bridge-It® S-Adenosyl Methionine (SAM) Fluorescence Assay Kit (Mediomics, United States), following the manufacturer's instruction. Briefly, 0.3 g frozen ground root samples were shaken in soluble protein extraction buffer at 4 °C for 30 minutes, before spinning at 12,000 rpm for 10 minutes. 30 µl of the supernatant was transferred to 30 µl of CM Buffer (included in the kit) and incubated at 24 °C for 1 hour. Suspension was centrifuged at 10,000 g in 4 °C for 5 min, and the supernatant was collected to measure the fluorescence. The excitation and emission absorbance were 485 nm and 655 nm, respectively.

Statistical analysis

Data analysis, graphs and statistics were done using R (<https://www.r-project.org/>). The significant difference of mean for all traits in this study was

performed by t-test. Multiple comparisons were conducted using Tukey HSD method.

Acknowledgments

We thank Dr. Sascha Laubinger (Tübingen, Germany) for *ddc* and *ros1* mutant seeds. We also thank the China Scholarship Council for support.

Author contributions

X.C. and U.L. conceived the experiment; X.C., B.S. and J.M. performed the experimental work; X.C., B.S., J.M. and U.L. analyzed data; X.C., B.S., J.M. and U.L. wrote the paper.

Competing interests

The authors declare no competing financial interests.

References (part 8 References)

Supporting tables and figures

Supporting Table S1: Full list of microarray evaluation (data not shown).

Supporting Table S2: Description of whole-genome bisulfite sequencing.

	Clean reads	Unique mapping rate (%)	Multiple mapping rate (%)	Bisulfite non- conversion rate (%)	Average coverage
+Zn_R1	37491819	31.7	5.8	0.4	19.0
+Zn_R2	36702677	28.8	5.7	0.4	16.9
+Zn_R3	30004414	15.5	2.9	0.3	7.5
-Zn_R1	44103843	39.0	7.3	0.6	27.6
-Zn_R2	47999999	37.2	4.9	0.5	28.6
-Zn_R3	43313476	41.3	7.8	0.5	28.7
Average	39936038	32.3	5.7	0.5	21.4

Supporting Table S3: 84 genes that contain Zn deficiency responsive motif in promoters. (red indicates the gene was changed in microarray analysis)

Nr.	AGI code	Nr.	AGI code	Nr.	AGI code	Nr.	AGI code
1	AT1G02700	22	AT1G34047	43	AT3G08960	64	AT4G20470
2	AT1G03190	23	AT1G47810	44	AT3G09240	65	AT4G20730
3	AT1G05300	24	AT1G50550	45	AT3G09250	66	AT4G22720
4	AT1G05340	25	AT1G60960	46	AT3G10815	67	AT4G38050
5	AT1G08010	26	AT1G60960	47	AT3G10820	68	AT4G39795
6	AT1G10970	27	AT1G63810	48	AT3G11160	69	AT5G02090
7	AT1G12640	28	AT1G64405	49	AT3G16730	70	AT5G02100
8	AT1G16858	29	AT1G65907	50	AT3G19120	71	AT5G04420
9	AT1G16860	30	AT1G77920	51	AT3G26150	72	AT5G14740
10	AT1G17340	31	AT1G80420	52	AT3G45460	73	AT5G18170
11	AT1G23330	32	AT2G05020	53	AT3G50610	74	AT5G23350
12	AT1G24260	33	AT2G15970	54	AT3G59068	75	AT5G26770
13	AT1G24800	34	AT2G22760	55	AT4G04990	76	AT5G29041
14	AT1G24881	35	AT2G24440	56	AT4G11393	77	AT5G41570
15	AT1G25055	36	AT2G26200	57	AT4G13840	78	AT5G41600
16	AT1G25150	37	AT2G32800	58	AT4G14670	79	AT5G44750
17	AT1G25211	38	AT2G34250	59	AT4G16144	80	AT5G51870
18	AT1G27840	39	AT2G45920	60	AT4G16450	81	AT5G51880
19	AT1G31260	40	AT2G46600	61	AT4G16610	82	AT5G62160
20	AT1G31270	41	AT2G47060	62	AT4G18650	83	AT5G62990
21	AT1G32600	42	AT3G01500	63	AT4G20460	84	AT5G63380

Supporting Table S4: Single-cytosine methylation level of 57 genes that contain Zn deficiency responsive motif in promoters.

Cytosine 1_CpG				
AGI	Chromosome	Coordinate	Methylation_+Zn	Methylation_-Zn
AT1G03190	chr1	775132	0	0
AT1G05300	chr1	1548677	0	0
AT1G10970	chr1	3667175	0	0
AT1G16858	chr1	5767231	0	0
AT1G16860	chr1	5767231	0	0
AT1G17340	chr1	5933215	0	0
AT1G23330	chr1	8282070	4.76190476	0
AT1G24260	chr1	8596650	0	0
AT1G32600	chr1	11794659	0	0
AT1G34047	chr1	12391296	0	4.16666667
AT1G47810	chr1	17603369	6.66666667	0
AT1G60960	chr1	22447222	0	0
AT1G60960	chr1	22447320	0	0
AT1G63810	chr1	23676540	0	0
AT1G64405	chr1	23923348	0	0
AT1G65907	chr1	24519835	0	0
AT1G77920	chr1	29298138	0	0
AT1G80420	chr1	30239473	0	0
AT2G05020	chr2	1769592	79.54545455	88.38383838
AT2G15970	chr2	6949897	0	0
AT2G22760	chr2	9677164	0	0
AT2G26200	chr2	11151999	0	0
AT2G32800	chr2	13915619	0	0
AT2G34250	chr2	14461893	0	3.33333333
AT2G45920	chr2	18898951	0	0
AT2G46600	chr2	19135646	0	0
AT2G47060	chr2	19335058	0	0
AT3G01500	chr3	198690	0	0
AT3G10815	chr3	3387064	0	0
AT3G10820	chr3	3387063	0	0
AT3G11160	chr3	3497307	0	0
AT3G16730	chr3	5699776	0	0
AT3G19120	chr3	6611603	0	1.11111111
AT3G45460	chr3	16680751	2.56410256	0
AT3G50610	chr3	18781099	0	0

Supporting Table S4: Continued

Cytosine 1_CpG				
AGI	Chromosome	Coordinate	Methylation_+Zn	Methylation_-Zn
<i>AT3G59068</i>	chr3	21831961	0	0
<i>AT4G13840</i>	chr4	8017065	11.11111111	0
<i>AT4G14670</i>	chr4	8409829	0	0
<i>AT4G16450</i>	chr4	9279830	0	0
<i>AT4G16610</i>	chr4	9355994	0	0
<i>AT4G20460</i>	chr4	11033250	0	0
<i>AT4G20470</i>	chr4	11033250	0	0
<i>AT4G20730</i>	chr4	11121284	0	0
<i>AT4G38050</i>	chr4	17872629	0	0
<i>AT4G39795</i>	chr4	18466116	0	2.56410256
<i>AT5G04420</i>	chr5	1250454	0	0
<i>AT5G18170</i>	chr5	6005607	0	0
<i>AT5G23350</i>	chr5	7860270	0	0
<i>AT5G29041</i>	chr5	11101607	52.77777778	68.25396825
<i>AT5G41570</i>	chr5	16623940	0	0
<i>AT5G41600</i>	chr5	16635499	0	0
<i>AT5G44750</i>	chr5	18051728	0	0
<i>AT5G51870</i>	chr5	21088792	0	0
<i>AT5G62160</i>	chr5	24959944	0	3.7037037
<i>AT5G62990</i>	chr5	25276569	11.11111111	0
<i>AT5G63380</i>	chr5	25390547	0	0

Supporting Table S4: Continued

Cytosine 2_CHH				
AGI	Chromosome	Coordinate	Methylation_+Zn	Methylation_-Zn
<i>AT1G03190</i>	chr1	775135	0	0
<i>AT1G05300</i>	chr1	1548674	0	0
<i>AT1G10970</i>	chr1	3667172	0	0
<i>AT1G16858</i>	chr1	5767234	0	0
<i>AT1G16860</i>	chr1	5767234	0	0
<i>AT1G17340</i>	chr1	5933218	0	0
<i>AT1G23330</i>	chr1	8282067	0	0
<i>AT1G24260</i>	chr1	8596647	0	0
<i>AT1G32600</i>	chr1	11794662	0	0
<i>AT1G34047</i>	chr1	12391293	0	0

Supporting Table S4: Continued

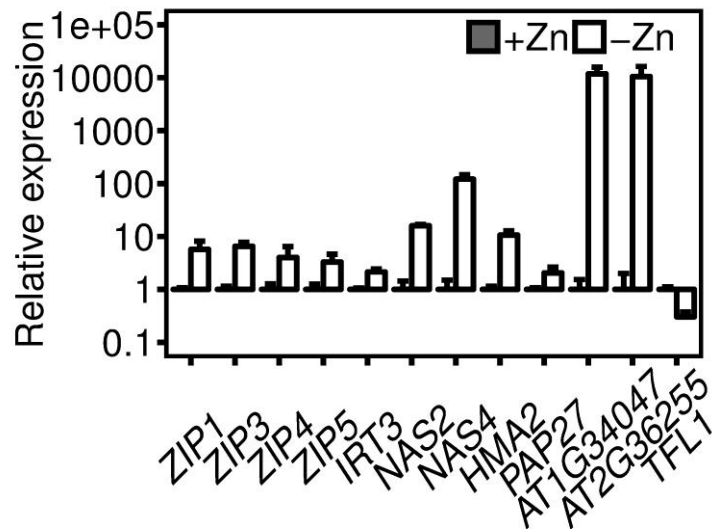
Cytosine 2_CHH				
AGI	Chromosome	Coordinate	Methylation_+Zn	Methylation_-Zn
<i>AT1G47810</i>	chr1	17603372	0	3.50877193
<i>AT1G60960</i>	chr1	22447219	0	0
<i>AT1G60960</i>	chr1	22447317	0	1.75438596
<i>AT1G63810</i>	chr1	23676537	0	0
<i>AT1G64405</i>	chr1	23923351	0	0
<i>AT1G65907</i>	chr1	24519838	0	0
<i>AT1G77920</i>	chr1	29298141	0	0
<i>AT1G80420</i>	chr1	30239470	0	0
<i>AT2G05020</i>	chr2	1769595	0	1.11111111
<i>AT2G15970</i>	chr2	6949900	0	0
<i>AT2G22760</i>	chr2	9677167	0	0
<i>AT2G26200</i>	chr2	11152002	11.11111111	0
<i>AT2G32800</i>	chr2	13915622	0	0
<i>AT2G34250</i>	chr2	14461896	0	0
<i>AT2G45920</i>	chr2	18898954	0	0
<i>AT2G46600</i>	chr2	19135649	0	0
<i>AT2G47060</i>	chr2	19335055	0	0
<i>AT3G01500</i>	chr3	198687	0	0
<i>AT3G10815</i>	chr3	3387061	0	3.33333333
<i>AT3G10820</i>	chr3	3387066	0	0
<i>AT3G11160</i>	chr3	3497304	0	0
<i>AT3G16730</i>	chr3	5699773	0	0
<i>AT3G19120</i>	chr3	6611600	0	0
<i>AT3G26150</i>	chr3	9567811	0	0
<i>AT3G45460</i>	chr3	16680748	0	0
<i>AT3G59068</i>	chr3	21831964	0	0
<i>AT4G13840</i>	chr4	8017062	0	0
<i>AT4G14670</i>	chr4	8409832	0	0
<i>AT4G16450</i>	chr4	9279833	0	0
<i>AT4G16610</i>	chr4	9355991	0	0
<i>AT4G20460</i>	chr4	11033247	0	0
<i>AT4G20470</i>	chr4	11033247	0	0
<i>AT4G20730</i>	chr4	11121281	0	0
<i>AT4G38050</i>	chr4	17872626	0	0
<i>AT4G39795</i>	chr4	18466119	0	0

Supporting Table S4: Continued

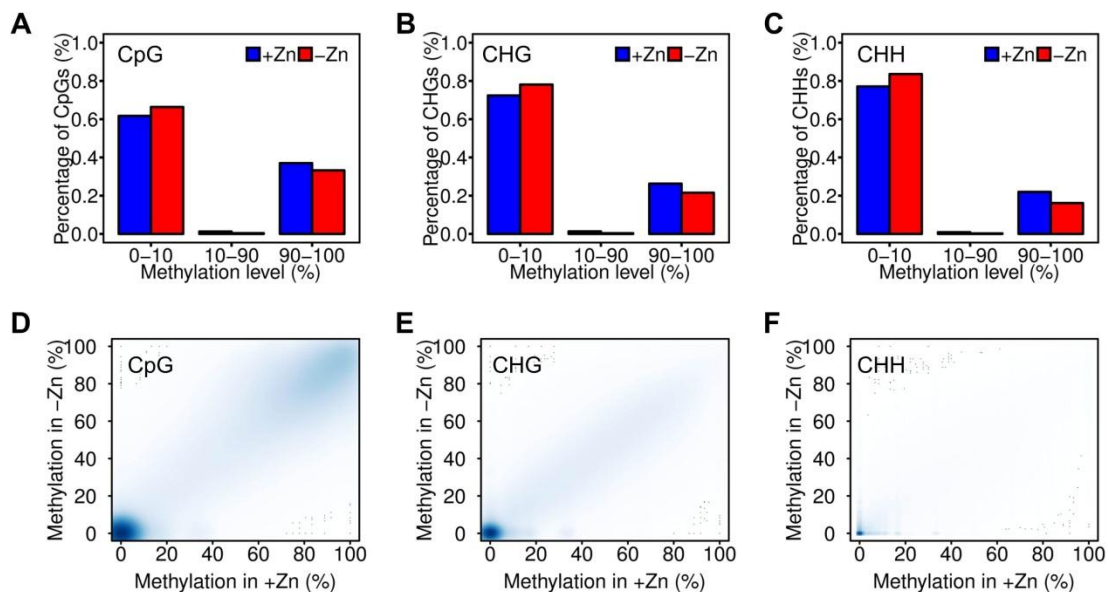
Cytosine 2_CHH				
AGI	Chromosome	Coordinate	Methylation_+Zn	Methylation_-Zn
<i>AT5G02100</i>	chr5	412533	0	4.76190476
<i>AT5G04420</i>	chr5	1250451	0	0
<i>AT5G18170</i>	chr5	6005610	0	0
<i>AT5G23350</i>	chr5	7860267	0	0
<i>AT5G29041</i>	chr5	11101604	0	4.76190476
<i>AT5G41570</i>	chr5	16623943	0	0
<i>AT5G41600</i>	chr5	16635502	0	0
<i>AT5G44750</i>	chr5	18051731	0	0
<i>AT5G51870</i>	chr5	21088789	0	0
<i>AT5G62160</i>	chr5	24959947	0	0
<i>AT5G62990</i>	chr5	25276572	0	0
<i>AT5G63380</i>	chr5	25390544	0	1.2345679

Supporting Table S5: Primers used for qRT-PCR in this study.

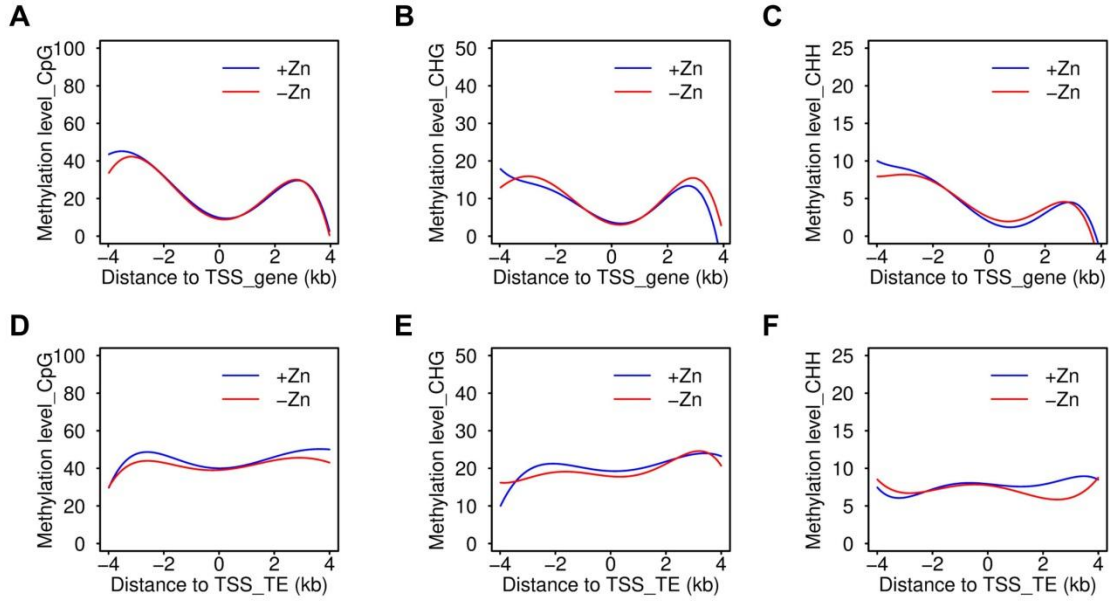
Gene	Primer orientation	Primer sequence
<i>ZIP1</i>	Forward	5'-TGGATGTTTTTCGGCAACAACT -3'
	Reverse	5'-CGCTTTCTCTGCTTCGTCTTG-3'
<i>ZIP3</i>	Forward	5'-CCTCCGTTGACTCCGAGAAG -3'
	Reverse	5'-ATTCCCAACTCCAATACCTGTGC -3'
<i>ZIP4</i>	Forward	5'-GATCTTCGTGCGATGTTCTTTGG -3'
	Reverse	5'-TGAGAGGTATGGCTACACCAGCAGC-3'
<i>ZIP5</i>	Forward	5'-TGAGATAAATACATCGATCACTCCC-3'
	Reverse	5'-CACTCGCATTTAGACTCGCC-3'
<i>IRT3</i>	Forward	5'-TCTCTCAGCAACAGAGTCCAT-3'
	Reverse	5'-GACGGTTCCTGCCAATGAGT-3'
<i>NAS2</i>	Forward	5'-CGGTCCGATGCCACTTACTT -3'
	Reverse	5'-TTTGAAGCGAGTGTGTTGGC -3'
<i>NAS4</i>	Forward	5'-TCGGATCTCGCGTGTAAGT-3'
	Reverse	5'-TTAGCACCTGCGAACTCCTC -3'
<i>HMA2</i>	Forward	5'-TACTCTCCCTTCCGTTGGC -3'
	Reverse	5'-GCTCCCACGGTTACAACAAC-3'
<i>PAP27</i>	Forward	5'-TCCTTTGCCCTCTTCACTGG -3'
	Reverse	5'-ACGGTCATCTCGTCCCATT -3'
<i>AT1G34047</i>	Forward	5'-TGTGCTGGACGTGTTGAAGT -3'
	Reverse	5'-TGTCTCACACGGAATGGAAG -3'
<i>AT2G36255</i>	Forward	5'-TTCTAATGGACTCCCAAAGGC -3'
	Reverse	5'-ACAGTGCCTCTCGTTGTCTT -3'
<i>TFL1</i>	Forward	5'-ACACCTGCACTGGATCGTTAC -3'
	Reverse	5'-GCTTGGCCTTGGCAATTCAT -3'
<i>SAND</i>	Forward	5'-AACTCTATGCAGCATTTGATCCACT-3'
	Reverse	5'-TGATTGCATATCTTTATCGCCATC-3'
<i>PDF2</i>	Forward	5'-TAACGTGGCCAAAATGATGC-3'
	Reverse	5'-GTTCTCCACAAC^CGCTTGGT-3'



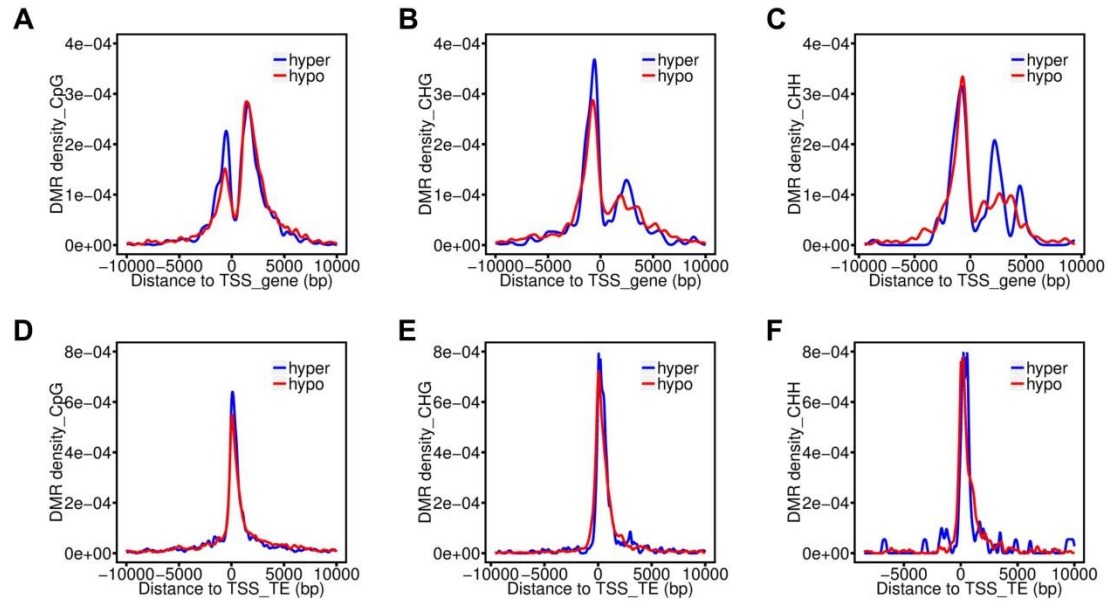
Supporting Figure S1: Relative transcript levels of the differentially expressed genes identified in microarray analysis. Transcript levels in +Zn was normalized to 1.



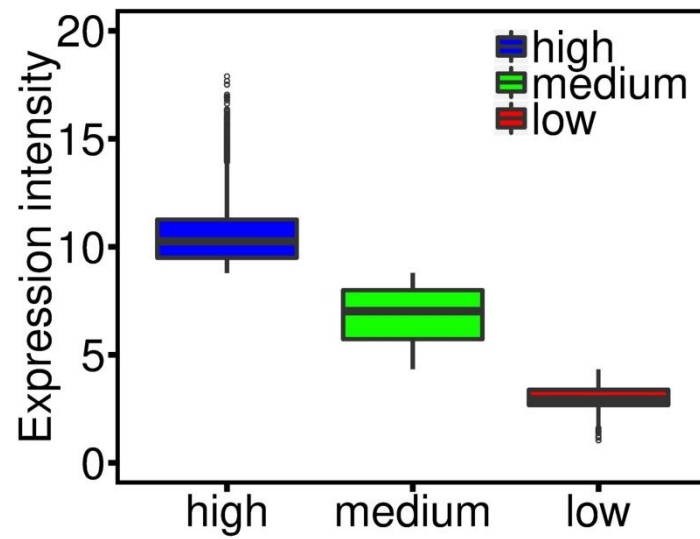
Supporting Figure S2: Percentage of methylation, and the correlation between +Zn and -Zn treatment. A-C, Percentage of methylation level enriched in either 0-10% or 90-100%. **D-F,** Correlation of methylation level between +Zn and -Zn treatment.



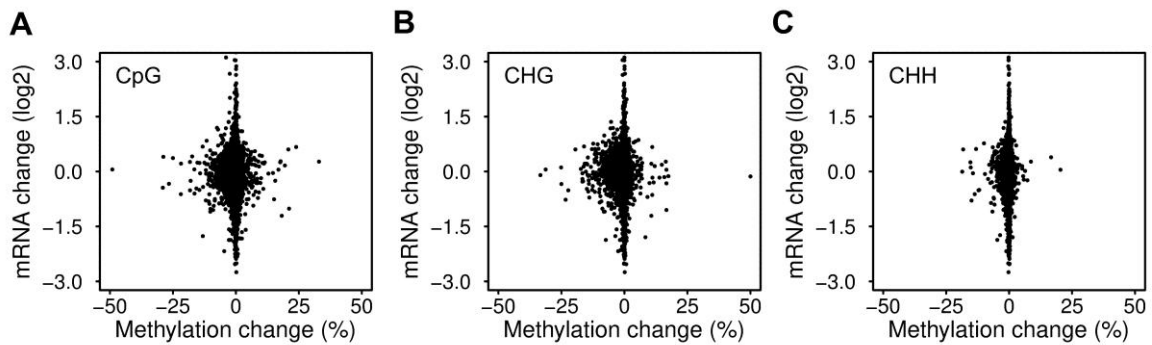
Supporting Figure S3: Description of methylation profile across genes and TEs. A-C, Methylation level across transcription start site (TSS) of genes. **D-F,** Methylation level across transposon start site (TSS) of TEs.



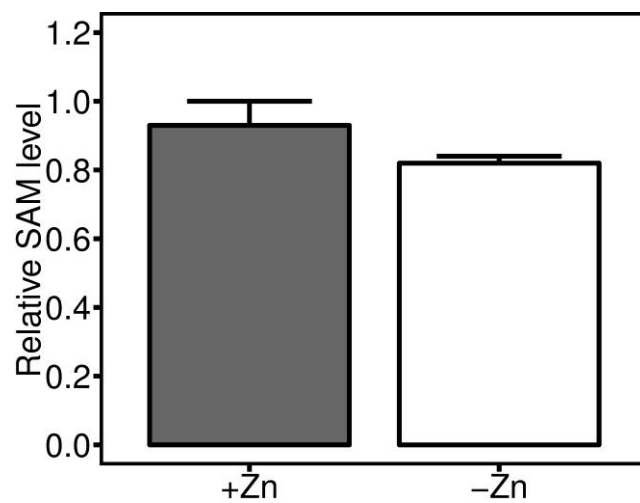
Supporting Figure S4: Description of DMR distribution across genes and TEs. A-C, DMR distribution across transcription start site (TSS) of genes. **D-F,** DMR distribution across transposon start site (TSS) of TEs. Hyper and hypo indicate hypermethylation and hypomethylation in the -Zn relative to the +Zn treatment.



Supporting Figure S5: Expression density of high-, medium- and low-expression genes.



Supporting Figure S6: Relationship of gene transcription and DNA methylation in the whole genome.



Supporting Figure S7: Relative SAM level in roots. SAM: S-adenosyl methionine.

5 Chapter II

Zinc controls leaf size by promotion of *FLOWERING LOCUS T* in early-flowering *Arabidopsis thaliana*.

Xiaochao Chen and Uwe Ludewig

Institute of Crop Science, Nutritional Crop Physiology, University of Hohenheim, Fruwirthstr. 20, 70593 Stuttgart, Germany

Abbreviations: DAS: days after sowing, FDR: false discovery rate, GWA: genome-wide association, MAC: minor allele count, SNP: single nucleotide polymorphism, Zn: zinc

Abstract

Plant growth is generally limited if an essential element is insufficiently available in soil. However, a subset of *Arabidopsis* accessions, including Columbia (Col-0), produced larger rosettes in soil low in Zn than in Zn-amended soil. Vegetative growth promotion by Zn deficiency was genome-wide associated with flowering genes, including the key flowering integrator *FLOWERING LOCUS T* (*FT*). Both in early and late-flowering genotypes, Zn deficiency inhibited *FT* expression, but in certain early-flowering accessions, Zn deficiency promoted the rosette size. This was overcome in a *loss-of-function* mutant of *FT*, but not in mutants promoting early flowering. The promotion of leaf size induced by Zn deficiency temporally coincided with the delayed transition to flowering, followed by a gradual increase in cell divisions. Interestingly, the leaf promotion by Zn deficiency was not observed in environmental conditions that repressed *FT* and delayed flowering. Our results uncover an unusual vegetative biomass increase under nutrient deficiency that masks the full genotypic yield potential because of Zn-dependence of early flowering.

Keywords: micronutrients, genome-wide association, candidate genes, nutrition, flowering, rosette size, zinc, vegetative growth, cell proliferation

Introduction

The appropriate decision for flowering in annual plants is crucial for their lifespan and under very complex genetic control, with over 360 genes implicated (Fornara et al., 2010; Bouché et al., 2016). The transition to flowering depends on several endogenous and environmental signals in *Arabidopsis thaliana*. Several flowering pathways were identified, such as photoperiod, temperature, vernalization, gibberellin, sugar pathways (Searle and Coupland, 2004; Fornara et al., 2010; Capovilla et al., 2014; Bouché et al., 2016). The flowering time of accessions in natural environments and the underlying genetic loci drastically differ in greenhouse conditions (Brachi et al., 2010). Flowering signals converge in the activation of the *FLOWERING LOCUS T (FT)* gene in source leaves, its translated gene product (florigen) is phloem mobile and is translocated to the shoot apical meristem, where *FT* dimerizes with the transcription factor *FLOWERING LOCUS D (FD)* to activate another central integrator, *SUPPRESSOR OF OVEREXPRESSION OF CONSTANS 1 (SOC1)*. This terminates the vegetative fate of the meristem and initiates flower development (Corbesier et al., 2007; Jaeger and Wigge, 2007; Mathieu et al., 2007; Notaguchi et al., 2008).

Low nutrient levels promote flowering in *Arabidopsis* and the ornamental plant *Pharbitis nil*, where it correlated with elevated *FT* expression (Kolář and Seňková, 2008; Wada et al., 2010). The macronutrients nitrate and phosphate act in an antagonistic way, as nitrate deficiency promotes and low phosphate delays flowering in *Arabidopsis* (Kant et al., 2011). At higher concentrations, nitrate promotes flowering independent of the phytohormone gibberellin, which integrates several environmental stimuli and acts downstream of other known floral induction pathways (Marín et al., 2010). Flowering is also promoted by mineral stress (50 μ M cadmium, toxic for *Arabidopsis*) via up-regulation of

CONSTANS (CO) and *FT* (Wang et al., 2012), but the micronutrient zinc (Zn) has not been associated with flowering. Zn is essential for plant growth and development (Marschner, 2012), but in many natural habitats and crop production systems its availability is low, often as a result of high CaCO₃ content and high pH. This renders many food products low in Zn, causing malnutrition in humans (Cakmak, 2007). In *Arabidopsis*, over 2000 Zn-related genes, primarily with catalytic and transcriptional regulator activity require Zn and deficiency leads to abnormal leaf and seed growth (Broadley et al., 2007; Talukdar and Aarts, 2007). Zn-responsive key genes and transporters involved in Zn uptake and translocation have been reported using molecular and genetic tools (Sinclair and Krämer, 2012). *ZIP* (*ZRT*, *IRT-LIKE PROTEIN*) gene family is the important metal transporter family in transporting several cations, including Zn, iron (Fe) and Manganese (Mn); and *Arabidopsis* contains 15 *ZIP* genes (Guerinot, 2000). Among them, *ZIP1* to *ZIP5*, *ZIP9* to *ZIP12* and *IRT3* were highly expressed in Zn deficiency (Grotz et al., 1998; Mortel et al., 2006; Krämer et al., 2007; Lin et al., 2009).

Here, we were interested in how *Arabidopsis* accessions perform in low Zn and Zn-amended soil-sand mixtures and quantified the rosette size of 168 accessions. Unexpectedly, Zn deficiency promoted vegetative growth in some early-flowering accessions. Meanwhile Zn deficiency delayed flowering time, followed by rosette growth promotion relative to control condition. Genetic evidence suggests that flowering via *FT* was crucial for Zn-dependent vegetative regulation.

Results and discussion

Natural variation of rosette size with two different levels of Zn

To explore the natural variation of plant growth in response to low Zn soil, 168 *Arabidopsis thaliana* accessions were grown in a fertilized soil-sand mix without (-Zn) or with added Zn (+Zn) in the greenhouse. The set of accessions included six main populations (Central Europe, Northern Europe, Iberian Peninsula,

Mediterranean, Central Asia and North America) and three small populations (Cape Verde, Canary Islands and Japan) (Supplementary Fig. S1, Supplementary Table S1) (Stetter et al., 2015; Chen et al., 2016).

There was substantial natural variation in the vegetative shoot growth and rosette size among these accessions in +Zn and -Zn, which represent Zn sufficiency and Zn deficiency conditions, respectively (Fig. 1, A and B). The rosette diameter, a proxy for the maximal vegetative leaf length, ranged from 1.3 cm to 12.6 cm in +Zn, with a distribution peak of around 10 cm. In -Zn, the rosette size ranged from 2.3 cm to 9.6 cm, with the majority of accessions having a rosette of around 7.5 cm (Fig. 1D; Supplementary Table S2). One-way ANOVA indicated that significant genetic differences were observed among accessions ($p < 2e-16$ and $p < 2e-16$), in both conditions (Supplementary Table S3). Broad-sense heritability of rosette size was 0.69 for +Zn, but only 0.38 for -Zn (Supplementary Table S2). The lower heritability in -Zn contrasted the large environment x genetic interaction in +Zn. As expected, the rosette size in -Zn highly correlated with that in +Zn ($p < 2.5e-8$), as the leaf size is majorly controlled genetically. However, the 168 accessions could be divided into two groups based on their contrasting effect of Zn on the rosette size (Fig. 1E). Most genotypes had reduced rosette diameter in -Zn, as expected for growth depression resulting from Zn limitation. Whereas the remaining genotypes had a larger rosette diameter in -Zn compared to +Zn, suggesting that other factors controlled vegetative growth under +Zn for these accessions.

As a measure of how the different accessions responded to Zn deficiency, we calculated the Zn sensitivity of the rosette size $[(+Zn) - (-Zn)] * 100 / +Zn$, a relative measure of the reduction under Zn deficiency. As the genetic factors that are responsible for the leaf length are identical in individual genotypes and irrespective of Zn levels, Zn sensitivity is a measure for the environmental control for the longitudinal expansion of the largest leaves (rosette size in this study). In addition, leaf shape is little affected by Zn (see below). Therefore, Zn sensitivity of rosette size is appropriate to generally reflect -Zn effect on leaf growth.

Chapter II

126 accessions (67% of 168 accessions, including e.g. Sf-2) had decreased rosette diameter in Zn-deficient soil (Fig. 1C, “positive” effect of Zn on leaf size). By contrast, the other 42 accessions (33% of 168 accessions, such as Col-0) had a decreased rosette size, despite having sufficient Zn in soil (Fig. 1C, “negative” effect of Zn). The average Zn sensitivity was -64.5% for negative response and 24.8% for the positive response. Zn sensitivity of the rosette size was determined by +Zn soil ($r=0.85$, $p<2.2e-16$), but not -Zn soil ($r=0.06$, $p=0.4478$, Fig. 1F, Supplementary Fig. S2).

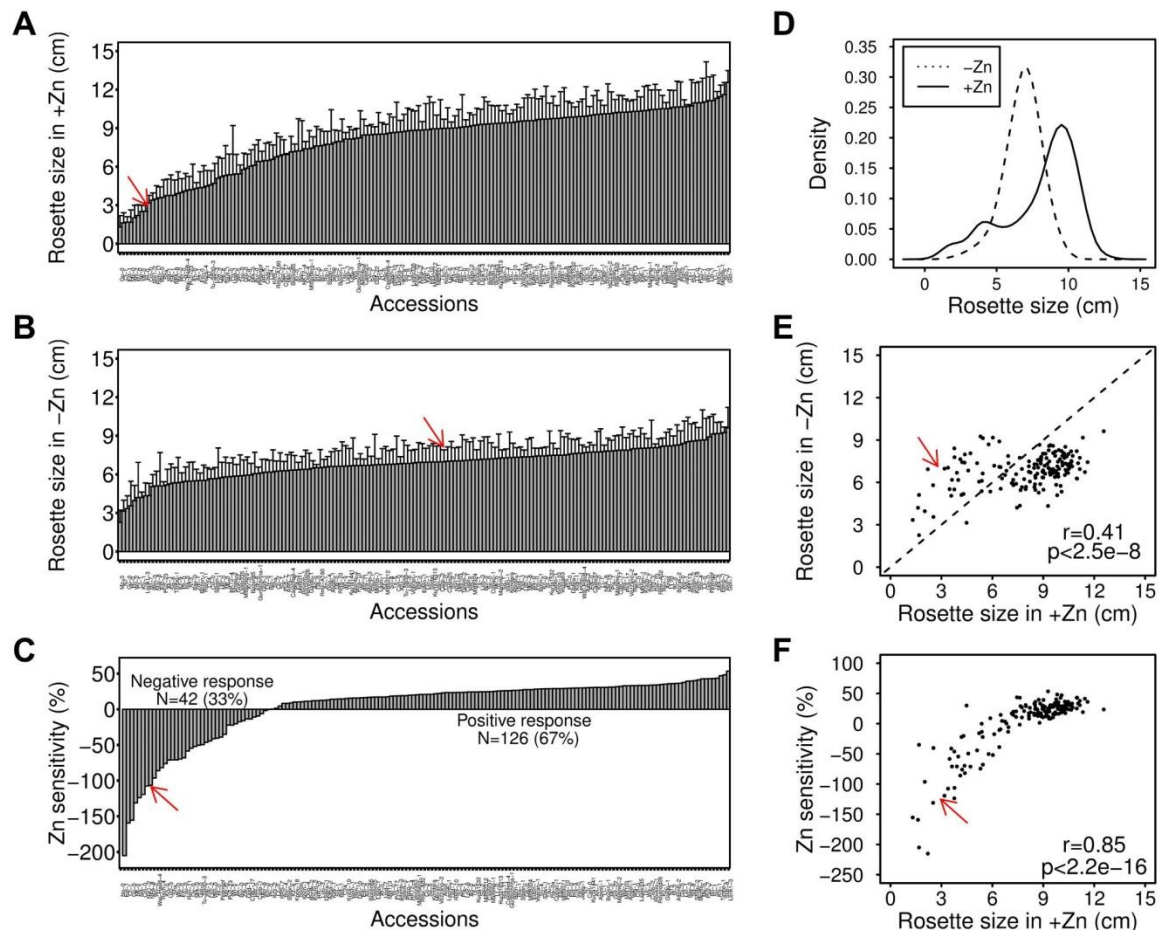


Figure 1: Natural variation of rosette size in response to Zn deficiency. A-C, Natural variation of 168 accessions in control (+Zn), Zn deficiency (-Zn) and Zn sensitivity. Data plotted are mean + SD, $n=6$. D, Kernel density of rosette size in +Zn and -Zn. E and F, Rosette size in +Zn was highly correlated with rosette size in -Zn and Zn sensitivity. Dashed line in E divided the 168 accessions into two groups. Red arrows indicate the accession Col-0 in each panel.

Genome-wide association mapping

To identify the underlying genetics of Zn sensitivity, we carried out genome-wide association (GWA) with 147 accessions for which high density single nucleotide polymorphisms (SNPs) were available; GWAPP were used that contains 1386 accessions and 206,000 SNPs (Seren et al., 2012). Natural genetic variation and GWA have been extensively used in *Arabidopsis* to dissect the genetics of various traits, including nutrients accumulation, flowering time, light sensitivity and root architecture (Brachi et al., 2010; Chao et al., 2012; Chao et al., 2014a; Meijón et al., 2014; Chao et al., 2014b). Even though larger population size may be required, a panel with only 96 accessions was evidently sufficient for several traits with large phenotypic variance in practice (Atwell et al., 2010; Gifford et al., 2013; Korte and Farlow, 2013; Ogura and Busch, 2015). Population structure is a strong confounding factor to produce false discovery results, which is partially overcome by the multi-locus mixed model (Cardon and Palmer, 2003; Platt et al., 2010; Segura et al., 2012). A stringent P-value cutoff with 5% false discovery rate (FDR) was set for quantifying the significance. Only SNPs with minor allele count (MAC) ≥ 15 were considered, to reduce potential false positive SNPs. The GWA did not identify any significant SNP for the rosette diameter in +Zn, but two SNPs for -Zn (Supplementary Fig. S3, A and B), *1G_27415858* and *4G_16195683*. *1G_27415858* is located around 500 bp distant from *AT1G72850* and *AT1G72860*, both encoding disease resistance proteins. *4G_16195683* is located in the genebody (first intron) of *At4G33770*, encoding an inositol 1,3,4-trisphosphate 5/6-kinase family protein. However, we were majorly interested in how rosette size was regulated by -Zn, we further focused on the more Zn-specific trait Zn sensitivity. The raw Zn sensitivity data was logarithmically transformed to reduce scale effects, so that extreme values have less impact on the outcome (Seren et al., 2012).

GWA identified several potentially interesting SNPs (Supplementary Fig. S3C). In particular, at position *1G_16581335* and *5G_18589544*, two flowering-related genes were associated, *AT1G43800* (*FTM1*, *FLORAL TRANSITION AT THE MERISTEM1*) and *AT5G45830* (*DOG1*, *DELAY OF GERMINATION 1*). *FTM1* is

activated independently of *FLOWERING LOCUS T* (*FT*) and *SUPPRESSOR OF OVEREXPRESSION OF CONSTANS1* (*SOC1*) during the floral induction (Torti et al., 2012). *DOG1* was initially identified to control the seed dormancy and germination (Bentsink et al., 2006); but later also found as candidate for differences in flowering in several GWA studies (Atwell et al., 2010; Brachi et al., 2010; Li et al., 2010). As potential SNPs might be covered by other SNPs due to population structure, here we further performed stepwise GWA with cofactors, which are identified SNPs (Segura et al., 2012). After four rounds of stepwise GWA with cofactors, four SNPs explained 74% of the total variance, while only 3% of genetic variance remained (23% accounted for error variance, Supplementary Table S4). Intriguingly, another significant SNP (*1G_24327565*) appeared among the cofactors (Fig. 2A). *1G_24327565* locates at 3862 bp upstream of *AT1G65480* (*FT*, *FLOWERING LOCUS T*), the central regulator of flowering. At SNP *1G_24327565*, most accessions contained the allele A (such as Sf-2), while fewer accessions contained the allele G (such as Col-0) (Fig. 2B). Accessions with allele G presented a more negative Zn sensitivity value (Fig. 2C). A closer look at the LD map (r^2) was conducted between the identified SNP *1G_24327565* and SNPs in *FT*. There are two SNPs in *FT*, *1G_24331677* and *1G_24333548* (Supplementary Fig. S4B). The GWA identified SNP *1G_24327565* was moderately linked to *1G_24333548*, locating in the exon of *FT*, with r^2 of 0.491.

Moreover, gene ontology enrichment analysis was conducted with agriGO (Du et al., 2010). The 50 genes located in +/- 20 kb distance of SNPs with $-\log_{10}(p_value) > 5$ were enriched for developmental and reproduction processes, involving transcriptional regulators (Supplementary Fig. S5), further supporting that flowering was regulated by Zn sensitivity.

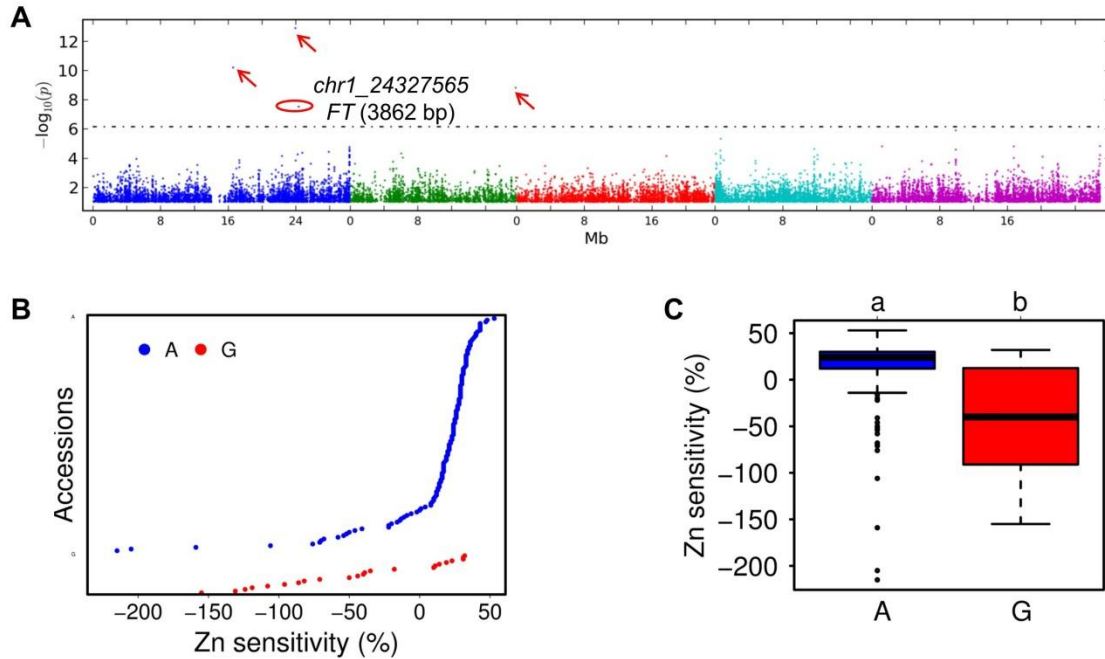


Figure 2: Genome-wide association mapping of Zn sensitivity. **A**, Manhattan plot for Zn sensitivity of rosette size. The value of Zn sensitivity was used after logarithmic transformation. Stepwise GWA was conducted with AMM model. SNPs with minor allele count (MAC) ≥ 15 were presented. The 5% FDR threshold was denoted by a dashed line. Red arrows indicate the other three SNPs. **B** and **C**, Zn sensitivity of allele A and allele G.

Relationship of rosette size and flowering

Next we set out to determine the relationship of rosette size and the flowering status after 6 weeks, two traits with typically minor correlation (Atwell et al., 2010). When grouped into accessions that had larger rosette under Zn-deficiency and those with positive Zn response (Fig. 1C), flowering was significantly more prominent in “negative” response accessions compared to positive response accessions, both in -Zn and +Zn conditions (Fig. 3A). Interestingly, the flowering status was clearly dependent on Zn, as the fraction of flowering plants was significantly stimulated by the presence of Zn irrespective of response types (Fig. 3A). This revealed that -Zn potentially inhibited flowering. Therefore, we further investigated *FT* transcript levels in both +Zn and -Zn soils, for negative-response accessions (Col-0, Po-0, Ct-1, No-0) and positive-response accessions (Lerik1-3,

Koz-2, Sf-2, Cvi-0). -Zn greatly reduced *FT* expression in all accessions (Fig. 3B). Moreover, negative-response accessions presented high *FT* level compare to late-response accessions, confirming that the flowering was casual for the response types. The same pattern also exhibited in another flowering central integrator *SOC1* (Supplementary Fig. S6).

We assumed that very early-flowering accessions might produce smaller rosette sizes just due to their shorter vegetative growth time. Indeed, *Arabidopsis ft* (and *soc1*) mutants are well known for their different shoot size, the *FT* homolog in tomato accelerates leaf maturation and is associated with termination of vegetative leaf growth (Melzer et al., 2008; Shalit et al., 2009). To further explore the correlation of rosette growth with flowering, we quantified the flowering times for 158 accessions (included in the 168 accessions mentioned above) at 23°C temperature in soils with full nutrition. It took around 25 days for the majority of accessions to bolting (highly correlated with bud-opening, Supplementary Fig. S7). The chronological flowering time strongly correlated with the physiological age (Salomé et al., 2011), except for a few ultimately non-flowering accessions (Supplementary Fig. S7B). The correlation between rosette size and flowering in +Zn was best described by the “*linear plus plateau model*” (Fig. 3C). Apparently, the rosette size in many accessions was repressed by flowering time (up to a threshold of 30 days, 71 of 158 accessions). By contrast, late-flowering accessions, harboring the winter annuals, all had large rosette size. The same model nicely fitted the correlation of Zn sensitivity and flowering (Supplementary Fig. S8). The germination rate, by contrast, was not different in +Zn and -Zn (all plants germinated in two days).

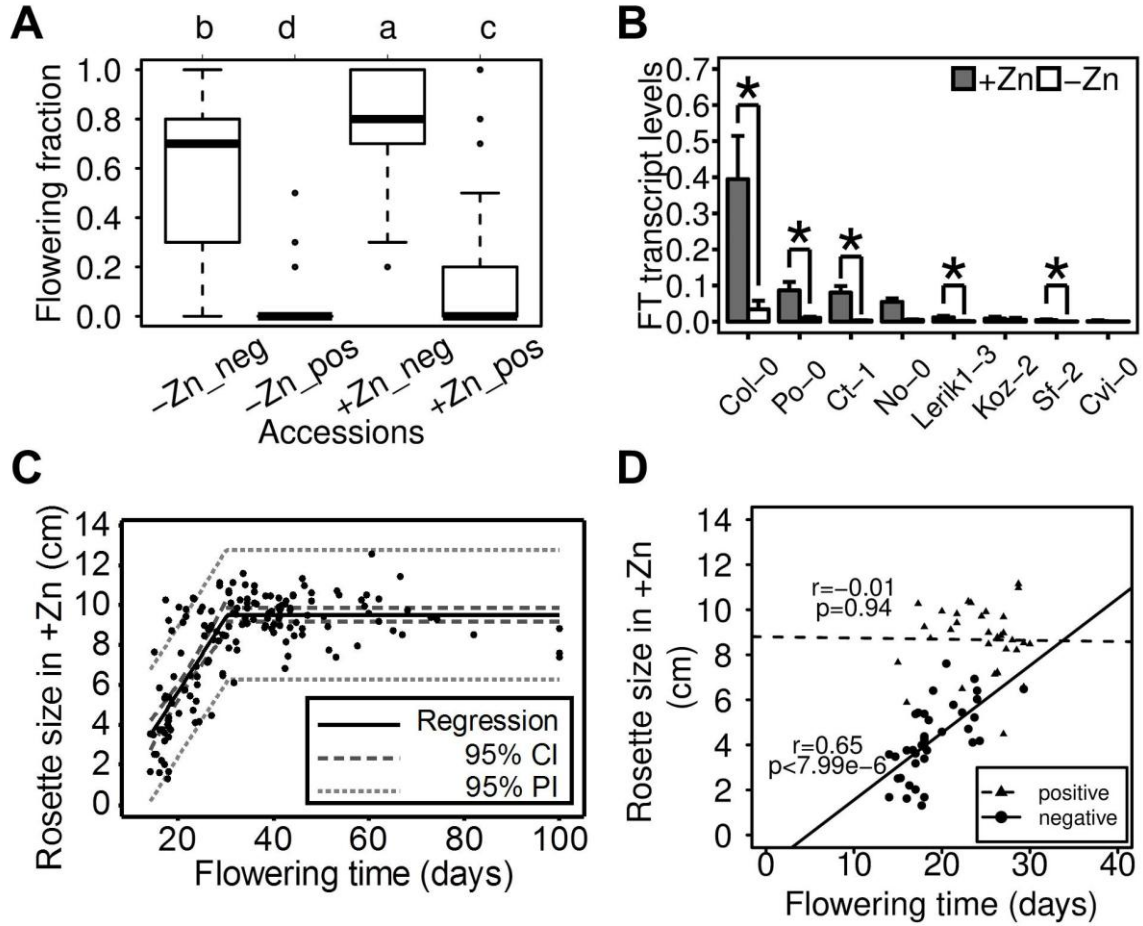


Figure 3: **A**, Fraction of flowering plants at 6 weeks, separated for negative and positive response accessions in both growth conditions. Different small letters above the figure denote the significant difference at $p < 0.05$ level. The multiple comparisons were calculated by Tukey HSD. “neg” means negative, “pos” means positive. -Zn_neg, -Zn_pos, +Zn_neg and +Zn_pos indicate negative and positive accessions in -Zn and +Zn soils. **B**, FT transcript levels in negative (Col-0, Po-0, Ct-1, No-1) and positive accessions (Lerik1-3, Koz-2, Sf-2, Cvi-0). Data were referenced to reference genes *SAND* and *PDF2*. * denotes the significant difference at $p < 0.05$ level. Values were mean + SD. **C**, Relationship of rosette size and flowering time in control, which is simulated by “linear-plus-plateau” model. Flowering time was documented as the days to bolting. CI and PI mean the confidence interval and prediction interval. **D**, Relationship of rosette size and flowering time for early-flowering accessions. The early-flowering accessions were generated from Figure 3C, which were also grouped into negative and positive response according to Figure 1C.

A closer look at the 71 early-flowering accessions (flowering before day 30) identified that 39 accessions of these grouped into the “negative response”, while the other 32 accessions belonged into the “positive response” (Fig. 3D; Fig. 1C). No correlation of rosette size and flowering was observed for the 32 positive response accessions, as these accessions had already reached near maximal rosette size before they started to bolt. However, within the 39 negative response accessions, there was significant positive correlation between flowering time and rosette size (Fig. 3D), indicating that for these accessions (such as Col-0), Zn sensitivity was determined by a terminal transition to flowering, which apparently repressed vegetative growth. In other words, Zn deficiency apparently delayed the transition from vegetative to generative growth, leading to larger leaf size. Therefore, Zn limitation of vegetative growth was then only apparent in accessions with large leaf blades, notably late-flowering accessions.

Genetics of zinc-deficiency repression on flowering

Further genetic analysis was performed in Col-0, a negative response accession (Zn sensitivity was -119 %) with strong *FT* and *SOC1* inhibition by -Zn. The phenotypic differences and growth variance in a batch were shown in Fig. 4A; obviously, -Zn repressed flowering in Col-0 (Fig. 4A). To get more insight whether photoperiod, metabolic, vernalization, gibberellin or ambient temperature were affected by Zn deficiency (Amasino, 2004; Fornara et al., 2010), we further investigated null-mutant of these flowering pathways. All the mutants used in this study are knock-out in Col-0 background (Balasubramanian et al., 2006; Posé et al., 2012). To confirm the Zn effectiveness, shoot Zn concentration was analyzed. -Zn indeed strongly reduced Zn uptake in all genotypes, including late-flowering accession sf-2 (Fig. 4B). In addition, Transcript levels in -Zn were also compared to +Zn in Col-0 and Sf-2, for several known Zn transporters, which were previously reported being induced upon -Zn in roots (Grotz et al., 1998; Mortel et al., 2006; Lin et al., 2009). Here, we also found the strongly induction effect in leaves in response to -Zn (Fig. 4C). Next we checked the expression of key genes representative of these flowering pathways. However, the expression of the diurnal integrator *CONSTANS* (*CO*), trehalose biosynthesis enzyme

TREHALOSE-6-PHOSPHATASE SYNTHASES 1 (TPS1), the transcriptional repressors *FLOWERING LOCUS C (FLC)*, *FLOWERING LOCUS M (FLM)* and *SHORT VEGETATIVE PHASE (SVP)*, two inhibitors of the elevated temperature-induced early flowering via de-repression of *FT*, were all unaffected by Zn. Furthermore, flowering promoting *GIBBERELLIN 3-OXIDASE1 (GA4)*, as well as expression of *FTM1*, identified from the GWA (supplementary Fig. S3C), were also not different between -Zn and +Zn (Fig. 4D). *DOG1* was another candidate identified from the GWA (supplementary Fig. S3C), but a *dog1-2* allele was indistinguishable from the wild-type with respect to Zn dependence of rosette size and flowering (data not shown), excluding this gene to be causally linked to the Zn-dependent regulation.

Using mutant alleles of flowering genes upstream and downstream of *FT*, we ruled out several upstream repressors of early flowering as direct targets of Zn. Compared to Col-0, *flc-3* and *flm-3* did not delay flowering time (Fig. 4E), which might be because that Col-0 is an extremely early-flowering accession, which contains low level of *FLC* and *FLM* (Lempe et al., 2005; Balasubramanian et al., 2006). Therefore, Col-0 was not distinguishable from *flc-3* and *flm-3* in current study that all plants flowered relatively early. Nevertheless, *svp-32* and double mutant *svp-32/flm-3* still exhibited pretty earlier flowering compared to Col-0 (Fig. 4E). Concomitantly, rosette size reduced in these mutants irrespective of Zn supply (Fig. 4F). By contrast, in alleles that lack major activators of flowering, *ft-10* and *soc1-2*, flowering was delayed, but still inhibited by -Zn (Fig. 4E). The loss of *SOC1* was reported to increase the lifespan of plants independent of flowering time (Melzer et al., 2008), but -Zn rosettes were still bigger than those from +Zn. Interestingly, the rosette of *ft-10* was large irrespective of Zn supply (Fig. 3 F, Supplementary Fig. S9), indicating that the -Zn promotion of rosette growth was lost in the absence of *FT*. As a consequence, the final vegetative dry biomass (determined by the number of rosette leaves and their size) was significantly higher in -Zn in wild type and early flowering mutant *svp-32*, but identical despite different Zn supply in the late flowering *ft-10* and *soc1-2* (Fig. 4G).

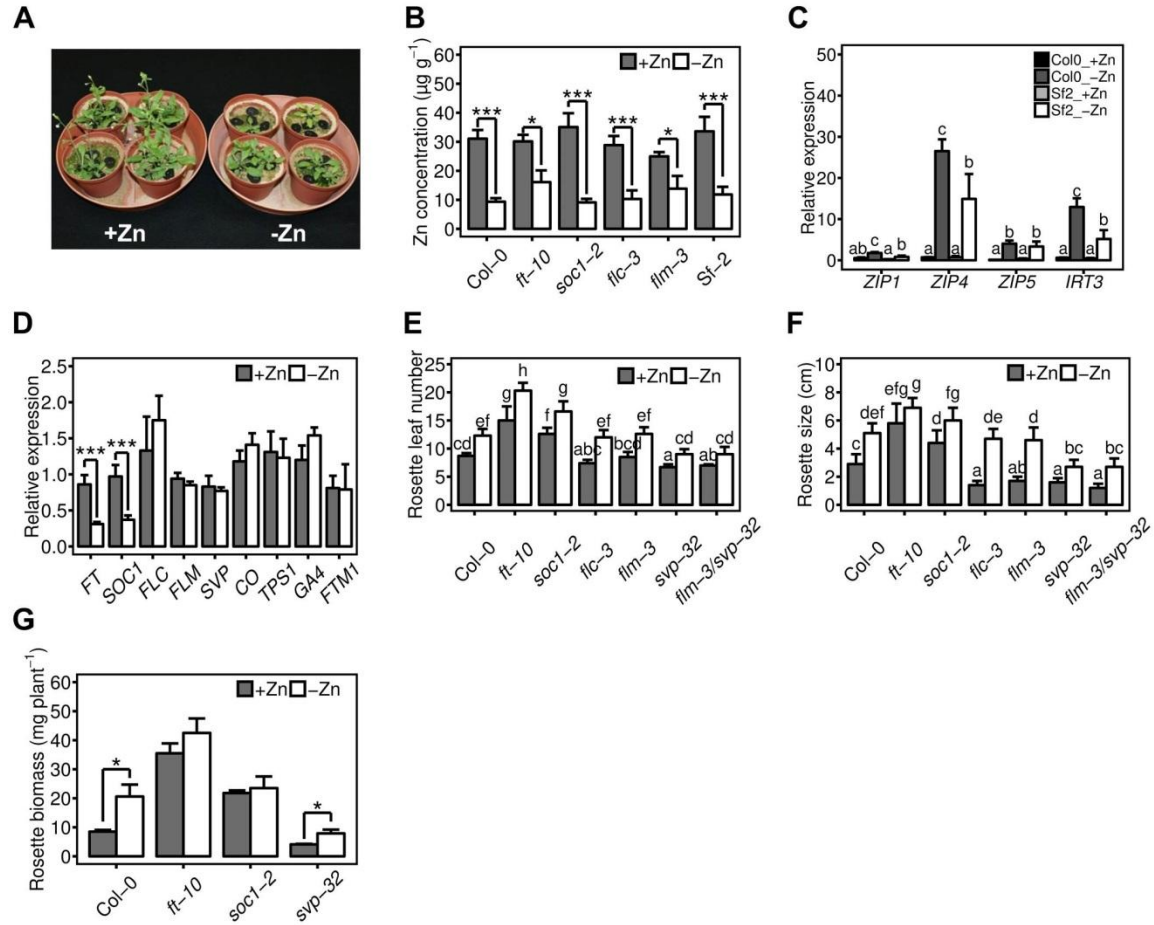


Figure 4: Genetic basis of Zn regulation of flowering and rosette size. **A**, Col-0 plants grown in +Zn and -Zn soils. -Zn delayed flowering. **B**, Zn concentration in wild-type (Col-0 and Sf-2) and flowering null mutants, indicating the Zn effectiveness. **C**, Relative expression level of known Zn transporters in Col-0 at vegetative stage (14 DAS). Data were referenced to reference genes *SAND* and *PDF2*, then normalized to the first replicate of +Zn. **D**, Relative expression level for central flowering genes in Col-0 and Sf-2 at vegetative stage (14 DAS). Data were referenced to reference genes *SAND* and *PDF2*. **E** and **F**, Rosette leaf number and rosette size, at bolting stage in wild-type (Col-0) and flowering null mutants. **G**, Rosette dry biomass of wild-type (Col-0) and flowering null mutants at 7 weeks at the point that all plants have finished flowering. *, ** and *** denote $p < 0.05$, $p < 0.01$ and $p < 0.001$, respectively. Different small letters between columns denote significant difference at $p < 0.05$ level. Data plotted are mean + SD.

Loss of zinc-deficiency repression on flowering by growth in unfavorable environments

The flowering in many *Arabidopsis* accessions is stimulated by growth at elevated temperatures, but delayed in short days, at lower temperatures or growth in unfavorable light conditions (Lempe et al., 2005; Balasubramanian et al., 2006). Based on the observation that -Zn repression of early flowering and the associated vegetative growth promotion were only observed in accessions that flowered earlier than day 30 (Fig. 3), we hypothesized that -Zn should not affect rosette diameter when flowering is sufficiently delayed, even in the genetic background of Col-0. At two weeks, *FT* and *SOC1* expression were greatly reduced by -Zn irrespective of accessions or grown temperatures (Fig. 5 A, B and D). However, the reduction was not able to be maintained at seven weeks in -Zn (Fig. 5 C and E). In other word, when grown in low temperature (16°C, or low light or short days, data not shown), -Zn only transiently decreased *FT* and *SOC1* expression. Meanwhile, the relative low *FT* level in +Zn were also insufficient to induce early flowering in 16°C (Fig. 5 B and G). Accordingly, rosette size was also not regulated by -Zn (Fig. 5H). Similarly, in the late-flowering accession Sf-2, the reduction of *FT* level was not persistent by -Zn (Fig. 5E), and *FT* expression was not high enough to trigger flowering in +Zn plants (Fig. 5 D and H). As a result, vegetative growth was not promoted in -Zn (Fig. 5H). Ultimately the rosette size was limited by other factors than *FT* or *SOC1*, which repressed leaf growth only during the early growth. Indeed, many other factors that restrict organ size in plants have been identified, including genes involved in auxin, cytokinin and gibberellin signaling (Bögre et al., 2008; Powell and Lenhard, 2012).

On the other hand, when the flowering time of the late-flowering accession Sf-2 was shortened via a 3-weeks vernalization process at 4°C, flowering was promoted and the rosette diameter mildly decreased, compared to the non-vernalized Sf-2 (Fig. 5, G and H). Again, -Zn increased the *FT* transcript levels (though not significantly), leading to earlier flowering (Fig. 5 F and G). However, Zn did not reduce the rosette size (Fig. 5H), since maximal leaf elongation potential had already been reached.

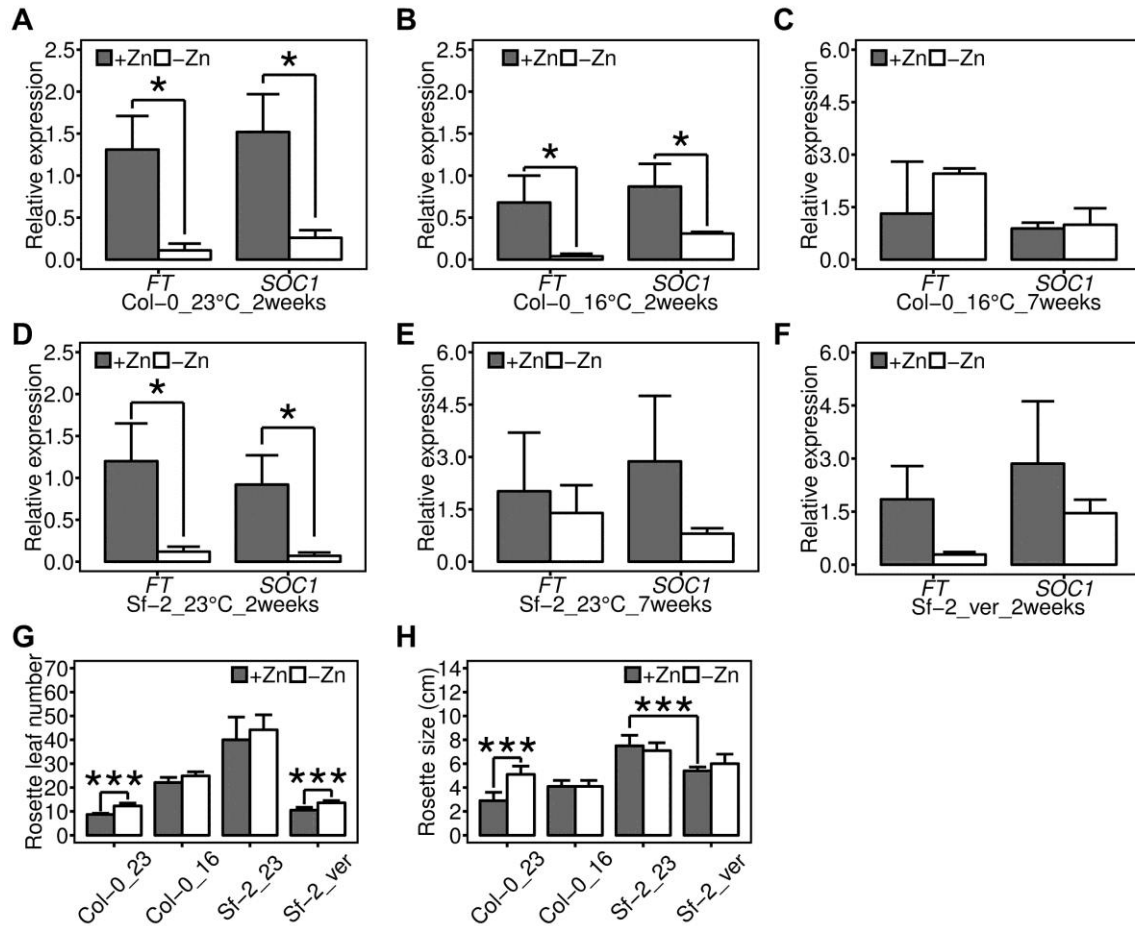


Figure 5: Low temperature and vernalization changed the -Zn regulation of flowering in natural accessions. A-F, Relative *FT* and *SOC1* expression level of Col-0 and Sf-2 in variable conditions and stages. Data were referenced to reference genes *SAND* and *PDF2*, then normalized to the first replicate of +Zn. **G and H,** Rosette leaf number and rosette size of Col-0 and Sf-2 at bolting stage in different conditions. “ver” means vernalization. * and *** denote p<0.05 and p<0.001, respectively. Data plotted are mean + SD.

Zn-deficiency promotion of vegetative growth via *FT*

While the transition to flowering fate in the apical meristem is well explained by *FT* (Amasino, 2010; Fornara et al., 2010), its role in termination of vegetative leaf growth is less well understood (Melzer et al., 2008; Shalit et al., 2009). Final rosette diameter and leaf size are ultimately controlled by the complex

coordination of primordium size, cell proliferation and cell expansion (Gonzalez et al., 2012; Powell and Lenhard, 2012). To get insight into the underlying mechanism behind the reduced rosette diameter in higher *FT* plants, the leaf length, petiole and cell sizes were documented during leaf growth. Interestingly, the rosette diameters were initially indistinguishable between +Zn and -Zn, in agreement with a mild Zn-deficiency; but differed at the time of the transition to flowering in the apical meristem (Fig. 6A), consistent with a repressing signal transmitted at the time of flower initiation in +Zn (21 DAS, Fig. 6A). Unexpectedly, the longitudinal leaf growth rate was not terminated, but only reduced in +Zn after the transition to flowering, while the longitudinal leaf growth rate increased in -Zn until termination at around 33 DAS (Fig. 6A). This signal was lost in *ft-10*, leading to strong leaf expansion irrespective of Zn supply (Fig. 6, B and D). Absolute flowering time and rosette size were somewhat variable in different growth batches, but flowering was generally faster on the soils used than in previous studies and -Zn repression of flowering was highly consistent (Fig 4F, Fig 6, Supplementary Fig. S9). The petiole elongation in response to -Zn explained only ~35 % of the rosette leaf length differences. Cell expansion accounted for almost 40 % of the leaf enlargement between 19 DAS and 33 DAS, but was identical in -Zn and +Zn, and was unchanged in *ft-10* (Fig. 6, C-E). The combined data suggest repressing functions of *FT* outside the leaf meristem. Reduced cell proliferation and less cell divisions in the wild type, especially in +Zn, accounted for the growth inhibition of the largest leaves and were also responsible for minor differences in leaf shape (Fig. 6D).

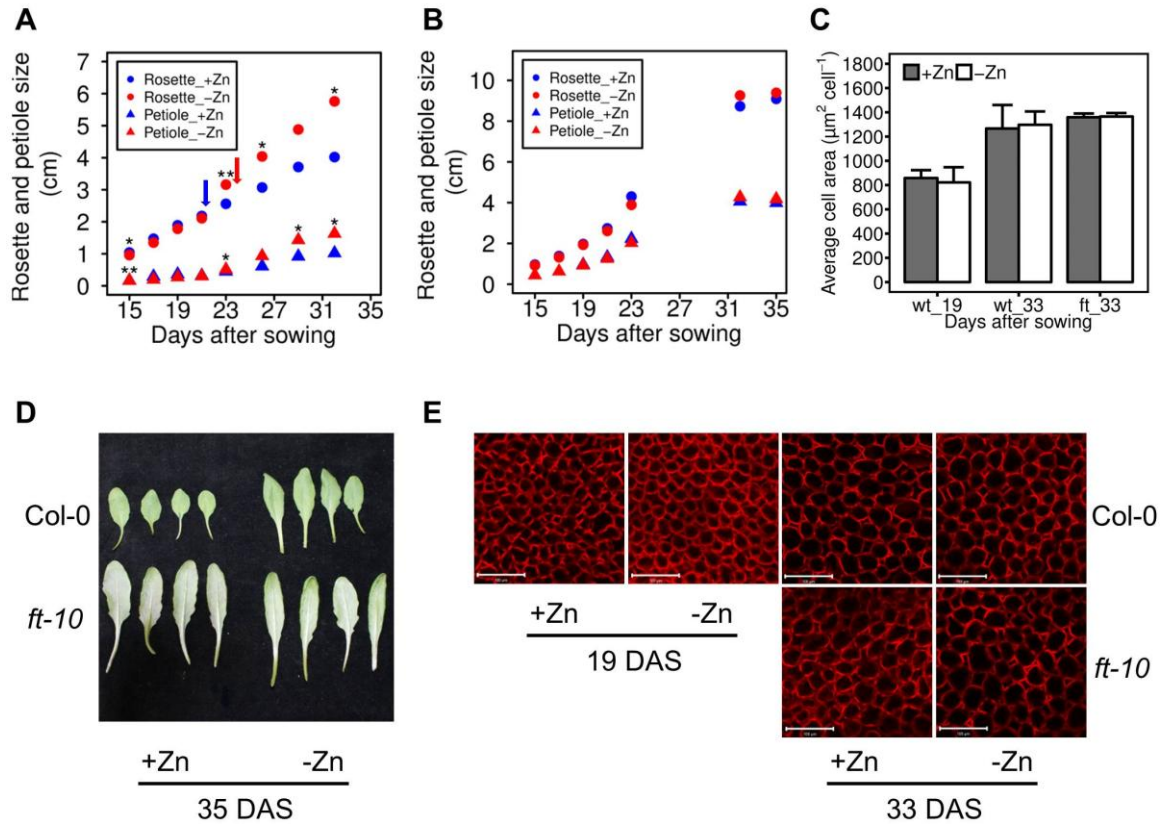


Figure 6: Zn regulation of rosette expansion and cell proliferation. **A**, Growth of rosette size (circle) and petiole size (triangle) in Col-0 with +Zn (blue) and -Zn (red). * and ** denote $p < 0.05$ and $p < 0.01$. Arrows indicate the flowering time in +Zn (blue) and -Zn (red). **B**, Rosette growth of *ft-10*. **C**, Average cell size of first four wild type and *ft-10* leaves at 19 DAS (days after sowing) and 33 DAS. Data plotted are mean + SD. **D**, First four leaves at 35 DAS. **E**, confocal mesophyll cell images after staining with propidium iodide of wild type and *ft-10*. Scale bar: 100 µm.

The transition to flowering, which occurs in apical leaf meristems, was stimulated by Zn even in the *ft* or *soc1* background. By contrast, promotion of vegetative growth by -Zn required reduction of *FT*, but not *SOC1*. Leaf cell numbers and cell size in the *ft-10* mutant were in agreement with the hypothesis that *FT* restricts leaf size, as the loss of *FT* massively increased leaf size via increased cell numbers, similar as in Zn-deficiency in the wild type (Fig. 6). The dual action of *FT* in promoting flowering and restricting leaf size and its regulation by Zn are

summarized in Fig. 7A. Additional roles of *FT* in regulating the fate of meristems and consequently reduction in growth had been especially noted under short days (Melzer et al., 2008), while the above data confirm its importance under long day conditions. The direct mechanistic targets of Zn are likely upstream components of *FT* and only restrict leaf blade size as long as leaves are small and proliferate, while in many later-flowering genotypes Zn-deficiency slightly reduces leaf blade size (Fig. 7B; Fig. 1C). As general nutrient deficiencies promote flowering in *Arabidopsis* (Kolář and Seňková, 2008), the observed flowering delay and rosette repression may be Zn-specific. Whether nutritional regulation of flowering and the concomitant restriction of vegetative growth are relevant in ecosystems and crops, are interesting questions for future research.

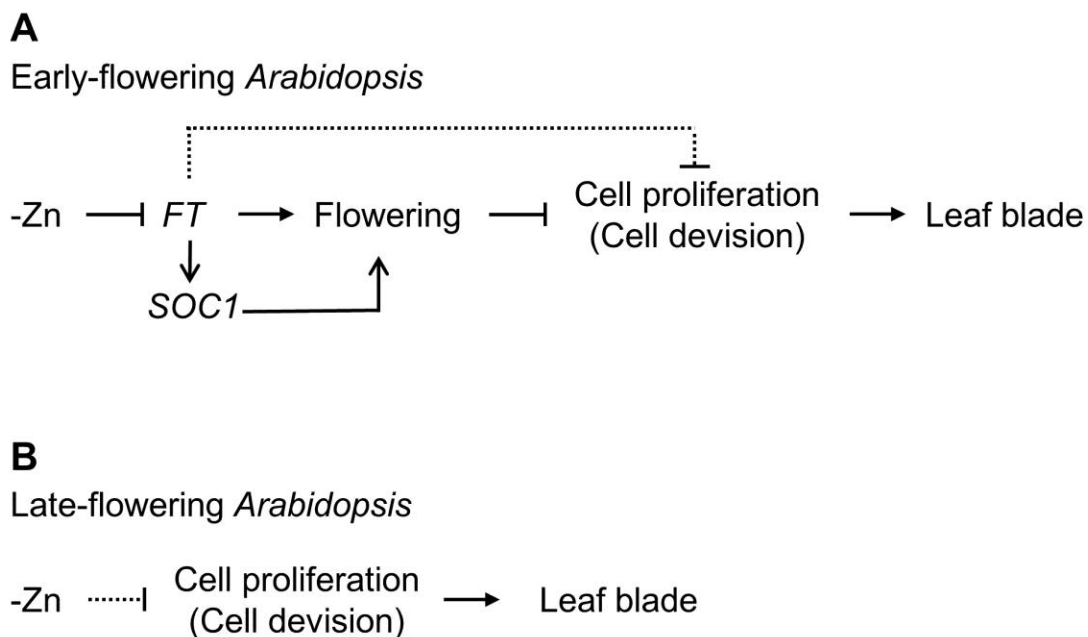


Figure 7: Working models of Zn-regulation of flowering and rosette leaf size. Note that Zn-deficiency only represses *FT*, flowering and promotes leaf cell division in early-flowering accessions that have not fully expanded their leaves (**A**); whereas in many late-flowering accessions, mild Zn-deficiency slightly restricts shoot growth (**B**). Arrows and block lines denote activation and repression, respectively. Dashed lines indicate putative regulation.

Conclusion

The analysis of a population of *Arabidopsis* accessions on Zn-deficient and Zn-amended soil revealed a close inter-connection of -Zn repression of flowering via *FT* and improved vegetative growth. Confounding effects of nutrient deficiency on flowering may thus mask the growth potential of sensitive genotypes, leading to the unusual situation that nutrient-deficient plants accumulate more vegetative shoot biomass than plants on full nutrients.

Materials and methods

Plant material, soil-sand preparation and growth conditions

168 *Arabidopsis thaliana* accessions used in this study are listed in the Supplementary Table S1. Seeds for all accessions were obtained from Dr. Karl Schmid (Germany). The *ft-10*, *soc1-2*, *flc-3*, *flm-3*, *svp-32*, *flm-3/svp-32* mutants in the Col-0 background were gifted by Dr. Markus Schmid (Umea, Sweden). All accessions and mutants have been previously described (Balasubramanian et al., 2006; Posé et al., 2012; Stetter et al., 2015; Chen et al., 2016).

Soil-sand mixtures of a Zn-scarce soil from a C-horizon of a loess soil (0.7 mg kg⁻¹ Zn, pH 7.2) was mixed at 1:1 ratio with quartz sand (0.6-1.2 mm diameter), which was washed with HCl (rinsed with tap water, pH<1 adjusted with HCl, incubated for one day, rinsed with deionized water to pH>5) to wash out trace nutrients, biological contaminations and dust. The soil-sand mix was fertilized with 1.1 g kg⁻¹ NH₄NO₃, 0.9 g kg⁻¹ K₂SO₄, 2.1 g kg⁻¹ MgSO₄ and 1.6 g kg⁻¹ Ca(H₂PO₄)₂. 200 g of soil-sand per plant (or 120 g for qRT-PCR experiments and mutant experiments) was placed in the pot before watering with 7-8 ml micronutrients, according to a modified Hoagland's solution (1 mM NH₄NO₃, 1 mM KH₂PO₄, 0.5 mM MgSO₄, 1 mM CaCl₂, 0.1 mM Na₂EDTA-Fe, 2 µM ZnSO₄, 9 µM MnSO₄, 0.32 µM CuSO₄, 46 µM H₃BO₃, 0.016 µM Na₂MoO₄). In addition, 3 mg kg⁻¹ Zn was added into soil for the control treatment (+Zn).

Seeds were stratified at 4°C for 3 days to promote germination. Plants were cultivated in greenhouse (GWA, during a warm period in may 2013) or in controlled growth chambers (all other experiments). The growth conditions were generally set as: long days (16h light/ 8h dark), 23°C light / 20°C dark, 120-140 $\mu\text{mol m}^{-2} \text{s}^{-1}$ and 65% humidity, or 16°C light / 16°C dark for ambient temperature experiment.

Phenotype scoring

For the genome-wide association (GWA), 6 randomized replicates per accession were analyzed. For each plant, the rosette size was measured from two pairs of diameters of four biggest leaves, after 6 weeks of growth. The flowering status was documented as well. For the flowering time requantification, 3 replicates were recorded for each accession. The flowering time was quantified as the number of days required for a 1 cm visible bolt or a visible flower-bud (chronological time) and the number of leaves until bolting or flower-budding (physiological age). 100 days were set as the flowering time for the ultimate non-flowering accessions. In mutant experiments, 5-17 plants were analyzed at bolting stage (1 cm visible bolt) for rosette size diameter, leaf number and flowering days as previously described (Lempe et al., 2005; Salomé et al., 2011). The Zn sensitivity was calculated as: $(\text{plus Zn} - \text{minus Zn}) / \text{plus Zn} \times 100$.

Genome-wide association (GWA)

GWA was conducted using the online web application GWAPP, containing 1386 accessions and 206,000 SNPs (Seren et al., 2012). Only 147 accessions were uploaded in GWAPP as the SNP data of the other 21 accessions are not yet available. For the Zn sensitivity, we transformed the phenotypes using a logarithmic transformation, which yields extreme value to be less extreme. The AMM approach was used to correct for the population structure for all association mapping (Segura et al., 2012). Except for the original GWAS for the Zn sensitivity, a step-wise GWAS including cofactors was performed, which finally identified the key flowering regulator *FLOWERING LOCUS T (FT)*.

Enrichment analysis

The enrichment analysis was performed using the online web application agriGO (Du et al., 2010). The gene list was generated from step-wise GWAS of Zn sensitivity (described above), including 50 genes (Supplementary Table S6). In detail, genes located within +/-20 kb of the SNPs with $-\log_{10}(p_value) > 5$ were selected. Singular Enrichment Analysis (SEA) was conducted for cellular components, molecular function and biological process. TAIR 10 was used as the reference database (<http://www.arabidopsis.org/>).

Zinc concentration determination

6-week-old plants were harvested, dried in 60°C for a week and milled. Around 0.1 g milled materials were digested with 2.5 ml 69 % HNO₃ and 2 ml 30% HCl for 1 hour. The samples were placed in a microwave at 170 °C for 25 minutes, followed by 200 °C for 40 minutes. The extract was measured by atomic absorption spectrometry (Thermo Fisher Scientific, United Kingdom) to determine Zn concentration.

Quantitative RT-PCR analysis

Plants were grown in +Zn and -Zn soils (described above) with 3-5 replicates. For each replicate, 10-20 seedlings were harvested and pooled between 12:00-13:00 at 14 DAS (days after sowing, not yet bolting) with liquid nitrogen before storing in -80°C. Total RNA of all seedlings was extracted with the innuPREP Plant RNA Kit (Analytik Jena, Germany) after plants were homogenized (Retsch, Germany). Around 1 µg total RNA was used to synthesis cDNA library using the QuantiTect Reverse Transcription Kit (Qiagen, Germany). Gene-specific primes for qRT-PCR were designed according to the *Arabidopsis* genome sequence information TAIR10 (<https://www.arabidopsis.org/>) and Primer-BLAST (<http://www.ncbi.nlm.nih.gov/tools/primer-blast/>), quality-checked by using PCR Primer Stats (http://www.bioinformatics.org/sms2/pcr_primer_stats.html). Primers were ordered from Invitrogen (United States) and listed in the Supplementary Table S7. For the PCR procedure, 15 µl reaction was carried out, containing 6 µl 20x diluted cDNA, 7.5 µl SYBR Green Supermix (KAPA

Biosystems, United States), 0.3 μ l forward primers, 0.3 μ l reverse primers and 0.9 μ l RNase-free H₂O. The reaction was conducted in 384-well plates in RT-PCR systems (Bio-Rad, United States). The standard protocol was set as: 3 min at 95 °C, followed by 44 cycles of 3 s at 95 °C and 25 s at 60 °C, and then 5 s at 65 °C for the melt curve. Two reference genes, *SAND* (AT2G28390) and *PDF2* (AT1G13320), were used. Reactions were performed in 3 technical replicates and 3-5 biological replicates. Relative transcript levels were calculated with the 2- $\Delta\Delta$ CT method by the Bio-Rad software (Livak and Schmittgen, 2001). All kits described here were used according to the manufacturer's instructions.

Histological analysis

Palisade cell sizes were measured as previously described (Sicard et al., 2015). Briefly, first four leaves were harvested and fixed overnight at 4 °C in FAA solution (20 ml formalin, 10 ml acetic acid, 100 ml alcohol, and 70 ml water), and dehydrated through a series of 70, 80, 90, 100% ethonal, with 5-min incubation per step. Then the samples were transferred into acetone for 5-min incubation at 95 °C, and cleared overnight in the clearing solution (100 g chloral hydrate, 10 g glycerol, and 25 ml water). Finally the samples were stained with 10 μ g ml⁻¹ propidium iodide for two days, and imaged with the confocal microscope (LSM700, Carl Zeiss, Germany). Four regions were measured for every leaf and cell size was averaged from four leaves. Three biological replicates were performed.

Statistical analysis

Data analysis, graphs and statistics were done by using Microsoft Excel, Minitab and R (<https://www.r-project.org/>). The significant difference of mean for all traits in this study was performed by t-test. Multiple comparisons were done using Tukey HSD method in R. Broad-sense heritability was calculated as genotypic variance divided by total variance (Visscher et al., 2008). The total variance was partitioned into genetic variance and residuals.

Acknowledgments: We thank Karl Schmidt (Stuttgart, Germany) for all accessions seeds, Markus Schmidt (Umea, Sweden) and Wim Swoppe (Cologne, Germany) for mutant seeds, Dr Huaiyu Yang for initial help with lab work and Dominik Hedderich for help with determination of flowering times. We also thank the China Scholarship Council for support.

Author contributions

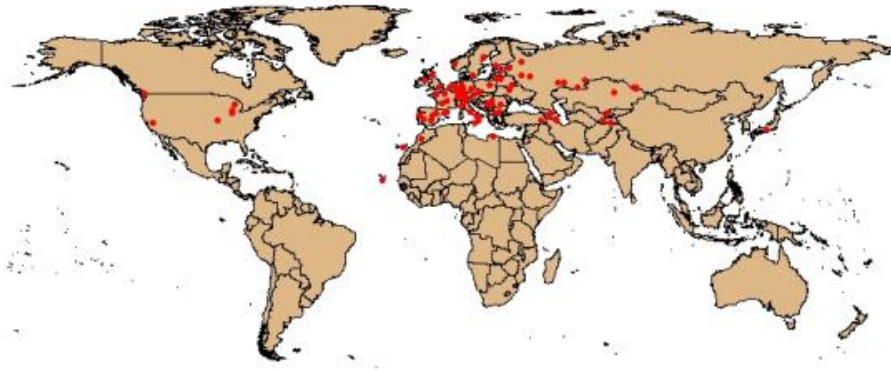
X.C. and U.L. conceived the experiment; X.C. performed the experimental work; X.C. and U.L. analyzed data; X.C. and U.L. wrote the paper.

Competing interests

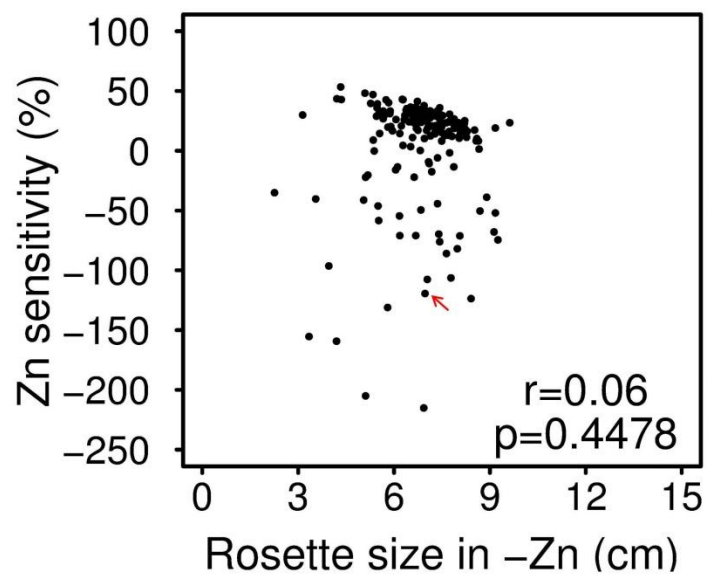
The authors declare no competing financial interests.

References (part 8 References)

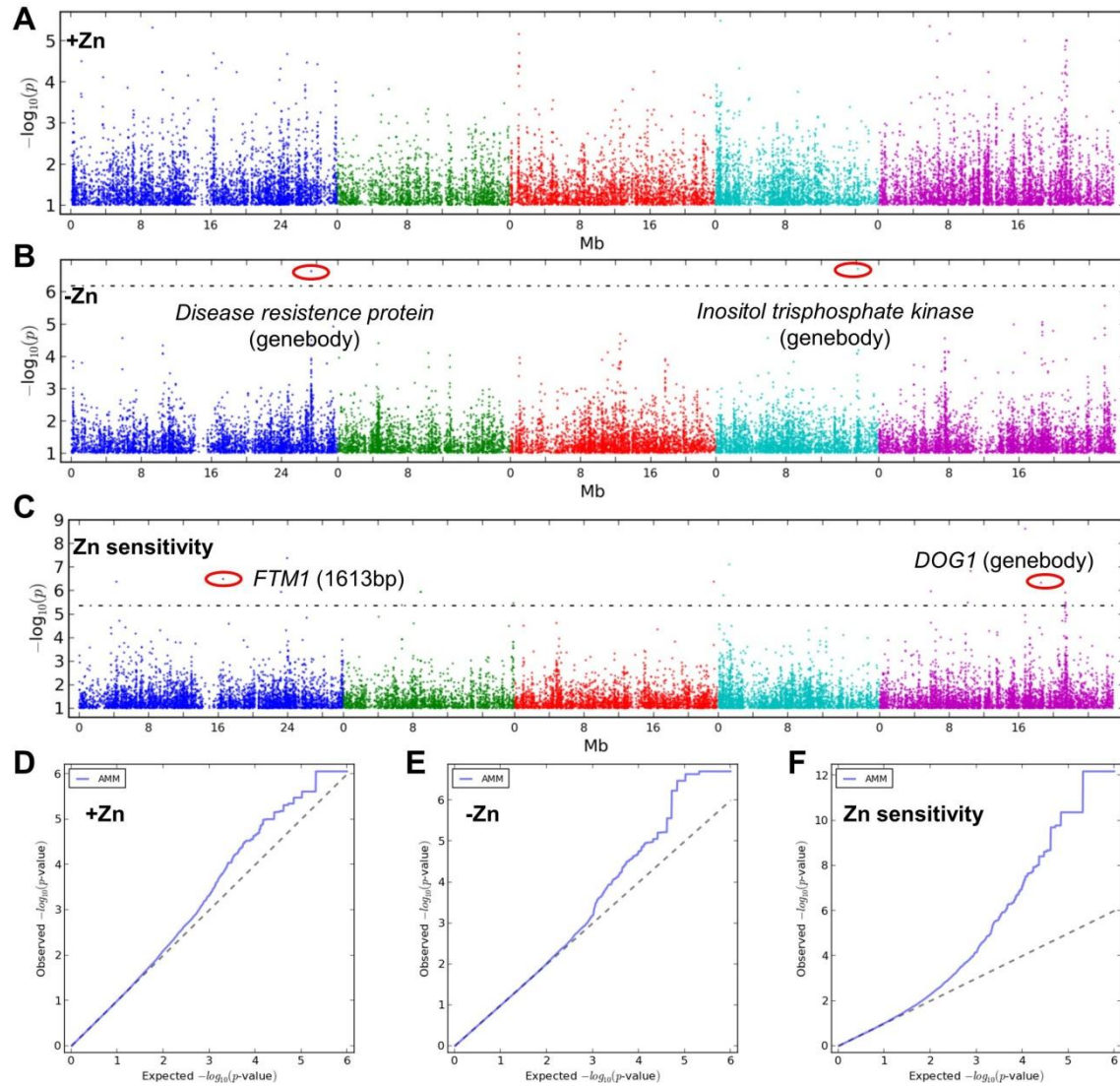
Supplementary figures and tables



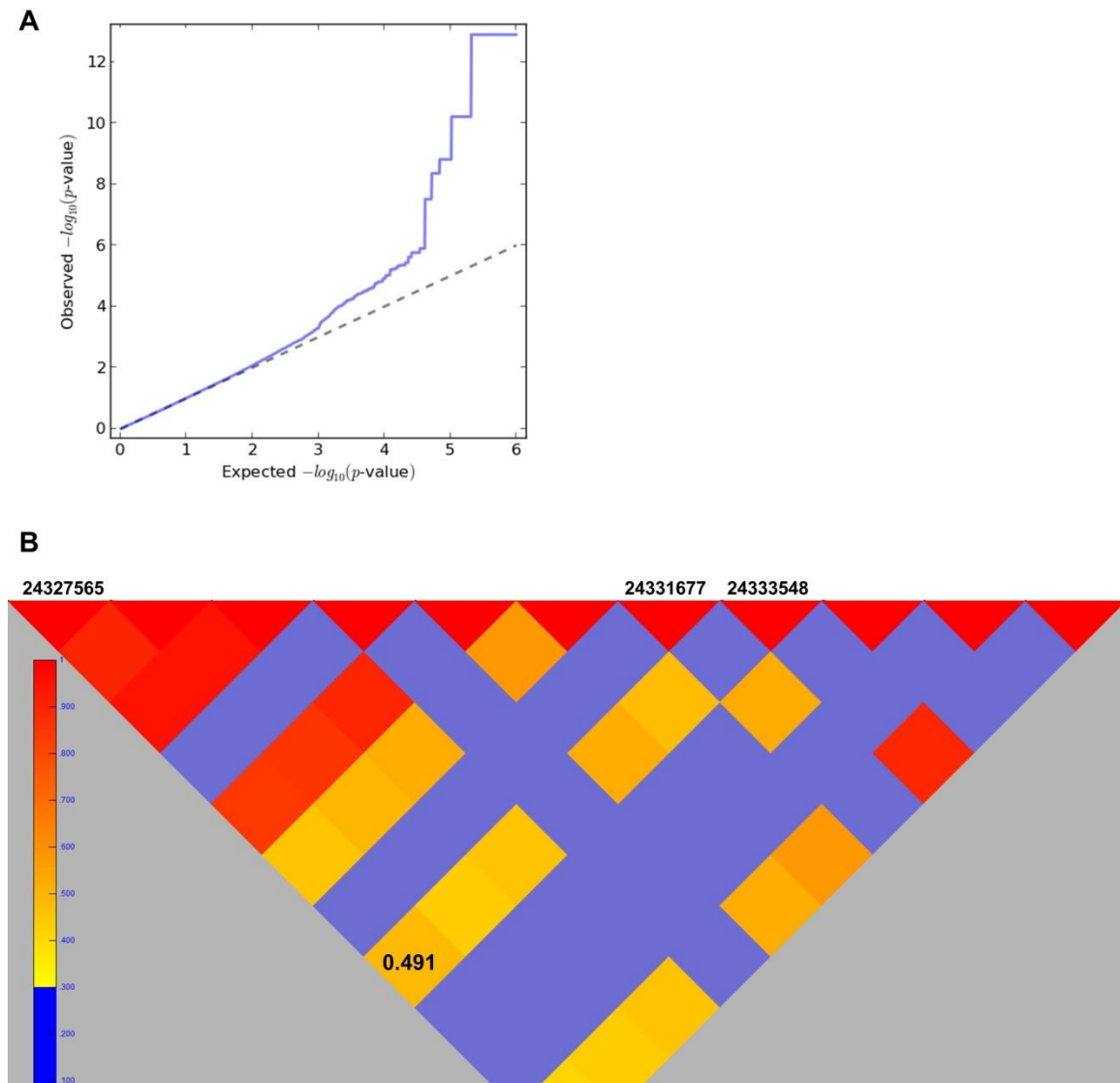
Supplementary Figure S1: The worldwide population distribution of 168 *Arabidopsis* accessions used in this study. Every red dot represents one accession.



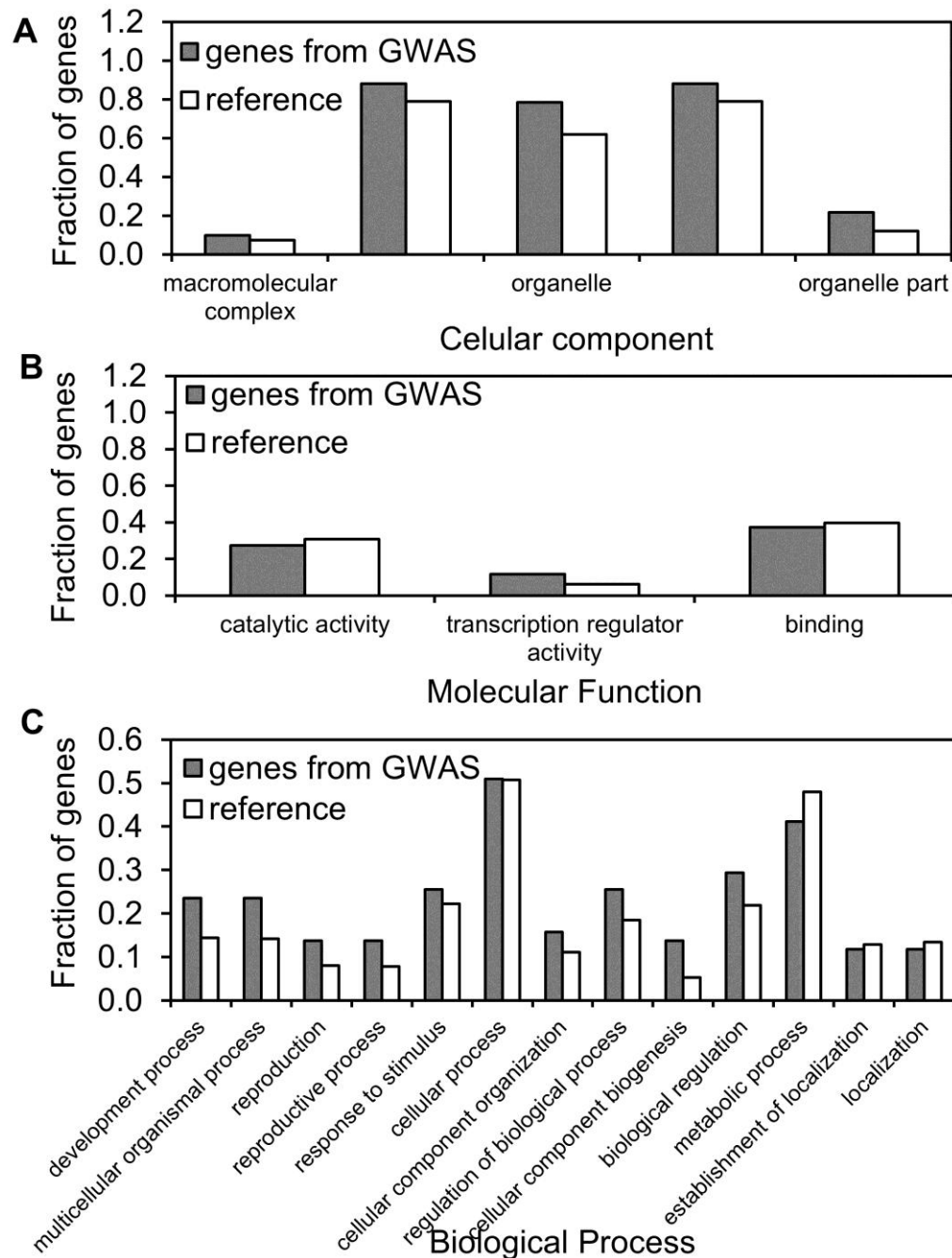
Supplementary Figure S2: Relationship between rosette size in -Zn and Zn sensitivity.



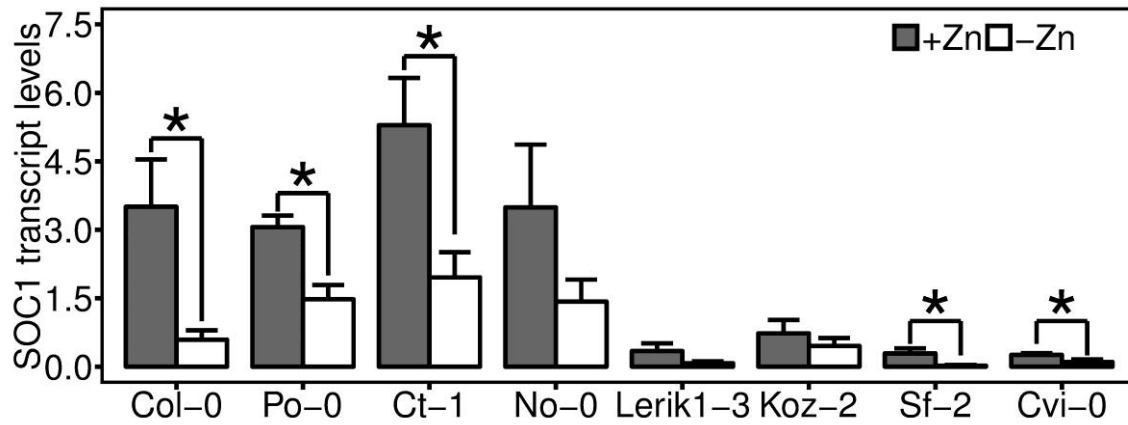
Supplementary Figure S3: Genome-wide association for rosette size in +Zn (A), -Zn (B) and Zn sensitivity (C) with AMM model (no cofactors). The value of Zn sensitivity was used after logarithmic transformation. SNPs with minor allele count (MAC) ≥ 15 were presented. The 5% FDR threshold is denoted by a dashed line. D-F, QQ-plots of GWA mapping with AMM model.



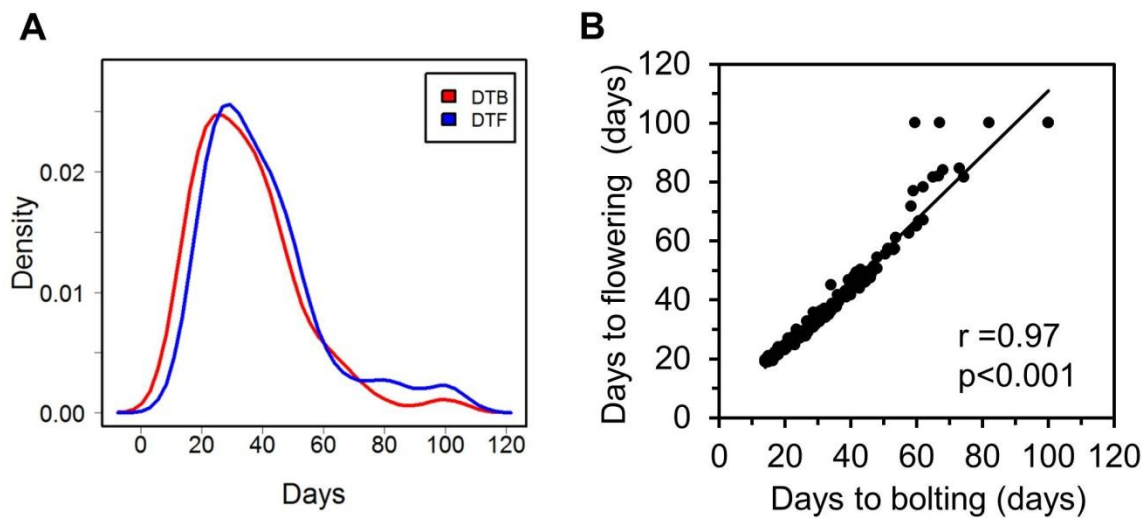
Supplementary Figure S4: QQ-plot and LD mapping plot from GWAS with co-factors for Zn sensitivity. A, QQ-plot from AMM model. **B**, LD values (r^2) between identified SNP (*1G_24327565*) and *FT* (*AT1G65480*, *Chr1:24331428..24333934*). Two SNPs locate in genebody of *FT* were also presented. r^2 was 0.491 between *1G_24327565* and *1G_24333548*. r^2 lower than 0.3 was colored with blue.



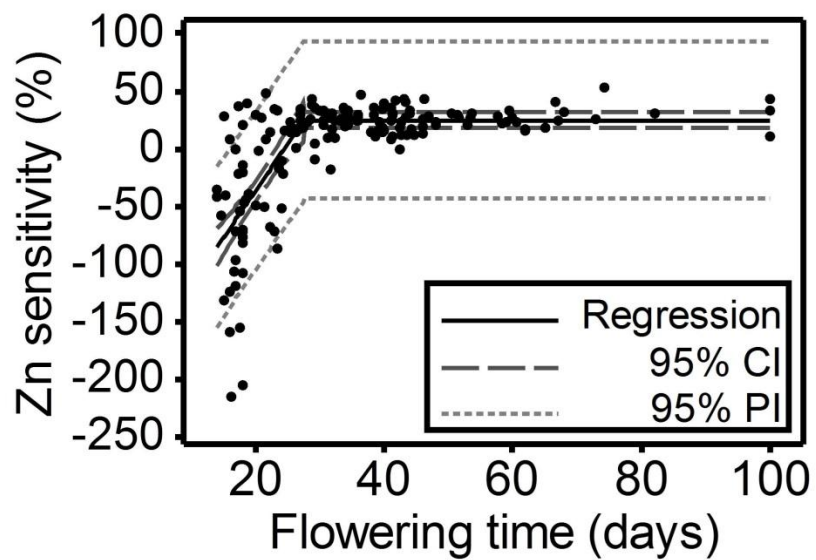
Supplementary Figure S5: Gene ontology enrichment analysis for cellular component (A), molecular function (B), and biological process (C). The figures depict the fractions of genes from a list including 50 top genes, which were generated from GWA. The selected genes located within ± 20 kb of the SNPs with $-\log_{10}(p_value) > 5$. Reference genome: TAIR 10.



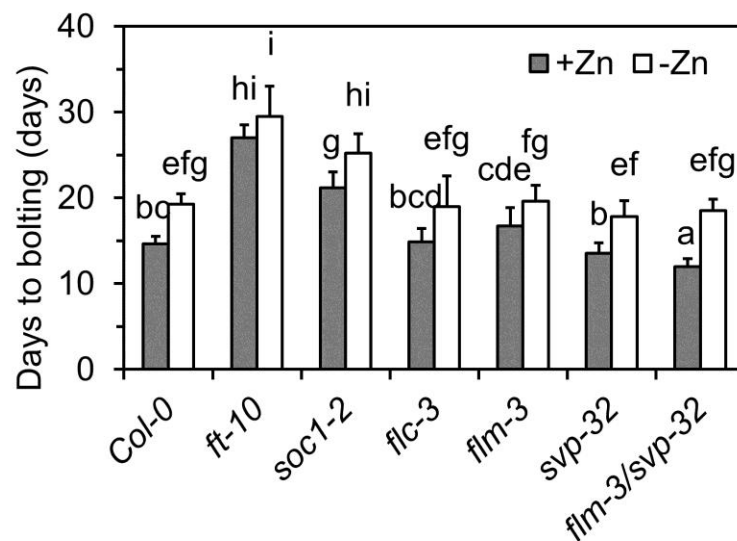
Supplementary Figure S6: *SOC1* transcript levels in negative (Col-0, Po-0, Ct-1, No-1) and positive accessions (Lerik1-3, Koz-2, Sf-2, Cvi-0). Data were referenced to reference genes *SAND* and *PDF2*. Values were mean + SD. * denotes $p < 0.05$.



Supplementary Figure S7: Distribution and correlation of days to bolting and days to flowering. DTB and DTF indicate days to bolting and days to flowering, respectively.



Supplementary Figure S8: Relationship of flowering time and Zn sensitivity. Flowering time was documented as the days to bolting. CI and PI indicate confidence interval and prediction interval.



Supplementary Figure 9: Days to bolting for wild-type (Col-0) and flowering null mutants. Different small letters between columns denote significant difference at p<0.05 level. Data plotted are mean + SD.

Supplementary Table S1: List of all accessions used in this study.

Number	Name	GWAS_ID	NASC_ID	Origin
1	Ag-0	6897	22630	France
2	Aitba-2	98034	76347	Tunesia
3	Ak-1	6987	6602	Germany
4	Alc-0	6988	1656	Spain
5	Altenb-2	98020	76353	Italy
6	Altenb-3			Italy
7	An-1	6898	6603	Belgium
8	Angel-1	98046	76362	Italy
9	Angit	98047	76366	Italy
10	Apost-1	98048	76368	Italy
11	Bay-0	6899	22633	Germany
12	Bil-7	6901	22579	Sweden
13	Bla-1	7015	970	Spain
14	Bla-11	7017	985	Spain
15	Bolin-1	98024	76373	Romania
16	Bor-1	5837	22590	Czech Republic
17	Bor-4	6903	22591	Czech Republic
18	Borsk-2	98039	76421	Russia
19	Bozen-1	98021	76357	Italy
20	Bozen85			Italy
21	Bur-0	5719	22656	Ireland
22	C24	6906	22620	Portugal
23	Can-0	8274	1064	Canary Islands
24	Caste25			Italy
25	Caste37			Italy
26	Castelfed-4	98025	76355	Italy
27	CIBC-17	6907	22603	United Kingdom
28	Ciste-1	98049	76359	Italy
29	Ciste-2	98050	76360	Italy
30	Co-2	7078	1086	Portugal
31	Col-0	6909	22625	Poland
32	Copac-1	98038	76420	Romania
33	Ct-1	6910	N6674	Italy
34	Cvi-0	6911	902	Cape Verdi
35	Del-10	9230	28890	Serbia
36	Dobra-1	98033	76369	Serbia

Supplementary Table S1 Continued.

Number	Name	GWAS_ID	NASC_ID	Origin
37	Dog-4	9060	76386	Turkey
38	Eden-1	6009	22572	Sweden
39	Edi-0	6914	N6688	Scotland
40	Est-1	6916	22629	Estonia
41	Fei-0	8215	22645	Portugal
42	Ga-0	6919	22634	Germany
43	Galdo-1	98005	76423	Italy
44	Gie-0	7147	6720	Germany
45	Got-22	6920	22609	Germany
46	Got-7	6921	22608	Germany
47	Gu-0	6922	22617	Germany
48	Guntschnna-1			Italy
49	Gy-0	8214	22631	France
50	Hi-0	8304	N6736	Netherlands
51	HKT2-4	98004	76404	Germany
52	HR-10	6923	22597	United Kingdom
53	HR-5	6924	22596	United Kingdom
54	Jablo-1	98032	76372	Greece
55	Kidr-1	98042	76376	Russia
56	Kin-0	6926	22654	Lithuania
57	Kly-1	753	9630	Russia
58	Kn-0	7186	N6762	Lthuania
59	Knox-10	6927	22566	USA
60	Knox-18	6928	22567	UAS
61	Koch-1	9185	22823	Ukraine
62	Kondara	6929	22651	Tajikistan
63	Koz-2	98015	9637	Russia
64	Kr-0	7201	1296	Germany
65	Krazo-2	98043	76422	Russia
66	Kurta1441			Italy
67	Kurta1532			Italy
68	Kurta16313			Italy
69	Kz-1	6930	22606	Kazakhstan
70	Kz-9	6931	22607	Kazakhstan
71	Laats335			Italy
72	Lago-1	98006	76367	Italy
73	Leb-3		9641	Russia

Supplementary Table S1 Continued.

Number	Name	GWAS_ID	NASC_ID	Origin
74	Lecho-1	98045	76371	Bulgaria
75	Ler-1	6932	22618	Poland
76	Lerik1-3	9074	22712	Azerbaijan
77	LL-0	6933	22650	Spain
78	LI-1	7238	1341	Spain
79	Lp2-2	7520	22594	Czech Republic
80	Lp2-6	7521	22595	Czech Republic
81	Lz-0	6936	22615	France
82	Mammo-1	98007	76365	Italy
83	Mammo-2	98008	76364	Italy
84	Mer-6	98053	76414	Spain
85	Mitt103			Italy
86	Mitt113			Italy
87	Mitt62212			Italy
88	Mitt8324			Italy
89	Mitt9311			Italy
90	Mitterberg-1	98023	76354	Italy
91	Monte-1	98009	76361	Italy
92	Moran-1	98010	76363	Italy
93	Mr-0	7522	22640	Italy
94	Mrk-0	6937	22635	Germany
95	Ms-0	6938	22655	Russia
96	Mt-0	6939	1380	Libya
97	Mz-0	6940	22636	Germany
98	N13	7438	22491	Russia
99	N7	7449	22485	Russia
100	Nd-1	6942	22619	Germany
101	NFA-8	6944	22598	United Kingdom
102	Nie1-2	98054	76402	Germany
103	No-0	7275	3081	Germany
104	Oy-0	6946	22658	Norway
105	Petergof	7296	926	Russia
106	Petro-1	98028	76370	Serbia
107	Pla-0	7300	6834	Spain
108	Pla-1	7301	1461	Spain
109	Pla-3	7303	1464	Spain
110	Pna-10	7526	22571	USA

Supplementary Table S1 Continued.

Number	Name	GWAS_ID	NASC_ID	Origin
111	Pna-17	7523	22570	USA
112	Po-0	7308	6839	Germany
113	Pu2-23	6951	22593	Czech Republic
114	Pu2-7	6956	22592	Czech Republic
115	Ra-0	6958	22632	France
116	Ren-1	6959	22610	France
117	Ren-11	6960	22611	France
118	Rmx-A02	7524	22568	USA
119	Rmx-A180	7525	22569	USA
120	Rovero-1	98027	76351	Italy
121	Roverod26			Italy
122	RRS-10	7515	22565	USA
123	RRS-7	7514	22564	USA
124	Rsch-4	8374	6850	Russia
125	Se-0	6961	22646	Spain
126	Sf-2	7328	1517	Spain
127	Sha	98059	6180	Tadjikistan
128	Shigu-2	98041	76374	Russia
129	Sij-1	98017	76379	Usbekistan
130	Sij-2	98018	76380	Usbekistan
131	Sij-4	98019	9656	Usbekistan
132	Slavi-1	98031	76419	Bulgaria
133	Sorbo	6963	22653	Tajikistan
134	Sq-1	6966	22600	United Kingdom
135	Sq-8	6967	22601	United Kingdom
136	Star-8	98060	76400	Germany
137	Stepn-1	98037	76378	Russia
138	Stepn-2	98036	76377	Russia
139	Tamm-2	6968	22604	Finland
140	Timpo-1	98011	76424	Italy
141	Toufl-1	98035	76348	Morocco
142	Ts-1	6970	22647	Spain
143	Ts-5	6971	22648	Spain
144	Tsu-0	7373	6874	Japan
145	Tsu-1	6972	22641	Japan
146	Tu-SB30-3	98061	76403	Germany
147	UII2-3	6973	22587	Sweden

Supplementary Table S1 Continued.

Number	Name	GWAS_ID	NASC_ID	Origin
148	Uod-1	6975	22612	Austria
149	Uod-7	6976	22613	Austria
150	Van-0	6977	22627	Canada
151	Vash-1	9116	22754	Georgia
152	Vezza63			Italy
153	Vezzano-2	98029	76349	Italy
154	Voeran-1	98044	76352	Italy
155	Wa-1	6978	1587	Poland
156	Wal-HasB-4	98066	76408	Germany
157	Wei-0	6979	22622	Switzerland
158	Wil-2	7413	6889	Russia
159	WS	7397		Russia
160	Ws-0	6980	1602	Russia
161	Wt-5	6982	22637	Germany
162	Wu-0		6897	Germany
163	Xan-1	9065	76387	Azerbaijan
164	Yeg-1	9127	76394	Armenia
165	Yo-0	6983	1623	USA
166	Zdr-1	6984	22588	Czech Republic
167	Zdr-6	6985	22589	Czech Republic
168	Zu-0	7417	6902	Germany

Supplementary Table S2: Summary of rosette size in +Zn and -Zn.

	Accessions	Mean (cm)	Median (cm)	Standard deviation	Minimum	Maximum	Heritability
+Zn	168	8.04	8.86	2.53	1.3	12.6	0.69
-Zn	168	6.82	6.94	1.22	2.3	9.6	0.38

Supplementary Table S3: One-way anova of rosette size in +Zn and -Zn.

	Source	Df	Sum square	Mean square	F value	Pr(>F)	Phenotype variance	Genotype variance	Residual error
+Zn	Genotypes	167	5453	32.65	14.47	<2e-16	7.33	5.07	2.26
	Residuals	709	1599	2.26					
-Zn	Genotypes	167	1309	7.84	4.71	<2e-16	2.69	1.03	1.66
	Residuals	729	1213	1.66					

Supplementary Table S4: Cofactors in step-wise GWAS and explained variance.

Step	Chromosome	Position	% var. explained	% gen. var. remaining	% err. var. remaining
0			0	0.86	0.14
1	1	23946852	0.33	0.55	0.12
2	1	16581335	0.48	0.37	0.15
3	2	19572960	0.59	0.27	0.14
4	1	24327565	0.74	0.03	0.23

Supplementary Table S5: Significant SNPs identified in GWA.

Chromosome	SNP	Phenotype	-log ₁₀ (p)	MAC
1	4325711	Zn sensitivity	6.37	17
1	16581335	Zn sensitivity/Zn sensitivity_stepwise	6.49/10.21	15
1	23253933	Zn sensitivity	5.94	30
1	23946852	Zn sensitivity/Zn sensitivity_stepwise	7.37/12.89	19
1	24327565	Zn sensitivity_stepwise	7.51	22
1	27415858	Zn deficiency	6.64	55
2	8932364	Zn sensitivity	5.94	15
2	19572960	Zn sensitivity/Zn sensitivity_stepwise	5.46/8.81	23
3	22959554	Zn sensitivity	6.37	20
4	627989	Zn sensitivity	5.80	21
4	1292368	Zn sensitivity	7.10	25
4	16195683	Zn deficiency	6.71	19
5	5918773	Zn sensitivity	5.96	33
5	10138088	Zn sensitivity	5.48	19
5	10499501	Zn sensitivity	6.83	39
5	16773585	Zn sensitivity	8.62	22
5	18589544	Zn sensitivity	6.34	15
5	21365007	Zn sensitivity	5.40	34
5	21393570	Zn sensitivity	5.91	15
5	21416265	Zn sensitivity	5.49	18

Note: MAC, minor allele count

Supplementary Table S6: List of genes used for enrichment analysis.

Number	AGI code	Number	AGI code	Number	AGI code
1	<i>AT1G64430</i>	18	<i>AT1G65470</i>	35	<i>AT4G01535</i>
2	<i>AT1G64440</i>	19	<i>AT1G65480</i>	36	<i>AT4G01540</i>
3	<i>AT1G64450</i>	20	<i>AT1G65481</i>	37	<i>AT4G01550</i>
4	<i>AT1G64460</i>	21	<i>AT1G65483</i>	38	<i>AT4G01560</i>
5	<i>AT1G64470</i>	22	<i>AT2G47700</i>	39	<i>AT4G01570</i>
6	<i>AT1G64480</i>	23	<i>AT2G47710</i>	40	<i>AT4G01575</i>
7	<i>AT1G64490</i>	24	<i>AT2G47720</i>	41	<i>AT4G01580</i>
8	<i>AT1G64500</i>	25	<i>AT2G47730</i>	42	<i>AT4G01590</i>
9	<i>AT1G64510</i>	26	<i>AT2G47750</i>	43	<i>AT4G01595</i>
10	<i>AT1G64520</i>	27	<i>AT2G47760</i>	44	<i>AT4G01600</i>
11	<i>AT1G64530</i>	28	<i>AT2G47770</i>	45	<i>AT4G01610</i>
12	<i>AT1G43780</i>	29	<i>AT2G47780</i>	46	<i>AT4G01630</i>
13	<i>AT1G43790</i>	30	<i>AT2G47790</i>	47	<i>AT4G01640</i>
14	<i>AT1G43800</i>	31	<i>AT2G47800</i>	48	<i>AT4G01650</i>
15	<i>AT1G43810</i>	32	<i>AT2G47810</i>	49	<i>AT5G27880</i>
16	<i>AT1G65440</i>	33	<i>AT2G47820</i>	50	<i>AT5G27889</i>
17	<i>AT1G65450</i>	34	<i>AT2G47830</i>	51	<i>AT5G27890</i>

Supplementary Table S7: List of primers used in qRT-PCR.

Gene	Primer orientation	Primer sequence
<i>FT</i>	Forward	5'-GGTGGAGAAGACCTCAGGAAC-3'
	Reverse	5'-TCAGTCACCAACCAATGGAGAT-3'
<i>SOC1</i>	Forward	5'-TGGTGAGGGGCAAACTCAG-3'
	Reverse	5'-CAGCATCACAAAGCACTGAGAG-3'
<i>FLC</i>	Forward	5'-GCCACCTTAAATCGGCGGTTG-3'
	Reverse	5'-CACAAAGTCTCTTGGCCAAAGAGAGAG-3'
<i>FLM</i>	Forward	5'-CTTCCTCCGGTGACGACATT-3'
	Reverse	5'-AGGCTCTAAGTTCATCAGCATGT-3'
<i>SVP</i>	Forward	5'-CGGAAAACGTTCGAGTTCTGT-3'
	Reverse	5'-CTGTTCTCAACCAGCTGTAAC-3'
<i>CO</i>	Forward	5'-AGCCCCTTCTTTCAGATACCAG-3'
	Reverse	5'-TGCCCTGTTGTTCTCTCCAC-3'
<i>TPS1</i>	Forward	5'-GAAACTCAAGACGTCCTTCACCAG-3'
	Reverse	5'-TCTAGCATTGGTGCGAGTACG AC-3'
<i>GA4</i>	Forward	5'-CAACATCACCTCAACTACTGCGAT-3'
	Reverse	5'-TTCGCTGACCCCAAGTGAAT-3'
<i>FTM1</i>	Forward	5'-GTTTACCGACCAGGTTTCGTG-3'
	Reverse	5'-CTCGTCCCTTACGCCATCAA-3'
<i>ZIP1</i>	Forward	5'-TGGATGTTTTTCGGCAACAAC-3'
	Reverse	5'-CGCTTTCTCTGCTTCGTCTTG-3'
<i>ZIP4</i>	Forward	5'-GATCTTCGTCGATGTTCTTTGG-3'
	Reverse	5'-TGAGAGGTATGGCTACACCAGCAGC-3'
<i>ZIP5</i>	Forward	5'-TGAGATAAATACATCGATCACTCCC-3'
	Reverse	5'-CACTCGCATTTAGACTCGCC-3'
<i>IRT3</i>	Forward	5'-TCTCTCAGCAACAGAGTCCAT-3'
	Reverse	5'-GACGGTTCCTGCCAATGAGT-3'
<i>SAND</i>	Forward	5'-AACTCTATGCAGCATTTGATCCACT-3'
	Reverse	5'-TGATTGCATATCTTTATCGCCATC-3'
<i>PDF2</i>	Forward	5'-TAACGTGGCCAAAATGATGC-3'
	Reverse	5'-GTTCTCCACAAC^CGCTTGGT-3'

6 Chapter III

Natural genetic variation of seed micronutrients of *Arabidopsis thaliana* grown in zinc-deficient and zinc-amended soil

Xiaochao Chen¹, Lixing Yuan² and Uwe Ludewig^{1*}

¹Institute of Crop Science, Nutritional Crop Physiology, University of Hohenheim, Stuttgart, Germany

²Key Laboratory of Plant-Soil Interaction, Ministry of Education, Center for Resources, Environment and Food Security, College Resources and Environmental Sciences, China Agricultural University, Beijing, China

Abstract

The quality of edible seeds for human and animal nutrition is crucially dependent on high zinc (Zn) and iron (Fe) seed concentrations. The micronutrient bioavailability is strongly reduced by seed phytate that forms complexes with seed cations. Superior genotypes with increased seed Zn concentrations had been identified, but low micronutrient seed levels often prevail when the plants are grown in Zn-deficient soils, which are globally widespread and correlate with human Zn-deficiency. Here, seed Zn concentrations of *Arabidopsis* accessions grown in Zn-deficient and Zn-amended conditions were measured together with seed Fe and manganese (Mn), in a panel of 108 accessions. By applying genome-wide association, *de novo* candidate genes potentially involved in the seed micronutrient accumulation were identified. However, a candidate inositol 1,3,4-trisphosphate 5/6-kinase 3 gene (*ITPK3*), located close to a significant nucleotide polymorphism associated with relative Zn seed concentrations, was dispensable for seed micronutrients accumulation in Col-0. Loss of this gene in *itpk3-1* did neither affect phytate seed levels, nor seed Zn, Fe, and Mn. It is concluded that large natural variance of micronutrient seed levels is identified in the population and several accessions maintain high seed Zn despite growth in Zn-deficient conditions.

Front. Plant Sci., 26 July 2016 | <http://dx.doi.org/10.3389/fpls.2016.01070>

7 General discussion

7.1 How to limit Zn bioavailability in *Arabidopsis*?

As a micronutrient, a small amount of Zinc (Zn) is enough for plant growth and development; 20 $\mu\text{g g}^{-1}$ Zn was reported to be sufficient for adequate plant growth (Marschner, 2012). Thus it is a problem to achieve a Zn-deficiency effect in small-biomass plants like *Arabidopsis thaliana*. In addition, chemicals and water inevitably contain Zn though distilled water was used. Our nutrient analyses also found that around 40 $\mu\text{g g}^{-1}$ Zn exists in *Arabidopsis* seeds across around 100 accessions (Chen et al., 2016). Such amount of Zn may also be sufficient to support plant growth for some time. In this case, first problem I had to solve was how to reduce Zn concentrations in *Arabidopsis*.

Hydroponic culture is an ideal solution to perform nutrient experiments as the nutrient components are concisely controlled, and it is beneficial for root analysis. So in most cases, root experiments were conducted in hydroponic culture when investigating nutrient functions, such as for nitrogen and phosphorus (Gruber et al., 2013; Wang et al., 2014; Yang et al., 2015). Whereas soil culture is able to represent natural conditions and limits nutrient bioavailability as well. In this study, I used hydroponic system for the first experiment due to the required sequencing of root samples. For the second and third experiments, soil culture was performed as I just investigated leaves, flowers and seeds; and Zn bioavailability was also more limited in soils.

In addition to the culture medium, another factor to be considered was to select a proper accession. In the first experiment, I selected a late-flowering accession Sf-2 for microarray analysis and whole-genome bisulfite sequencing, as which produces a higher biomass to dilute Zn concentration in plants. Whereas in other experiments, Col-0 was chosen for detailed genetic validation, as the specific mutants are available in Col-0 background.

7.2 How to perform a powerful GWAS?

As an outstanding output of next-generation sequencing, genome-wide association study (GWAS) is becoming a straightforward tool in identification of causal genetics for interested biological questions (Nordborg and Weigel, 2008; Weigel, 2012; Ogura and Busch, 2015). In *Arabidopsis*, the landmark GWAS was conducted by Atwell *et al.* (2010) on 107 phenotypes, using 126,130 SNPs and 96-199 natural accessions (Atwell *et al.*, 2010). The diverse set of phenotypes was related to flowering, ionomics, development and disease resistance. Since then, a series of GWAS were performed on *Arabidopsis*, especially in the field of leaf nutrients and flowering time (Baxter *et al.*, 2010; Brachi *et al.*, 2010; Li *et al.*, 2010; Chao *et al.*, 2012; Chao *et al.*, 2014a; Meijón *et al.*, 2014; Chao *et al.*, 2014b; Rooijen *et al.*, 2015). However, not all analyses provided powerful associations, as the GWAS results rely on the applied population size and traits. If a trait is controlled by a small number of large-effect loci, then the loci are likely identified with a small panel of accessions. However, many traits are regulated by a large number of small-effect loci. In this case, large population can be used to improve the association power (Korte and Farlow, 2013; Ogura and Busch, 2015). In most cases, over 300 accessions were used for a successful GWAS in *Arabidopsis* (Li *et al.*, 2010; Baxter *et al.*, 2012; Chao *et al.*, 2014a; Chao *et al.*, 2014b), but in our study, the plant materials were limited and just 168 *Arabidopsis* accessions were available. Nevertheless, 96 accessions have also been reported to be successful in some cases (Atwell *et al.*, 2010). Therefore, I just used this small panel for all GWAS.

With 147 accessions, GWAS did not produce any significant SNP ($p < 0.05$) for rosette size under +Zn (control) soil, but 2 SNPs under -Zn (deficiency) soil. Then the Zn sensitivity was calculated, which indicates the relative reduction of rosette size due to Zn deficiency. Interestingly, 17 significant SNPs were identified by GWAS for Zn sensitivity. As a more Zn-specific trait, Zn sensitivity greatly increased the power in GWAS. However, significant SNPs were more difficult to generate in seed nutrient experiment. The reason might be that the used panel was only around 100 accessions, which strongly limited the

association power. Alternatively, seed nutrient is a more complicated trait to identify the underlying genetics, as its accumulation depends on a series of complex processes: the ion bioavailability in soils, uptake efficiency by roots, translocation to shoot and loading into seeds (Grusak and DellaPenna, 1999; Olsen and Palmgren, 2014). Hence, the only significant SNP produced by GWAS was conducted for relative Zn concentration. Relative Zn was calculated as $Zn / (Zn + Fe + Mn)$, which is likely to reflect the correlation between Zn and other two micronutrients Fe and Mn, especially Fe, as it is extremely higher than Mn.

7.3 How does *Arabidopsis thaliana* respond to Zn deficiency?

Plants have developed a series of strategies to adapt to environmental stress, such as nutrient deficiencies. Plant roots show a strong morphological plasticity in response to nutrient deficiencies (Gruber et al., 2013). For example, phosphorus (P) deficiency produced a shallower but more highly branched root system. In addition, P deficiency decreased the lateral root length of first order, but increased that of second order (Gruber et al., 2013). In regard of Zn, Gruber *et al.* (2013) reported that primary root length was unaffected by Zn deficiency, whereas Jain *et al.* (2013) showed a reduction of primary root length under Zn deficiency condition (Gruber et al., 2013; Jain et al., 2013). The inconsistent conclusions indicate the complexity of Zn-deficiency experiments in practice. Nevertheless, both studies presented an increment of lateral root density, especially the first order lateral roots. Despite the limit responses in the root system to Zn deficiency, transcriptional changes still widely occur in roots (Grotz et al., 1998; Mortel et al., 2006; Krämer et al., 2007; Lin et al., 2009; Assunção et al., 2010). Together with transcriptional responses, I further investigated epigenetic changes in roots. Moreover, responses in flowering time, leaf size and seed mineral nutrients were also analyzed.

7.3.1 Transcriptional and epigenetic responses to Zn deficiency in roots

Previous microarray analysis identified over 300 differentially expressed transcripts in response to Zn deficiency (Mortel et al., 2006). The limited identification in this study might be a consequence of the heterogeneity among the three biological replicates. Indeed, another 50 transcripts, including additional Zn transporters, appeared in regard of 4-fold expression intensity between two Zn treatments, irrespective of the adjusted p value which was set as 0.05 before. On the other hand, the relatively late harvest developmental stage (long days in this study, compared to short days in the previous microarray analysis (Mortel et al., 2006)), potentially induced nutrient reallocation to the following reproductive growth. Secco *et al.* (2015) also found that large amount phosphate-deficiency responsive genes were recovered at 52 days compared to 21 days due to floral transition in rice (Secco et al., 2015). Nevertheless, this study still presented 15 differentially expressed transcripts in adaptation to Zn deficiency.

ZIP (*ZRT*, *IRT-LIKE PROTEIN*) family genes are important Zn transporters in *Arabidopsis*, including *ZIP1* to *ZIP5*, *ZIP9* to *ZIP12* and *IRT3*, which were highly expressed under Zn deficiency (Grotz et al., 1998; Guerinot, 2000; Mortel et al., 2006; Krämer et al., 2007; Lin et al., 2009). In addition to *ZIP*, *HMA2* (*HEAVY METAL ATPASE 2*) and *HMA4* are known to be involved in the Zn loading from root symplast to xylem (Olsen and Palmgren, 2014). Indeed, microarray analysis and qRT-PCR results found that the expression levels of *ZIP1*, *ZIP3*, *ZIP4*, *ZIP5*, *IRT3* and *HMA2* were increased under Zn deficiency condition in roots. Further, *NAS2* (*NICOTIANAMINE SYNTHASE 2*) and *NAS4* were characterized as well in microarray analysis, because Zn-nicotianamine complex is the major form to travel Zn (Mortel et al., 2006; Deinlein et al., 2012; Clemens et al., 2013). Interestingly, four defensin-like proteins were strongly up-regulated upon Zn deficiency. There is limited research about why and how these genes function biologically to regulate the Zn uptake (Zargar et al., 2014). However, I found that these defensin-like genes contain the specific Zn binding motif in promoters (unpublished data). The motif (RTGTCGACAY) was identified by Assunção *et al.* (2010), which was bound by transcription factors *BZIP19* (*BASIC-REGION*

LEUCINE ZIPPER 19) and *BZIP23* (Assunção et al., 2010). Therefore, these defensin-like genes are likely non-functional, which are just recognized by *trans-acting* elements in response to Zn deficiency. Another up-regulated transcript is *PAP27* (*PURPLE ACID PHOSPHATASE 27*), which was also reported previously in Zn-deficiency studies, but the biological function remains unclear (Mortel et al., 2006; Assunção et al., 2010). Surprisingly, *TFL1* (*TERMINAL FLOWER 1*) was significantly down-regulated in roots under Zn deficiency. *TFL1* acts as a floral inhibitor and controls plant architecture in *Arabidopsis* (Bradley et al., 1997; Ratcliffe et al., 1998; Ferrandiz et al., 2000; Kim et al., 2013). However, this study did neither identify floral promotion nor leaf architecture alteration under Zn deficiency.

Gene transcription is regulated by several epigenetic mechanisms, including DNA methylation, histone modifications and small-interfering RNA (siRNA) pathways (Henderson and Jacobsen, 2007; Zhang, 2008; Chen, 2009; Liu et al., 2010; He et al., 2011). To understand how epigenetics affect gene transcription upon Zn deficiency, this study also investigated the single base-resolution DNA methylome via whole-genome bisulfite sequencing. A similar study was conducted in phosphate (P) deficiency in rice previously (Secco et al., 2015). P deficiency drove DNA hypermethylation in transposable elements (TEs) that are proximal to the P deficiency responsive genes; and those hypermethylation predominantly occurred in CHH contexts. The *de novo* CHH methylation was reported to be more flexible to environmental stress (Downen et al., 2012; Dubin et al., 2015). However, Zn deficiency eliminated DNA methylation in TEs (all contexts) and gene bodies (CpG contexts) as well. These observations implicated nutrient-specific and species-specific effects on the DNA methylation response. Moreover, limited contribution of Zn deficiency-induced DNA demethylation to gene transcription was observed. The independence of DNA methylation and gene transcription in this case implied either the Zn-specific effect, or showed consistency to the finding that methylation is a consequence of transcription rather than a cause (Teixeira and Colot, 2009; Inagaki and Kakutani, 2012). Another example is that the *Arabidopsis* accession Cvi-0 presented much

less methylation, but a similar whole-genome transcription level, in comparison to other accessions (Kwak et al., 2016).

Overall, this study successfully presented Zn-deficiency effect in *Arabidopsis*, which was confirmed via the microarray analysis. However, the correlation between DNA methylation and gene transcription in response to Zn deficiency was complex.

7.3.2 Zn-dependence of flowering and leaf size

A basic principle of plant nutrition is that plants produce maximal biomass when all nutrients are adequately supplied (Marschner, 2012). Indeed, I found that 67% of *Arabidopsis* accessions (126 of 168) produced larger leaf size under adequate Zn condition, whereas the other 42 accessions produced larger leaf size under Zn deficiency condition. By performing genome-wide association mapping, *FT* (*FLOWERING LOCUS T*) was identified regulating the abnormal Zn regulation. *FT* is the central floral integrator in *Arabidopsis*, which is a floral promoter (Kim et al., 2009; Fornara et al., 2010; Jarillo and Piñero, 2011). These results indicated that flowering is involved in Zn-dependence of leaf growth. Hence I further determined the relationship between flowering time and leaf size, two traits with typically minor correlation (Levey and Wingler, 2005; Atwell et al., 2010). Interestingly, positive correlation only existed between two traits in 71 early-flowering accessions, suggesting that plants grew larger leaf when flowered later in early-flowering *Arabidopsis*. Therefore, I further asked how Zn regulates flowering and leaf size genetically.

The transition to flowering is controlled by several pathways, such as photoperiod, temperature, vernalization, gibberellin and sugar pathways (Searle and Coupland, 2004; Fornara et al., 2010; Capovilla et al., 2014; Bouché et al., 2016). In addition to these canonical pathways, nutrient deficiency was another environment cue affecting flowering time. For example, the macronutrients nitrate and phosphate act in an antagonistic way, as nitrate deficiency promotes and low phosphate delays flowering in *Arabidopsis* (Kant et al., 2011). Notably, this study found that Zn deficiency inhibited flowering in *Arabidopsis* in soil condition where

is more efficient to limit Zn bioavailability. Zn-dependence of flowering was not regulated by those canonical flowering pathways, revealed by the qRT-PCR results. However, the flowering regulation by Zn only occurred in early-flowering *Arabidopsis* accessions (such as Col-0). The flowering time was unaffected by Zn stress in natural late-flowering accessions (such as Sf-2), or artificial late-flowering plants (Col-0 grown in low temperature). On the other hand, in the artificial early-flowering plants (Sf-2 grown after vernalization), Zn deficiency again repressed flowering time. Due to the inhibition of flowering time under Zn deficiency, vegetative growth was prolonged resulting in a large leaf size. Loss of the *FT* in *ft-10* mutant plants, Zn-dependence of flowering and leaf size was eliminated.

Final leaf size are ultimately controlled by the complex coordination of primordium size, cell proliferation and cell expansion (Gonzalez et al., 2012; Powell and Lenhard, 2012). To get insight into the underlying mechanism behind the promoted leaf in lower *FT* plants induced by Zn deficiency, the leaf length, petiole and cell sizes were documented during leaf growth. Interestingly, leaf size and petiole size started to be distinguishable between Zn treatments unless plants flowered, consistent with the repressing signal of leaf growth when flowering. Moreover, the difference in leaf size was proved to be causal from cell number, but not cell size via microscope confocal images. As generally nutrient deficiencies promote flowering in *Arabidopsis* (Kolář and Seňková, 2008), the observed flowering delay and leaf size promotion may be Zn-specific. Taken together, I concluded that Zn deficiency inhibited *FT* expression resulting in late flowering; as flowering inhibited cell proliferation, hence Zn deficiency promoted leaf size.

7.3.3 Seed Zn accumulation under adverse Zn deficiency condition

Hidden hunger is becoming a major threat to human, due to the malnutrition and micronutrient deficiencies (e.g. Zn and Fe) in diets. Available seed Zn concentration is strongly restricted by soil Zn deficiency, elevated CO₂ and phytate (Cakmak, 2007; Alloway, 2008; Raboy, 2009; Lei et al., 2013; Loladze,

2014; Myers et al., 2014). Indeed, this work presented that soil Zn deficiency reduced seed Zn concentration from 47.4 $\mu\text{g g}^{-1}$ to 31.3 $\mu\text{g g}^{-1}$ across around 100 *Arabidopsis* accessions. Interestingly, few accessions still maintained seed Zn levels under Zn deficiency. For example, Zn concentration of Ts-1 was 37.16 $\mu\text{g g}^{-1}$ and 39.33 $\mu\text{g g}^{-1}$ in +Zn (control) and in -Zn (deficiency), respectively. This implied that there are genetic backgrounds in which high Zn is maintained in seeds even under -Zn growth. How these genotypes manage higher seed Zn is an interesting target for future research, to genetically improve the seed Zn content in the adverse Zn deficiency condition. Substantial natural variation in seed Zn concentration was found under both Zn conditions, providing the possibility to identify the underlying genetics. However, genome-wide association mapping did not yield any significant SNP in regulating seed Zn. The limited power in association mapping might be attributed to the small panel of accessions used in this study, whereas the seed nutrient is a complicated trait controlled by a series of processes, which is likely controlled by many small-effect loci (Olsen and Palmgren, 2014; Ogura and Busch, 2015).

Together with Zn, Fe and Mn concentration were analyzed as well. It was expected that Zn deficiency increases the Fe and Mn accumulation (especially Fe), as they partially share the same transporters. For example, Fe transporter *IRT3* (*IRON REGULATED TRANSPORTER 3*) is also overexpressed in roots under Zn deficiency conditions (Mortel et al., 2006; Lin et al., 2009). However, this was observed only in part of accessions, suggesting that the ultimate nutrients accumulation in seeds is more complicated than the root uptake. Similarly, previous reports found that the concentrations of *Arabidopsis* leaf minerals are a poor proxy for seed minerals (Ghandilyan et al., 2009; Baxter et al., 2012).

Nevertheless, association mapping still identified *ITPK-3* (Inositol 1,3,4-trisphosphate 5/6-kinase family protein) as the candidate gene affecting Zn accumulation. *ITPK-3* was expected to be ideal as the phytate strongly chelates Zn (Raboy, 2009; Kumar et al., 2010; Lei et al., 2013). However, the *itpk3* mutant

plants maintained Zn and phytate content compared to the wild type. The invalidation revealed that the significant SNP might be false positive due to the limited mapping population size and population structure (Atwell et al., 2010; Platt et al., 2010; Segura et al., 2012; Ogura and Busch, 2015). Alternatively, other neighboring genes are causal for the variation in seed minerals, which cannot be confirmed currently due to the unavailable mutants.

7.4 Future perspectives

The presented findings show that limited contribution of Zn deficiency-induced DNA methylation to gene transcription in roots in *Arabidopsis*. However, it still remains unclear how histone modification and siRNAs affect gene transcription in response to Zn deficiency. siRNAs play crucial roles in establishing *de novo* methylation, thus it might be also repressed by Zn deficiency where DNA methylation is eliminated. Histone modification (as well as chromatin structure) is pretty interesting to be investigated under Zn deficiency due to the specific Zn-finger domain. For example, it was reported that acute dietary Zn deficiency before conception compromises oocyte epigenetic programming and disrupts embryonic development in mice (Tian and Diaz, 2013). There was a dramatic decrease in histone H3K4 trimethylation and global DNA methylation in Zn deficient oocytes. In addition, single-cell epigenetics is particularly informative as the general bisulfite sequencing arbitrarily mixes the epigenetics changes together, whereas the cell-specific effect widely exists in response to environmental conditions. Moreover, the Zn deficiency response motif (RTGTGACAY) is bound by *bzip19* and *bzip23* in response to Zn deficiency, how this motif be methylated is also valuable to investigate in the future. Recently, the 1001 Genomes Consortium published the genome, transcriptome and DNA methylome data in 1135 *Arabidopsis* natural accessions (Alonso-Blanco et al., 2016; Kawakatsu et al., 2016), which will be greatly beneficial to evaluate transcriptional and methylation adaptation in different tissues for different accessions.

General discussion

Nutrient-dependence of flowering time is becoming a very important topic. Here I showed a novel insight in Zn-regulation of flowering time and biomass, which might be just Zn-specific. However, the mechanism of the interaction between Zn and flowering genes is unclear at molecular and biochemical levels, as the Zn-regulation is independent of other canonical flowering pathways. It would be interesting to identify whether it is achieved by epigenetics, such as the repression of *FLC* by histone modifications, the regulation of *SUPERMAN* and *FWA* by DNA methylation.

Superior nutrition of seeds is a vital pursuit for crop breeders and agronomists, but as being limited by the small panel in this study, association mapping did not yield powerful results. Further research can enlarge the mapping population and combine with QTL mapping for stronger identifications. Further, it is particularly essential to “release” the minerals from phytate in seeds and increase the mineral bioavailability. Alternatively, a reduced production of phytic acid without affecting mineral uptake could also prevent Zn malnutrition. Nevertheless, those accessions maintaining seed Zn concentrations under Zn deficiency are worthy to investigate further to potentially overcome Zn deficiency in plants and humans.

8 References

- Alloway** (2008) Zinc in Soils and Crop Nutrition. Wiley-Blackwell, pp 335–375
- Alloway BJ** (2009) Soil factors associated with zinc deficiency in crops and humans. *Environ Geochem Health* **31**: 537–548
- Alonso-Blanco C, Andrade J, Becker C, Bemm F, Bergelson J, Borgwardt KM, Cao J, Chae E, Dezwaan TM, Ding W, et al** (2016) 1,135 Genomes Reveal the Global Pattern of Polymorphism in *Arabidopsis thaliana*. *Cell* **166**: 481–491
- Alonso-Blanco C, El-Assal SE-D, Coupland G, Koornneef M** (1998) Analysis of Natural Allelic Variation at Flowering Time Loci in the Landsberg erecta and Cape Verde Islands Ecotypes of *Arabidopsis thaliana*. *Genetics* **149**: 749–764
- Amasino R** (2004) Vernalization, Competence, and the Epigenetic Memory of Winter. *Plant Cell Online* **16**: 2553–2559
- Amasino R** (2010) Seasonal and developmental timing of flowering. *Plant J* **61**: 1001–1013
- Assunção AGL, Herrero E, Lin Y-F, Huettel B, Talukdar S, Smaczniak C, Immink RGH, Eldik M van, Fiers M, Schat H, et al** (2010) *Arabidopsis thaliana* transcription factors bZIP19 and bZIP23 regulate the adaptation to zinc deficiency. *Proc Natl Acad Sci* **107**: 10296–10301
- Atwell S, Huang YS, Vilhjálmsson BJ, Willems G, Horton M, Li Y, Meng D, Platt A, Tarone AM, Hu TT, et al** (2010) Genome-wide association study of 107 phenotypes in *Arabidopsis thaliana* inbred lines. *Nature* **465**: 627–631
- Balasubramanian S, Sureshkumar S, Lempe J, Weigel D** (2006) Potent Induction of *Arabidopsis thaliana* Flowering by Elevated Growth Temperature. *PLoS Genet* **2**: e106
- Baxter I, Brazelton JN, Yu D, Huang YS, Lahner B, Yakubova E, Li Y, Bergelson J, Borevitz JO, Nordborg M, et al** (2010) A Coastal Cline in Sodium Accumulation in *Arabidopsis thaliana* Is Driven by Natural Variation of the Sodium Transporter AtHKT1;1. *PLOS Genet* **6**: e1001193
- Baxter I, Hermans C, Lahner B, Yakubova E, Tikhonova M, Verbruggen N, Chao D, Salt DE** (2012) Biodiversity of Mineral Nutrient and Trace Element Accumulation in *Arabidopsis thaliana*. *PLoS ONE* **7**: e35121
- Bej S, Basak J** (2014) MicroRNAs: The Potential Biomarkers in Plant Stress Response. *Am J Plant Sci* **05**: 748
- Benjamini Y, Hochberg Y** (1995) Controlling the False Discovery Rate: A Practical and Powerful Approach to Multiple Testing. *J R Stat Soc Ser B Methodol* **57**: 289–300

References

- Bentsink L, Jowett J, Hanhart CJ, Koornneef M** (2006) Cloning of DOG1, a quantitative trait locus controlling seed dormancy in Arabidopsis. *Proc Natl Acad Sci* **103**: 17042–17047
- Bögre L, Magyar Z, López-Juez E** (2008) New clues to organ size control in plants. *Genome Biol* **9**: 226
- Bouché F, Lobet G, Tocquin P, Périlleux C** (2016) FLOR-ID: an interactive database of flowering-time gene networks in Arabidopsis thaliana. *Nucleic Acids Res* **44**: D1167–D1171
- Brachi B, Faure N, Horton M, Flahauw E, Vazquez A, Nordborg M, Bergelson J, Cuguen J, Roux F** (2010) Linkage and Association Mapping of Arabidopsis thaliana Flowering Time in Nature. *PLOS Genet* **6**: e1000940
- Bradley D, Ratcliffe O, Vincent C, Carpenter R, Coen E** (1997) Inflorescence Commitment and Architecture in Arabidopsis. *Science* **275**: 80–83
- Broadley MR, White PJ, Hammond JP, Zelko I, Lux A** (2007) Zinc in plants. *New Phytol* **173**: 677–702
- Buescher E, Achberger T, Amusan I, Giannini A, Ochsenfeld C, Rus A, Lahner B, Hoekenga O, Yakubova E, Harper JF, et al** (2010) Natural Genetic Variation in Selected Populations of Arabidopsis thaliana Is Associated with Ionomic Differences. *PLoS ONE* **5**: e11081
- Buhtz A, Springer F, Chappell L, Baulcombe DC, Kehr J** (2008) Identification and characterization of small RNAs from the phloem of Brassica napus. *Plant J* **53**: 739–749
- Cakmak I** (2007) Enrichment of cereal grains with zinc: Agronomic or genetic biofortification? *Plant Soil* **302**: 1–17
- Capovilla G, Schmid M, Posé D** (2014) Control of flowering by ambient temperature. *J Exp Bot* eru416
- Cardon LR, Palmer LJ** (2003) Population stratification and spurious allelic association. *The Lancet* **361**: 598–604
- Chan SW-L, Henderson IR, Jacobsen SE** (2005) Gardening the genome: DNA methylation in Arabidopsis thaliana. *Nat Rev Genet* **6**: 351–360
- Chao D-Y, Baraniecka P, Danku J, Koprivova A, Lahner B, Luo H, Yakubova E, Dilkes B, Kopriva S, Salt DE** (2014a) Variation in Sulfur and Selenium Accumulation Is Controlled by Naturally Occurring Isoforms of the Key Sulfur Assimilation Enzyme ADENOSINE 5'-PHOSPHOSULFATE REDUCTASE2 across the Arabidopsis Species Range. *Plant Physiol* **166**: 1593–1608
- Chao D-Y, Chen Y, Chen J, Shi S, Chen Z, Wang C, Danku JM, Zhao F-J, Salt DE** (2014b) Genome-wide Association Mapping Identifies a New Arsenate

References

- Reductase Enzyme Critical for Limiting Arsenic Accumulation in Plants. *PLOS Biol* **12**: e1002009
- Chao D-Y, Silva A, Baxter I, Huang YS, Nordborg M, Danku J, Lahner B, Yakubova E, Salt DE** (2012) Genome-Wide Association Studies Identify Heavy Metal ATPase3 as the Primary Determinant of Natural Variation in Leaf Cadmium in *Arabidopsis thaliana*. *PLOS Genet* **8**: e1002923
- Chen X** (2009) Small RNAs and Their Roles in Plant Development. *Annu Rev Cell Dev Biol* **25**: 21–44
- Chen X, Yuan L, Ludewig U** (2016) Natural Genetic Variation of Seed Micronutrients of *Arabidopsis thaliana* Grown in Zinc-Deficient and Zinc-Amended Soil. *Front Plant Sci* **7**: 1070
- Chinnusamy V, Zhu J-K** (2009) Epigenetic regulation of stress responses in plants. *Curr Opin Plant Biol* **12**: 133–139
- Chiou T-J, Aung K, Lin S-I, Wu C-C, Chiang S-F, Su C** (2006) Regulation of Phosphate Homeostasis by MicroRNA in *Arabidopsis*. *Plant Cell* **18**: 412–421
- Clemens S, Deinlein U, Ahmadi H, Höreth S, Uraguchi S** (2013) Nicotianamine is a major player in plant Zn homeostasis. *BioMetals* **26**: 623–632
- Cokus SJ, Feng S, Zhang X, Chen Z, Merriman B, Haudenschield CD, Pradhan S, Nelson SF, Pellegrini M, Jacobsen SE** (2008) Shotgun bisulphite sequencing of the *Arabidopsis* genome reveals DNA methylation patterning. *Nature* **452**: 215–219
- Corbesier L, Vincent C, Jang S, Fornara F, Fan Q, Searle I, Giakountis A, Farrona S, Gissot L, Turnbull C, et al** (2007) FT Protein Movement Contributes to Long-Distance Signaling in Floral Induction of *Arabidopsis*. *Science* **316**: 1030–1033
- Deinlein U, Weber M, Schmidt H, Rensch S, Trampczynska A, Hansen TH, Husted S, Schjoerring JK, Talke IN, Krämer U, et al** (2012) Elevated Nicotianamine Levels in *Arabidopsis halleri* Roots Play a Key Role in Zinc Hyperaccumulation. *Plant Cell* **24**: 708–723
- Dowen RH, Pelizzola M, Schmitz RJ, Lister R, Dowen JM, Nery JR, Dixon JE, Ecker JR** (2012) Widespread dynamic DNA methylation in response to biotic stress. *Proc Natl Acad Sci* **109**: E2183–E2191
- Dubin MJ, Zhang P, Meng D, Remigereau M-S, Osborne EJ, Casale FP, Drewe P, Kahles A, Jean G, Vilhjálmsson B, et al** (2015) DNA methylation in *Arabidopsis* has a genetic basis and shows evidence of local adaptation. *eLife* **4**: e05255
- Du Z, Zhou X, Ling Y, Zhang Z, Su Z** (2010) agriGO: a GO analysis toolkit for the agricultural community. *Nucleic Acids Res* **38**: W64–W70

References

- Ferrandiz C, Gu Q, Martienssen R, Yanofsky MF** (2000) Redundant regulation of meristem identity and plant architecture by FRUITFULL, APETALA1 and CAULIFLOWER. *Development* **127**: 725–734
- Fornara F, de Montaigu A, Coupland G** (2010) SnapShot: Control of Flowering in Arabidopsis. *Cell* **141**: 550–550.e2
- Gaj T, Gersbach CA, Barbas III CF** (2013) ZFN, TALEN, and CRISPR/Cas-based methods for genome engineering. *Trends Biotechnol* **31**: 397–405
- Ghandilyan A, Ilk N, Hanhart C, Mbengue M, Barboza L, Schat H, Koornneef M, El-Lithy M, Vreugdenhil D, Reymond M, et al** (2009) A strong effect of growth medium and organ type on the identification of QTLs for phytate and mineral concentrations in three Arabidopsis thaliana RIL populations. *J Exp Bot* **60**: 1409–1425
- Ghandilyan A, Kutman UB, Kutman BY, Cakmak I, Aarts MGM** (2012) Genetic analysis of the effect of zinc deficiency on Arabidopsis growth and mineral concentrations. *Plant Soil* **361**: 227–239
- Gifford ML, Banta JA, Katari MS, Hulsmans J, Chen L, Ristova D, Tranchina D, Purugganan MD, Coruzzi GM, Birnbaum KD** (2013) Plasticity Regulators Modulate Specific Root Traits in Discrete Nitrogen Environments. *PLOS Genet* **9**: e1003760
- Gonzalez N, Vanhaeren H, Inzé D** (2012) Leaf size control: complex coordination of cell division and expansion. *Trends Plant Sci* **17**: 332–340
- Grotz N, Fox T, Connolly E, Park W, Guerinot ML, Eide D** (1998) Identification of a family of zinc transporter genes from Arabidopsis that respond to zinc deficiency. *Proc Natl Acad Sci* **95**: 7220–7224
- Gruber BD, Giehl RFH, Friedel S, Wirén N von** (2013) Plasticity of the Arabidopsis root system under nutrient deficiencies. *Plant Physiol* pp.113.218453
- Grusak MA, DellaPenna D** (1999) Improving the Nutrient Composition of Plants to Enhance Human Nutrition and Health. *Annu Rev Plant Physiol Plant Mol Biol* **50**: 133–161
- Guerinot ML** (2000) The ZIP family of metal transporters. *Biochim Biophys Acta BBA - Biomembr* **1465**: 190–198
- Hansen KD, Langmead B, Irizarry RA** (2012) BSmooth: from whole genome bisulfite sequencing reads to differentially methylated regions. *Genome Biol* **13**: R83
- He G, Elling AA, Deng XW** (2011) The Epigenome and Plant Development. *Annu Rev Plant Biol* **62**: 411–435
- Henderson IR, Jacobsen SE** (2007) Epigenetic inheritance in plants. *Nature* **447**: 418–424

References

- Hisamatsu T, King RW** (2008) The nature of floral signals in Arabidopsis. II. Roles for FLOWERING LOCUS T (FT) and gibberellin. *J Exp Bot* **59**: 3821–3829
- Holm PB, Kristiansen KN, Pedersen HB** (2002) Transgenic Approaches in Commonly Consumed Cereals to Improve Iron and Zinc Content and Bioavailability. *J Nutr* **132**: 514S–516S
- Hussain D, Haydon MJ, Wang Y, Wong E, Sherson SM, Young J, Camakaris J, Harper JF, Cobbett CS** (2004) P-Type ATPase Heavy Metal Transporters with Roles in Essential Zinc Homeostasis in Arabidopsis. *Plant Cell* **16**: 1327–1339
- Inagaki S, Kakutani T** (2012) What Triggers Differential DNA Methylation of Genes and TEs: Contribution of Body Methylation? *Cold Spring Harb Symp Quant Biol* **77**: 155–160
- Ito T, Sakai H, Meyerowitz EM** (2003) Whorl-Specific Expression of the SUPERMAN Gene of Arabidopsis Is Mediated by cis Elements in the Transcribed Region. *Curr Biol* **13**: 1524–1530
- Jacobsen SE, Meyerowitz EM** (1997) Hypermethylated SUPERMAN Epigenetic Alleles in Arabidopsis. *Science* **277**: 1100–1103
- Jaeger KE, Wigge PA** (2007) FT Protein Acts as a Long-Range Signal in Arabidopsis. *Curr Biol* **17**: 1050–1054
- Jain A, Sinilal B, Dhandapani G, Meagher RB, Sahi SV** (2013) Effects of Deficiency and Excess of Zinc on Morphophysiological Traits and Spatiotemporal Regulation of Zinc-Responsive Genes Reveal Incidence of Cross Talk between Micro- and Macronutrients. *Environ Sci Technol* **47**: 5327–5335
- Jarillo JA, Piñeiro M** (2011) Timing is everything in plant development. The central role of floral repressors. *Plant Sci* **181**: 364–378
- Kant S, Peng M, Rothstein SJ** (2011) Genetic Regulation by NLA and MicroRNA827 for Maintaining Nitrate-Dependent Phosphate Homeostasis in Arabidopsis. *PLOS Genet* **7**: e1002021
- Karan R, DeLeon T, Biradar H, Subudhi PK** (2012) Salt Stress Induced Variation in DNA Methylation Pattern and Its Influence on Gene Expression in Contrasting Rice Genotypes. *PLOS ONE* **7**: e40203
- Kawakatsu T, Huang SC, Jupe F, Sasaki E, Schmitz RJ, Urich MA, Castanon R, Nery JR, Barragan C, He Y, et al** (2016) Epigenomic Diversity in a Global Collection of Arabidopsis thaliana Accessions. *Cell* **166**: 492–505
- Khraiweh B, Zhu J-K, Zhu J** (2012) Role of miRNAs and siRNAs in biotic and abiotic stress responses of plants. *Biochim Biophys Acta BBA - Gene Regul Mech* **1819**: 137–148
- Kim D-H, Doyle MR, Sung S, Amasino RM** (2009) Vernalization: Winter and the Timing of Flowering in Plants. *Annu Rev Cell Dev Biol* **25**: 277–299

References

- Kim W, Park TI, Yoo SJ, Jun AR, Ahn JH** (2013) Generation and analysis of a complete mutant set for the Arabidopsis FT/TFL1 family shows specific effects on thermo-sensitive flowering regulation. *J Exp Bot* ert036
- Klug A** (2010) The Discovery of Zinc Fingers and Their Applications in Gene Regulation and Genome Manipulation. *Annu Rev Biochem* **79**: 213–231
- Kolář J, Seňková J** (2008) Reduction of mineral nutrient availability accelerates flowering of Arabidopsis thaliana. *J Plant Physiol* **165**: 1601–1609
- Korte A, Farlow A** (2013) The advantages and limitations of trait analysis with GWAS: a review. *Plant Methods* **9**: 29
- Krämer U, Talke IN, Hanikenne M** (2007) Transition metal transport. *FEBS Lett* **581**: 2263–2272
- Krueger F, Andrews SR** (2011) Bismark: a flexible aligner and methylation caller for Bisulfite-Seq applications. *Bioinformatics* **27**: 1571–1572
- Kumar V, Sinha AK, Makkar HPS, Becker K** (2010) Dietary roles of phytate and phytase in human nutrition: A review. *Food Chem* **120**: 945–959
- Law JA, Jacobsen SE** (2010) Establishing, maintaining and modifying DNA methylation patterns in plants and animals. *Nat Rev Genet* **11**: 204–220
- Lei XG, Weaver JD, Mullaney E, Ullah AH, Azain MJ** (2013) Phytase, a New Life for an “Old” Enzyme. *Annu Rev Anim Biosci* **1**: 283–309
- Lempe J, Balasubramanian S, Sureshkumar S, Singh A, Schmid M, Weigel D** (2005) Diversity of Flowering Responses in Wild Arabidopsis thaliana Strains. *PLoS Genet* **1**: e6
- Le T-N, Schumann U, Smith NA, Tiwari S, Au PCK, Zhu Q-H, Taylor JM, Kazan K, Llewellyn DJ, Zhang R, et al** (2014) DNA demethylases target promoter transposable elements to positively regulate stress responsive genes in Arabidopsis. *Genome Biol* **15**: 458
- Levey S, Wingler A** (2005) Natural variation in the regulation of leaf senescence and relation to other traits in Arabidopsis. *Plant Cell Environ* **28**: 223–231
- Lev Maor G, Yearim A, Ast G** (2015) The alternative role of DNA methylation in splicing regulation. *Trends Genet* **31**: 274–280
- Li H, Handsaker B, Wysoker A, Fennell T, Ruan J, Homer N, Marth G, Abecasis G, Durbin R** (2009) The Sequence Alignment/Map format and SAMtools. *Bioinformatics* **25**: 2078–2079
- Lin Y-F, Liang H-M, Yang S-Y, Boch A, Clemens S, Chen C-C, Wu J-F, Huang J-L, Yeh K-C** (2009) Arabidopsis IRT3 is a zinc-regulated and plasma membrane localized zinc/iron transporter. *New Phytol* **182**: 392–404

References

- Lister R, O'Malley RC, Tonti-Filippini J, Gregory BD, Berry CC, Millar AH, Ecker JR** (2008) Highly Integrated Single-Base Resolution Maps of the Epigenome in *Arabidopsis*. *Cell* **133**: 523–536
- Liu C, Lu F, Cui X, Cao X** (2010) Histone Methylation in Higher Plants. *Annu Rev Plant Biol* **61**: 395–420
- Livak KJ, Schmittgen TD** (2001) Analysis of Relative Gene Expression Data Using Real-Time Quantitative PCR and the 2- $\Delta\Delta$ CT Method. *Methods* **25**: 402–408
- Li Y, Huang Y, Bergelson J, Nordborg M, Borevitz JO** (2010) Association mapping of local climate-sensitive quantitative trait loci in *Arabidopsis thaliana*. *Proc Natl Acad Sci* **107**: 21199–21204
- Loladze I** (2014) Hidden shift of the ionome of plants exposed to elevated CO₂ depletes minerals at the base of human nutrition. *eLife* **3**: e02245
- Maathuis FJ** (2009) Physiological functions of mineral macronutrients. *Curr Opin Plant Biol* **12**: 250–258
- Marín IC, Loef I, Bartetzko L, Searle I, Coupland G, Stitt M, Osuna D** (2010) Nitrate regulates floral induction in *Arabidopsis*, acting independently of light, gibberellin and autonomous pathways. *Planta* **233**: 539–552
- Marschner** (2012) Marschner's Mineral Nutrition of Higher Plants - (Third Edition) - ScienceDirect. <http://www.sciencedirect.com/science/book/9780123849052>
- Mathieu J, Warthmann N, Küttner F, Schmid M** (2007) Export of FT Protein from Phloem Companion Cells Is Sufficient for Floral Induction in *Arabidopsis*. *Curr Biol* **17**: 1055–1060
- Mcgrath JM, Lobell DB** (2013) Reduction of transpiration and altered nutrient allocation contribute to nutrient decline of crops grown in elevated CO₂ concentrations. *Plant Cell Environ* **36**: 697–705
- Meijón M, Satbhai SB, Tsuchimatsu T, Busch W** (2014) Genome-wide association study using cellular traits identifies a new regulator of root development in *Arabidopsis*. *Nat Genet* **46**: 77–81
- Melzer S, Lens F, Gennen J, Vanneste S, Rohde A, Beeckman T** (2008) Flowering-time genes modulate meristem determinacy and growth form in *Arabidopsis thaliana*. *Nat Genet* **40**: 1489–1492
- Mortel JE van de, Villanueva LA, Schat H, Kwekkeboom J, Coughlan S, Moerland PD, Themaat EVL van, Koornneef M, Aarts MGM** (2006) Large Expression Differences in Genes for Iron and Zinc Homeostasis, Stress Response, and Lignin Biosynthesis Distinguish Roots of *Arabidopsis thaliana* and the Related Metal Hyperaccumulator *Thlaspi caerulescens*. *Plant Physiol* **142**: 1127–1147
- Mutasa-Göttgens E, Hedden P** (2009) Gibberellin as a factor in floral regulatory networks. *J Exp Bot* erp040

References

- Myers SS, Zanobetti A, Kloog I, Huybers P, Leakey ADB, Bloom AJ, Carlisle E, Dietterich LH, Fitzgerald G, Hasegawa T, et al** (2014) Increasing CO₂ threatens human nutrition. *Nature* **510**: 139–142
- Nordborg M, Weigel D** (2008) Next-generation genetics in plants. *Nature* **456**: 720–723
- Notaguchi M, Abe M, Kimura T, Daimon Y, Kobayashi T, Yamaguchi A, Tomita Y, Dohi K, Mori M, Araki T** (2008) Long-Distance, Graft-Transmissible Action of Arabidopsis FLOWERING LOCUS T Protein to Promote Flowering. *Plant Cell Physiol* **49**: 1645–1658
- Ogura T, Busch W** (2015) From phenotypes to causal sequences: using genome wide association studies to dissect the sequence basis for variation of plant development. *Curr Opin Plant Biol* **23**: 98–108
- Olsen LI, Palmgren MG** (2014) Many rivers to cross: the journey of zinc from soil to seed. *Plant Nutr* **5**: 30
- O'Malley RC, Huang SC, Song L, Lewsey MG, Bartlett A, Nery JR, Galli M, Gallavotti A, Ecker JR** (2016) Cistrome and Epicistrome Features Shape the Regulatory DNA Landscape. *Cell* **165**: 1280–1292
- Pérez-Pérez JM, Serrano-Cartagena J, Micol JL** (2002) Genetic Analysis of Natural Variations in the Architecture of Arabidopsis thaliana Vegetative Leaves. *Genetics* **162**: 893–915
- Persson DP, Hansen TH, Laursen KH, Schjoerring JK, Husted S** (2009) Simultaneous iron, zinc, sulfur and phosphorus speciation analysis of barley grain tissues using SEC-ICP-MS and IP-ICP-MS. *Metallomics* **1**: 418–426
- Platt A, Horton M, Huang YS, Li Y, Anastasio AE, Mulyati NW, Ågren J, Bossdorf O, Byers D, Donohue K, et al** (2010) The Scale of Population Structure in Arabidopsis thaliana. *PLOS Genet* **6**: e1000843
- Posé D, Verhage L, Ott F, Yant L, Mathieu J, Angenent GC, Immink RGH, Schmid M** (2013) Temperature-dependent regulation of flowering by antagonistic FLM variants. *Nature* **503**: 414–417
- Posé D, Yant L, Schmid M** (2012) The end of innocence: flowering networks explode in complexity. *Curr Opin Plant Biol* **15**: 45–50
- Powell AE, Lenhard M** (2012) Control of Organ Size in Plants. *Curr Biol* **22**: R360–R367
- Putterill J, Robson F, Lee K, Simon R, Coupland G** (1995) The CONSTANS gene of arabidopsis promotes flowering and encodes a protein showing similarities to zinc finger transcription factors. *Cell* **80**: 847–857
- Quinlan AR, Hall IM** (2010) BEDTools: a flexible suite of utilities for comparing genomic features. *Bioinformatics* **26**: 841–842

References

- Raboy V** (2009) Approaches and challenges to engineering seed phytate and total phosphorus. *Plant Sci* **177**: 281–296
- Ratcliffe OJ, Amaya I, Vincent CA, Rothstein S, Carpenter R, Coen ES, Bradley DJ** (1998) A common mechanism controls the life cycle and architecture of plants. *Development* **125**: 1609–1615
- Richard O, Pineau C, Loubet S, Charies C, Vile D, Marquès L, Berthomieu P** (2011) Diversity analysis of the response to Zn within the *Arabidopsis thaliana* species revealed a low contribution of Zn translocation to Zn tolerance and a new role for Zn in lateral root development. *Plant Cell Environ* **34**: 1065–1078
- Ristova D, Busch W** (2014) Natural variation of root traits: from development to nutrient uptake. *Plant Physiol* pp.114.244749
- Ritchie ME, Phipson B, Wu D, Hu Y, Law CW, Shi W, Smyth GK** (2015) limma powers differential expression analyses for RNA-sequencing and microarray studies. *Nucleic Acids Res* gkv007
- Rooijen R van, Aarts MGM, Harbinson J** (2015) Natural Genetic Variation for Acclimation of Photosynthetic Light Use Efficiency to Growth Irradiance in *Arabidopsis*. *Plant Physiol* **167**: 1412–1429
- Salomé PA, Bomblies K, Laitinen RAE, Yant L, Mott R, Weigel D** (2011) Genetic Architecture of Flowering-Time Variation in *Arabidopsis thaliana*. *Genetics* **188**: 421–433
- Searle I, Coupland G** (2004) Induction of flowering by seasonal changes in photoperiod. *EMBO J* **23**: 1217–1222
- Secco D, Wang C, Shou H, Schultz MD, Chiarenza S, Nussaume L, Ecker JR, Whelan J, Lister R** (2015) Stress induced gene expression drives transient DNA methylation changes at adjacent repetitive elements. *eLife* e09343
- Segura V, Vilhjálmsson BJ, Platt A, Korte A, Seren Ü, Long Q, Nordborg M** (2012) An efficient multi-locus mixed-model approach for genome-wide association studies in structured populations. *Nat Genet* **44**: 825–830
- Seren Ü, Vilhjálmsson BJ, Horton MW, Meng D, Forai P, Huang YS, Long Q, Segura V, Nordborg M** (2012) GWAPP: A Web Application for Genome-Wide Association Mapping in *Arabidopsis*. *Plant Cell* **24**: 4793–4805
- Shalit A, Rozman A, Goldshmidt A, Alvarez JP, Bowman JL, Eshed Y, Lifschitz E** (2009) The flowering hormone florigen functions as a general systemic regulator of growth and termination. *Proc Natl Acad Sci* **106**: 8392–8397
- Sharif R, Thomas P, Zalewski P, Fenech M** (2012) The role of zinc in genomic stability. *Mutat Res Mol Mech Mutagen* **733**: 111–121
- Sheldon CC, Jean Finnegan E, James Peacock W, Dennis ES** (2009) Mechanisms of gene repression by vernalization in *Arabidopsis*. *Plant J* **59**: 488–498

References

- Sicard A, Kappel C, Josephs EB, Lee YW, Marona C, Stinchcombe JR, Wright SI, Lenhard M** (2015) Divergent sorting of a balanced ancestral polymorphism underlies the establishment of gene-flow barriers in *Capsella*. *Nat Commun* **6**: 7960
- Sinclair SA, Krämer U** (2012) The zinc homeostasis network of land plants. *Biochim Biophys Acta BBA - Mol Cell Res* **1823**: 1553–1567
- Soppe WJJ, Jacobsen SE, Alonso-Blanco C, Jackson JP, Kakutani T, Koornneef M, Peeters AJM** (2000) The Late Flowering Phenotype of *fwa* Mutants Is Caused by Gain-of-Function Epigenetic Alleles of a Homeodomain Gene. *Mol Cell* **6**: 791–802
- Stetter MG, Schmid K, Ludewig U** (2015) Uncovering Genes and Ploidy Involved in the High Diversity in Root Hair Density, Length and Response to Local Scarce Phosphate in *Arabidopsis thaliana*. *PLOS ONE* **10**: e0120604
- Stroud H, Greenberg MVC, Feng S, Bernatavichute YV, Jacobsen SE** (2013) Comprehensive Analysis of Silencing Mutants Reveals Complex Regulation of the *Arabidopsis* Methylome. *Cell* **152**: 352–364
- Sung S, Amasino RM** (2004) Vernalization in *Arabidopsis thaliana* is mediated by the PHD finger protein VIN3. *Nature* **427**: 159–164
- Talukdar S, Aarts MGM** (2007) *Arabidopsis thaliana* and *Thlaspi caerulescens* respond comparably to low zinc supply. *Plant Soil* **306**: 85–94
- Tan M** (2010) Analysis of DNA methylation of maize in response to osmotic and salt stress based on methylation-sensitive amplified polymorphism. *Plant Physiol Biochem* **48**: 21–26
- Teixeira FK, Colot V** (2009) Gene body DNA methylation in plants: a means to an end or an end to a means? *EMBO J* **28**: 997–998
- Tian X, Diaz FJ** (2013) Acute dietary zinc deficiency before conception compromises oocyte epigenetic programming and disrupts embryonic development. *Dev Biol* **376**: 51–61
- Torti S, Fornara F, Vincent C, Andrés F, Nordström K, Göbel U, Knoll D, Schoof H, Coupland G** (2012) Analysis of the *Arabidopsis* Shoot Meristem Transcriptome during Floral Transition Identifies Distinct Regulatory Patterns and a Leucine-Rich Repeat Protein That Promotes Flowering. *Plant Cell Online* **24**: 444–462
- Verret F, Gravot A, Auroy P, Leonhardt N, David P, Nussaume L, Vavasseur A, Richaud P** (2004) Overexpression of *AtHMA4* enhances root-to-shoot translocation of zinc and cadmium and plant metal tolerance. *FEBS Lett* **576**: 306–312
- Visscher PM, Hill WG, Wray NR** (2008) Heritability in the genomics era — concepts and misconceptions. *Nat Rev Genet* **9**: 255–266

References

- Wada KC, Yamada M, Shiraya T, Takeno K** (2010) Salicylic acid and the flowering gene FLOWERING LOCUS T homolog are involved in poor-nutrition stress-induced flowering of *Pharbitis nil*. *J Plant Physiol* **167**: 447–452
- Wahl V, Ponnu J, Schlereth A, Arrivault S, Langenecker T, Franke A, Feil R, Lunn JE, Stitt M, Schmid M** (2013) Regulation of Flowering by Trehalose-6-Phosphate Signaling in *Arabidopsis thaliana*. *Science* **339**: 704–707
- Wang J-W, Czech B, Weigel D** (2009) miR156-Regulated SPL Transcription Factors Define an Endogenous Flowering Pathway in *Arabidopsis thaliana*. *Cell* **138**: 738–749
- Wang W-S, Pan Y-J, Zhao X-Q, Dwivedi D, Zhu L-H, Ali J, Fu B-Y, Li Z-K** (2010) Drought-induced site-specific DNA methylation and its association with drought tolerance in rice (*Oryza sativa* L.). *J Exp Bot* **erq391**
- Wang WY, Xu J, Liu XJ, Yu Y, Ge Q** (2012) Cadmium induces early flowering in *Arabidopsis*. *Biol Plant* **56**: 117–120
- Wang Z, Straub D, Yang H, Kania A, Shen J, Ludewig U, Neumann G** (2014) The regulatory network of cluster-root function and development in phosphate-deficient white lupin (*Lupinus albus*) identified by transcriptome sequencing. *Physiol Plant* **151**: 323–338
- Weigel D** (2012) Natural Variation in *Arabidopsis*: From Molecular Genetics to Ecological Genomics. *Plant Physiol* **158**: 2–22
- Wessells KR, Brown KH** (2012) Estimating the Global Prevalence of Zinc Deficiency: Results Based on Zinc Availability in National Food Supplies and the Prevalence of Stunting. *PLoS ONE* **7**: e50568
- Wong CKE, Jarvis RS, Sherson SM, Cobbett CS** (2009) Functional analysis of the heavy metal binding domains of the Zn/Cd-transporting ATPase, HMA2, in *Arabidopsis thaliana*. *New Phytol* **181**: 79–88
- Yang H, Menz J, Häussermann I, Benz M, Fujiwara T, Ludewig U** (2015) High and Low Affinity Urea Root Uptake: Involvement of NIP5;1. *Plant Cell Physiol* **pcv067**
- Yu S, Cao L, Zhou C-M, Zhang T-Q, Lian H, Sun Y, Wu J, Huang J, Wang G, Wang J-W** (2013) Sugar is an endogenous cue for juvenile-to-adult phase transition in plants. *eLife* **2**: e00269
- Zargar SM, Fujiwara M, Inaba S, Kobayashi M, Kurata R, Ogata Y, Fukao Y** (2014) Correlation analysis of proteins responsive to Zn, Mn, or Fe deficiency in *Arabidopsis* roots based on iTRAQ analysis. *Plant Cell Rep* **34**: 157–166
- Zhang X** (2008) The Epigenetic Landscape of Plants. *Science* **320**: 489–492
- Zhong L, Xu Y, Wang J** (2009) DNA-methylation changes induced by salt stress in wheat *Triticum aestivum*. *Afr. J. Biotechnol.* **8**:

References

- Zilberman D, Gehring M, Tran RK, Ballinger T, Henikoff S** (2007) Genome-wide analysis of *Arabidopsis thaliana* DNA methylation uncovers an interdependence between methylation and transcription. *Nat Genet* **39**: 61–69

9 Acknowledgement

First of all, I must acknowledge China Scholarship Council for the financial support during the last four years.

I would like to thank Prof. Dr. Uwe Ludewig, who accepted me to do my PhD study at University of Hohenheim. Importantly, he guided me to Epigenetics and GWAS, which are exciting topics to me. I am pretty sure I will continue these amazing researches for a long time in the future. I am also beneficial a lot from his erudition and wisdom. He was always able to connect knowledge from different disciplines and explore valuable information from “waste data”. In addition, I also thank his support to conferences and workshops.

I am particularly thankful to Dr. Huaiyu Yang and Dr. Yan Liu. They helped me to improve laboratory skills and solve many personal difficulties as well. Without them, my German life and study would be much harder.

I would also thank to my lab members who are not only colleagues but also friends. We discussed academic problems, and more importantly, we shared happiness and sorrows with each other. They are Dr. Zhengrui Wang, Dr. Benjamin Neuhäuser, Dr. Daniel Straub, Dr. Tatsiana Straub, Deborah Schnell, Jochen Menz, Brigitte Schönberger, Svenja Mager, Yuan Liu, Yaping Zhou, and all the others.

Many thanks to our technicians Helene Ochott, Hinrich Bremer, Charlotte Haake and Heidi Zimmermann, for plant growth and nutrient analyses. Especially to Frau Ochott, who helped me analyze around 3000 samples. I am also grateful to Frau Berghammer and Frau Schöllhammer, for their help with all administrative things.

I thank Prof. Dr. Günter Neumann, Prof. Dr. Torsten Müller and all their group members for their valuable discussions and suggestions during the regular colloquiums.

Lastly, I would thank to my family, especially my wife, for the encouragement and tolerance all the time with love.

10 Curriculum vitae

Personal information

Name: Xiaochao Chen

Date of birth: 22 October 1988

Place of birth: Anhui, China

Nationality: Chinese

Education

2012 - 2016 Ph.D.

Institute of Crop Science

University of Hohenheim

Stuttgart, Germany

2010 - 2012 M.Sc.

College of Resource and Environment

China Agricultural University

Beijing, China

2006 - 2010 B.Sc.

College of Resource and Environment

University of Science and Technology of Anhui

Anhui, China

Language skills

English, Chinese

Computer skills

DNA methylation data analysis (and related bioinformatics)

Transcriptome data analysis

Genome-wide association study

Data visualization in R

Workshop, summer school and conference

Sep. 2016 Epigenetics and Chromatin

New York, U.S.

Sep. 2016 German Plant Nutrition 2016 International Conference

Stuttgart, Germany

Dec. 2015 DNA Methylation Data Analysis

Leipzig, Germany

Aug. 2015 From Molecules to the Field, BOTANIKERTAGUNG 2015

Munich, Germany

Aug. 2015 2nd Summer Academy in Plant Molecular Biology

Freudenstadt, Germany

Feb. 2015 8th RegioPlantScience Meeting, Stuttgart-Tuebingen-Ulm

Ulm, Germany

Feb. 2014 7th RegioPlantScience Meeting, Stuttgart-Tuebingen-Ulm

Stuttgart, Germany

Publications

Chen X, Yuan L, Ludewig U (2016) Natural Genetic Variation of Seed

- Micronutrients of *Arabidopsis thaliana* Grown in Zinc-Deficient and Zinc-Amended Soil. **Frontiers in Plant Science** 7:1070
- Chen X**, Ludewig U, Zinc controls leaf size by promotion of *FLOWERING LOCUS T* in early-flowering *Arabidopsis thaliana*. **In revision**
- Chen X**, Ludewig U, Limited contribution of zinc deficiency-induced DNA demethylation to transcription in *Arabidopsis thaliana*. **Submitted**
- Chen X**, Chen F, Chen Y, Gao Q, Yang X, Yuan L, Zhang F, Mi G (2013a) Modern maize hybrids in Northeast China exhibit increased yield potential and resource use efficiency despite adverse climate change. **Global Change Biology** 19: 923–936
- Chen X**, Zhang J, Chen Y, Li Q, Chen F, Yuan L, Mi G (2013b) Changes in root size and distribution in relation to nitrogen accumulation during maize breeding in China. **Plant Soil** 374: 121–130
- Zhao J, Yang X, Lin X, Sassenrath GF, Dai S, Lv S, **Chen X**, Chen F, Mi G (2015) Radiation Interception and Use Efficiency Contributes to Higher Yields of Newer Maize Hybrids in Northeast China. **Agronomy Journal** 107: 1473–1480
- Lv S, Yang X, Lin X, Liu Z, Zhao J, Li K, Mu C, **Chen X**, Chen F, Mi G (2015) Yield gap simulations using ten maize cultivars commonly planted in Northeast China during the past five decades. **Agricultural and Forest Meteorology** 205: 1–10
- Chen Y, Xiao C, **Chen X**, Li Q, Zhang J, Chen F, Yuan L, Mi G (2014) Characterization of the plant traits contributed to high grain yield and high grain nitrogen concentration in maize. **Field Crops Research** 159: 1–9
- ZHANG Y, CHEN F, **CHEN X**, LONG L, GAO K, YUAN L, ZHANG F, MI G (2013) Genetic Improvement of Root Growth Contributes to Efficient Phosphorus Acquisition in maize (*Zea mays* L.). **Journal of Integrative Agriculture** 12: 1098–1111